UC Irvine
UC Irvine Previously Published Works

Title

Measurement of the inclusive jet cross-sections in proton-proton collisions at s=8 TeV with the ATLAS detector

Permalink

Journal

ISSN

Authors

The ATLAS collaboration
Aaboud, M
Aad, G
et al.

Publication Date

DOI

Copyright Information

Peer reviewed

Measurement of the inclusive jet cross-sections in proton-proton collisions at $\sqrt{s} = 8$ TeV with the ATLAS detector

The ATLAS collaboration

E-mail: atlas.publications@cern.ch

ABSTRACT: Inclusive jet production cross-sections are measured in proton-proton collisions at a centre-of-mass energy of $\sqrt{s} = 8$ TeV recorded by the ATLAS experiment at the Large Hadron Collider at CERN. The total integrated luminosity of the analysed data set amounts to $20.2\,\mathrm{fb}^{-1}$. Double-differential cross-sections are measured for jets defined by the anti-k_t jet clustering algorithm with radius parameters of $R = 0.4$ and $R = 0.6$ and are presented as a function of the jet transverse momentum, in the range between $70\,\mathrm{GeV}$ and $2.5\,\mathrm{TeV}$ and in six bins of the absolute jet rapidity, between 0 and 3.0. The measured cross-sections are compared to predictions of quantum chromodynamics, calculated at next-to-leading order in perturbation theory, and corrected for non-perturbative and electroweak effects. The level of agreement with predictions, using a selection of different parton distribution functions for the proton, is quantified. Tensions between the data and the theory predictions are observed.

Contents

1 Introduction

The Large Hadron Collider (LHC) [1] at CERN, colliding protons on protons, provides a unique opportunity to explore the production of hadronic jets in the TeV energy range. In Quantum Chromodynamics (QCD), jet production can be interpreted as the fragmentation of quarks and gluons produced in a short-distance scattering process. The inclusive jet production cross-section ($p + p \rightarrow jet + X$) gives valuable information about the strong coupling constant (α_{s}) and the structure of the proton. It is also among the processes directly testing the experimentally accessible space-time distances.

Next-to-leading-order (NLO) perturbative QCD calculations [2, 3] give quantitative predictions of the jet production cross-sections. Progress in next-to-next-to-leading-order (NNLO) QCD calculations has been made over the past several years [4–9]. After the completion of the first calculations of some sub-processes [10, 11], the complete NNLO QCD inclusive jet cross-section calculation was published recently [12].

As fixed-order QCD calculations only make predictions for the quarks and gluons associated with the short-distance scattering process, corrections for the fragmentation of these partons to particles need to be applied. The measurements can also be compared to Monte Carlo event generator predictions that directly simulate the particles entering the detector. These event generators can be based on calculations with leading-order (LO) or NLO accuracy for the description of the short-distance scattering process as well as additional QCD radiation, hadronisation and multiple parton interactions [13].

Inclusive jet production cross-sections have been measured in proton-antiproton collisions at the Tevatron collider at various centre-of-mass energies. The latest and most precise measurements at $\sqrt{s} = 1.96\,\mathrm{TeV}$ can be found in refs. [14, 15]. At the LHC, the ALICE, ATLAS and CMS collaborations have measured inclusive jet cross-sections in proton-proton collisions at centre-of-mass energies of $\sqrt{s} = 2.76\,\mathrm{TeV}$ [16–18] and $\sqrt{s} = 7\,\mathrm{TeV}$ [19–23], and recently the CMS Collaboration has also measured them at $\sqrt{s} = 8\,\mathrm{TeV}$ [24] and $\sqrt{s} = 13\,\mathrm{TeV}$ [25].

This paper presents the measurement of the inclusive jet cross-sections in proton-proton collisions at a centre-of-mass energy of $\sqrt{s} = 8\,\mathrm{TeV}$ using data collected by the ATLAS experiment in 2012 corresponding to an integrated luminosity of $20.2\,\mathrm{fb}^{-1}$. The cross-sections are measured double-differentially and presented as a function of the jet transverse momentum, p_{T}, in six equal-width bins of the absolute jet rapidity, $|y|$. Jets are reconstructed using the anti-k_t jet clustering algorithm [26] with radius parameters of $R = 0.4$ and $R = 0.6$. The measurement is performed for two jet radius parameters, since the uncertainties in the theoretical predictions are different. The kinematic region of $70\,\mathrm{GeV} \leq p_{\mathrm{T}} \leq 2.5\,\mathrm{TeV}$ and $|y| < 3$ is covered.

The measurements explore a higher centre-of-mass energy than the previous ATLAS measurements and are also more precise due to the higher integrated luminosity and the better knowledge of the jet energy measurement uncertainties. Fixed-order NLO QCD predictions calculated for a suite of proton parton distribution function (PDF) sets, corrected for non-perturbative (hadronisation and underlying event) and electroweak effects, are quantitatively compared to the measurement results, unfolded for detector effects. The

results are also compared to the predictions of a Monte Carlo event generator based on the NLO QCD calculation for the short-distance scattering process matched with parton showers, followed by hadronisation. The measurement is performed with two different jet radius parameters to test the sensitivity to perturbative (higher-order corrections and parton shower) and non-perturbative effects.

The outline of the paper is as follows. A brief description of the ATLAS detector is given in section 2. The inclusive jet production cross-section is defined in section 4. Section 3 gives an overview of the data set and Monte Carlo simulations used. The details of the experimental measurement are presented in the next sections. Section 5 describes the event and jet selection for the measurement. The jet energy calibration and the uncertainties associated with the jet energy measurements are outlined in section 6. The procedure to unfold the detector effects is detailed in section 7 and the propagation of the systematic uncertainties in the measurements is explained in section 8. The theoretical predictions are described in section 9. The results together with a quantitative comparison of the measurements to the theory predictions are presented in section 10.

2 ATLAS detector

The ATLAS experiment [27] at the LHC is a multipurpose particle detector with a forward-backward symmetric cylindrical geometry and a near 4π coverage in solid angle.[1] It consists of an inner tracking detector surrounded by a thin superconducting solenoid providing a 2 T axial magnetic field, electromagnetic and hadron calorimeters, and a muon spectrometer. The inner tracking detector covers the pseudorapidity range $|\eta| < 2.5$ and is made of silicon pixel, silicon microstrip, and transition-radiation tracking detectors. Lead/liquid-argon (LAr) sampling calorimeters provide electromagnetic (EM) energy measurements with high granularity. A hadron (steel/scintillator-tile) calorimeter covers the central pseudorapidity range ($|\eta| < 1.7$). The endcap and forward regions are instrumented with LAr calorimeters for EM and hadronic energy measurements up to $|\eta| = 4.9$. The muon spectrometer surrounds the calorimeters and is based on three large air-core toroid superconducting magnets with eight coils each. Its bending power ranges between 2.0 and 6.0 T m for most of the detector.

A three-level trigger system is used to select events. The first-level trigger is implemented in hardware and uses a subset of the detector information to reduce the accepted event rate to at most 75 kHz. This is followed by two software-based trigger levels that together reduce the accepted event rate to 400 Hz on average depending on the data-taking conditions during 2012.

The relevant systems used to select events with jets are the minimum-bias trigger scintillators (MBTS), located in front of the endcap cryostats covering $2.1 < |\eta| < 3.8$, as well as calorimeter-based jet triggers covering $|\eta| < 3.2$ for central jets [28].

---

[1]ATLAS uses a right-handed coordinate system with its origin at the nominal interaction point (IP)in the centre of the detector and the z-axis along the beam pipe. The x-axis points from the IP to the centre of the LHC ring, and the y-axis points upwards. Cylindrical coordinates (r, ϕ) are used in the transverse plane, ϕ being the azimuthal angle around the z-axis. The pseudorapidity is defined in terms of the polar angle θ as $\eta = -\ln\tan(\theta/2)$. Angular distance is measured in units of $\Delta R \equiv \sqrt{(\Delta y)^2 + (\Delta \phi)^2}$, where y is the jet rapidity.

3 Data set and Monte Carlo simulations

The measurement uses proton-proton collision data at a centre-of-mass energy of $\sqrt{s} = 8\,\text{TeV}$ collected by the ATLAS detector during the data-taking period of the LHC in 2012. The LHC beams were operated with proton bunches organised in "bunch trains", with bunch-crossing intervals (or bunch spacing) of $50\,\text{ns}$.

The absolute luminosity measurement is derived from beam-separation scans performed in November 2012 and corresponds to $20.2\,\text{fb}^{-1}$ with an uncertainty of 1.9%. The uncertainty in the luminosity is determined following the technique described in refs. [29]. The average number of interactions per bunch crossing, $\langle\mu\rangle$, was $10 \leq \langle\mu\rangle \leq 36$. All data events considered in this analysis have good detector status and data quality.

For the simulation of the detector response to scattered particles in proton-proton collisions, events are generated with the Pythia 8 [30] (v8.160) Monte Carlo event generator. It uses LO QCD matrix elements for $2 \rightarrow 2$ processes, along with a leading-logarithmic (LL) p_T-ordered parton shower [31] including photon radiation, underlying-event simulation with multiple parton interactions [32], and hadronisation with the Lund string model [33]. The MC event generator's parameter values are set according to the AU2 underlying event tune [34] and the CT10 PDF set [35] is used.

The stable particles from the generated events are passed through the ATLAS detector simulation [36] based on the Geant4 software toolkit [37] and are reconstructed using the same version of the ATLAS software as used to process the data. Effects from multiple proton-proton interactions in the same and neighbouring bunch crossings (pile-up) are included by overlaying inclusive proton-proton collision events (minimum bias), which consist of single-, double- and non-diffractive collisions generated by the Pythia 8 event generator using the A2 tune [34] based on the MSTW2008 LO PDF set [38]. The Monte Carlo events are weighted such that the distribution of the generated mean number of proton-proton collisions per bunch crossing matches that of the corresponding data-taking period. The particles from additional interactions are added before the signal digitisation and reconstruction steps of the detector simulation, but are not considered a signal and are therefore not used in the definition of the cross-section measurement defined in section 4.

For the evaluation of non-perturbative effects, the Pythia 8 [30] (v8.186) and Herwig++ [39] (v2.7.1) [40] event generators are also employed as described in section 9.3. The latter also uses LO matrix elements for the $2 \rightarrow 2$ short-distance process together with a LL angle-ordered parton shower [41]. It implements an underlying-event simulation based on an eikonal model [42] and the hadronisation process based on the cluster model [43].

The Powheg [44–46] method provides MC event generation based on an NLO QCD calculation matched to LL parton showers using the Powheg Box 1.0 package [47]. In this simulation the CT10 PDF set [35] is used. The simulation of parton showers, the hadronisation and the underlying event is based on Pythia 8 [30] using the AU2 tune [34]. These predictions are refered to as the Powheg predictions in the following.

The renormalisation and factorisation scales for the fixed-order NLO prediction are set to the transverse momentum of each of the outgoing partons of the $2 \rightarrow 2$ process, p_T^{Born}.

In addition to the hard scatter, Powheg also generates the hardest partonic emission in the event using the LO $2 \rightarrow 3$ matrix element or parton showers. The radiative emissions in the parton showers are limited by the matching scale μ_M provided by Powheg.

4 Inclusive jet cross-section definition

Jets are identified with the anti-k_t [26] clustering algorithm using the four-momentum recombination scheme, implemented in the FastJet [48] library, using two values of the jet radius parameter, $R = 0.4$ and $R = 0.6$. Throughout this paper, the jet cross-section measurements refer to jets built from stable particles defined by having a proper mean decay length of $c\tau > 10$ mm. Muons and neutrinos from decaying hadrons are included in this definition. More information about the particle definition can be found in ref. [49]. These jets are called "particle-level" jets in the following.

The inclusive jet double-differential cross-section, $\mathrm{d}^2\sigma/\mathrm{d}p_\mathrm{T}\mathrm{d}y$, is measured as a function of the jet transverse momentum p_T in bins of rapidity y. In this context, "inclusive" cross-section means that all reconstructed jets in accepted events contribute to the measurement in the bins corresponding to their p_T and y values.

The kinematic range of the measurement is $70\,\mathrm{GeV} \leq p_\mathrm{T} \leq 2.5\,\mathrm{TeV}$ and $|y| < 3$.

5 Event and jet selection

A set of single-jet triggers with various p_T thresholds are used to preselect events to be recorded. The highest threshold trigger accepts all events passing the threshold. To keep the trigger rate to an acceptable level, the triggers with lower p_T thresholds are only read out for a fraction of all events.

A p_T-dependent trigger strategy is adopted in order to optimise the statistical power of the measurement. Trigger efficiencies are studied using the trigger decisions in samples selected by lower-threshold jet triggers. The efficiency of the lowest p_T jet trigger is determined with an independent trigger based on the MBTS scintillators. For each measurement bin, the trigger is chosen such that the highest effective luminosity (i.e. the lowest prescale factor) is obtained and the trigger is fully efficient. This procedure is performed separately for each of the jet radius parameters and for each jet rapidity bin.

At least one reconstructed vertex with at least two associated well-reconstructed tracks is required. Jet quality criteria are applied to reject jets from beam-gas events, beam-halo events, cosmic-ray muons and calorimeter noise bursts following the procedure described in ref. [50].

In the 2012 data set the central hadron calorimeter had a few modules turned off for certain long time periods or suffered from power-supply trips that made them non-operational for a few minutes. The energy deposited in these modules is estimated using the energy depositions in the neighbouring modules [50]. This correction overestimates the true deposited energy. Therefore, events where a jet with $p_\mathrm{T} \geq 40\,\mathrm{GeV}$ points to such a calorimeter region are rejected both in data and simulation.

6 Jet energy calibration and resolution

6.1 Jet reconstruction

Jets are defined with the anti-k_t clustering algorithm with the jet radius parameters $R = 0.4$ and $R = 0.6$. The input objects for the jet algorithm are three-dimensional topological clusters (topoclusters) [51, 52] built from the energy deposits in calorimeter cells. A local cluster weighting calibration (LCW) based on the topology of the calorimeter energy deposits is then applied to each topocluster to improve the energy resolution for hadrons impinging on the calorimeter [51, 52]. The four-momentum of the LCW-scale jet is defined as the sum of four-momenta of the locally calibrated clusters in the calorimeter treating each cluster as a four-momentum with zero mass.

6.2 Jet energy calibration

Jets are calibrated using the procedure described in refs. [50, 51]. The jet energy is corrected for the effect of multiple proton-proton interactions (pile-up) both in collision data and in simulated events. Further corrections depending on the jet energy and the jet pseudorapidity (η) are applied to achieve a calibration that matches the energy of jets composed of stable particles in simulated events. Fluctuations in the particle content of jets and in hadronic calorimeter showers are reduced with the help of observables characterising internal jet properties. These corrections are applied sequentially (Global Sequential Calibration). Differences between data and Monte Carlo simulation are evaluated using *in situ* techniques exploiting the p_T balance of a jet and a well-measured object such as a photon (γ+jet balance), a Z boson (Z+jet balance) or a system of jets (multijet balance). These processes are used to calibrate the jet energy in the central detector region, while the p_T balance in dijet events is used to achieve an intercalibration of jets in the forward region with respect to central jets (dijet balance).

The calibration procedure that establishes the jet energy scale (JES) and the associated systematic uncertainty is given in more detail in the following:

Pile-up correction. Jets are corrected for the contributions from additional proton-proton interactions within the same (in-time) or nearby (out-of-time) bunch crossings [53]. First, for each event a correction based on the jet area and the median p_T density ρ [54, 55] is calculated. The jet area is a measure of the susceptibility of the jet to pile-up and is determined for each jet. The density, ρ, is a measure of the pile-up activity in the event. Subsequently, an average offset subtraction is performed based on the number of additional interactions and reconstructed vertices (N_{PV}) in the event. It is derived by comparing reconstructed calorimeter jets, with the jet-area correction applied, to particle jets in simulated inclusive jet events.

The correction for contributions from additional proton-proton interactions can also remove part of the soft physics contributions, e.g. the contribution from the underlying event. This contribution is restored on average by the MC-based jet energy scale correction discussed below. The impact of pile-up subtraction on the jet energy resolution is corrected for in the unfolding step (see section 7).

Jet energy scale. The energy and the direction of jets are corrected for instrumental effects (non-compensating response of the calorimeter, energy losses in dead material, and out-of-cone effects) and the jet energy scale is restored on average to that of the particles entering the calorimeter using an inclusive jet Monte Carlo simulation [56]. These corrections are derived in bins of energy and the pseudorapidity of the jet.

Global sequential correction. The topology of the calorimeter energy deposits and of the tracks associated with jets can be exploited to correct for fluctuations in the jet's particle content [51, 57]. The measured mean jet energy depends on quantities such as the number of tracks, the radial extent of the jets as measured from the tracks in the jets, the longitudinal and lateral extent of the hadronic shower in the calorimeter and the hits in the muon detector associated with the jet. A correction of the jet energy based on these quantities can therefore improve the jet resolution and reduce the dependence on jet fragmentation effects. The correction is constructed from a MC sample based on one generator such that the jet energy scale correction is unchanged for the inclusive jet sample, but the jet energy resolution is improved and the sensitivity to jet fragmentation effects such as differences between quark- or gluon-induced jets is moderated. The dependence of this correction on the MC generator is treated as uncertainty.

Correction for difference between data and Monte Carlo simulation. A residual calibration is applied to correct for remaining differences between the jet energy response in data and simulation. This correction is derived *insitu* by comparing the results of γ+jet, Z+jet, dijet and multijet p_T-balance techniques [56, 58, 59]. The level of agreement between the jet energy response in the Monte Carlo simulation and the one in the data is evaluated by exploiting the p_T balance between a photon or a Z boson and a jet. In the p_T range above about $800\,\mathrm{GeV}$, which cannot be reached by γ+jet events, the recoil system of low-p_T jets in events with more than two jets is used (multijet balance).

This correction is applied to the central detector region. The relative response in all detector regions is equalised using an intercalibration method that uses the p_T balance in dijet events where one jet is central and one jet is in the forward region of the detector (η-intercalibration).

In the region above $p_\mathrm{T} = 1.7\,\mathrm{TeV}$, where the *insitu* techniques do not have sufficient statistical precision, the uncertainty in the jet energy measurement is derived from single-hadron response measurements [60, 61].

6.3   Jet energy scale uncertainties

The jet calibration corrections are combined following the procedure described in ref. [56]. The systematic and statistical uncertainties of each of the above mentioned corrections contribute to the total JES uncertainty as independent systematic components.

The *insitu* techniques are based on various processes leading to jets with different fragmentation patterns. Differences in the calorimeter response to jets initiated by quarks

or gluons in the short-distance processes lead to an additional uncertainty. Limited knowledge of the exact flavour composition of the analysed data sample is also considered as an uncertainty. An estimation of flavour composition based on the Pythia and the Powheg + Pythia Monte Carlo simulations is used in order to reduce this uncertainty.

A systematic uncertainty needs to be assigned to the correction, based on the muon hits behind the jet, that corrects jets with large energy deposition behind the calorimeter (punch-through).

In total, 66 independent systematic components uncorrelated among each other and fully correlated across p_T and η, constitute the full JES uncertainty in the configuration with the most detailed description of correlations [56]. A simplification is performed in this standard configuration: the η-intercalibration statistical uncertainty being treated as one uncertainty component fully correlated between the jet rapidity and p_T bins for which the η-intercalibration was performed. However, at the level of precision achieved in this analysis a detailed description of the statistical uncertainties of the η-intercalibration calibration procedure is important. For this reason, in this measurement, the total statistical uncertainty of the η-intercalibration in the standard configuration is replaced by 240 (250) uncertainty components for jets with $R = 0.4$ ($R = 0.6$), propagated from the various bins of the *insitu* η-intercalibration analysis [58].

The total uncertainty in the JES is below 1% for $100\,\text{GeV} < p_T < 1500\,\text{GeV}$ in the central detector region ($|\eta| \leq 0.8$) rising both towards lower and higher p_T and larger $|\eta|$ [56].

6.4 Jet energy resolution and uncertainties

The fractional uncertainty in the jet p_T resolution (JER) is derived using the same *insitu* techniques as used to determine the JES uncertainty from the width of the ratio of the p_T of a jet to the p_T of a well-measured particle such as a photon or a Z boson [59]. In addition, the balance between the jet transverse momenta in events with two jets at high p_T can be used (η-intercalibration) [58]. This method allows measurement of the JER at high jet rapidities and in a wide range of transverse momenta. The results from individual methods are combined similarly to those for the JES [56]. This JER evaluation includes a correction for physics effects such as radiation of extra jets which can also alter the p_T ratio width. This correction is obtained from a Monte Carlo simulation.

The JER uncertainty has in total 11 systematic uncertainty components. Nine systematic components are obtained by combining the systematic uncertainties associated with the *insitu* methods. The last two are the uncertainty due to the electronic and pile-up noise measured in inclusive proton-proton collisions and the absolute JER difference between data and MC simulation as determined with the *insitu* methods. The latter is non-zero only for low-p_T jets in forward rapidity regions. In the rest of the phase-space region the JER in MC simulation is better than in data and this uncertainty is eliminated by smearing the jet p_T in simulation such that the resulting resolution matches closely the one in data. Each JER systematic component describes an uncertainty that is fully correlated in jet p_T and pseudorapidity. The 11 JER components are treated independently from each other.

6.5 Jet angular resolution and uncertainties

The jet angular resolution (JAR) is estimated from comparisons of the polar angles of a reconstructed jet and the matched particle-level jet using the Monte Carlo simulation. This estimate is cross-checked by comparing the standard jets using calorimeter energy deposits as inputs to the ones using tracks in the inner detector [50, 51]. A relative uncertainty of 10% is assigned to the JAR to account for possible differences between data and MC simulation.

7 Unfolding of detector effects

The reconstructed jet spectra in data are unfolded to correct for detector inefficiencies and resolution effects to obtain the inclusive jet cross-section that refers to the stable particles entering the detector. The detector unfolding is based on Monte Carlo simulation and is performed in three consecutive steps, namely, a correction for the matching impurity at reconstruction level, the unfolding for resolution effects and a correction for the matching inefficiency at particle level, as explained below. In order to account for migrations from lower p_T into the region of interest, this study is performed in a wider p_T range than the one for the final result.

The unfolding of the detector resolution in jet p_T is based on a modified Bayesian technique, the Iterative Dynamically Stabilised (IDS) method [62]. This unfolding method uses a transfer matrix describing the migrations of jets across the p_T bins, between the particle level and the reconstruction level. A minimal number of iterations in the IDS unfolding method is chosen such that the residual bias, evaluated through a data-driven closure test (see below), is within a tolerance of 1% in the bins with less than 10% statistical uncertainty. In this measurement this is achieved after one iteration.

The transfer matrix used in the unfolding is derived by matching a particle level jet with a reconstructed jet in Monte Carlo simulations, when both are closer to each other than to any other jet and lie within a radius of $\Delta R = 0.3$.

The matching purity, $\mathcal{P}$, is defined as the ratio of the number of matched reconstructed jets to the total number of reconstructed jets. The matching efficiency, $\mathcal{E}$, is defined as the ratio of the number of matched particle jets to the total number of particle jets. If jets migrate to other rapidity bins, they are considered together with the jets that are completely unmatched. In this way the migrations across rapidity bins are effectively taken into account by bin-to-bin corrections.

The final result is given by

$$\mathcal{N}_i^{\mathrm{part}} = \sum_j \mathcal{N}_j^{\mathrm{reco}} \cdot \mathcal{P}_j \cdot \mathcal{A}_{ij} \ / \ \mathcal{E}_i, \tag{7.1}$$

where i and j are the bin indices of the jets at particle- and reconstructed-levels and $\mathcal{N}^{\mathrm{part}}$ and $\mathcal{N}^{\mathrm{reco}}$ are the number of particle-level and reconstructed jets in a given bin. The symbol $\mathcal{A}$ denotes the unfolding matrix obtained by the IDS method from the transfer matrix. The element $\mathcal{A}_{ij}$ describes the probability for a reconstructed jet in p_T bin j to originate from particle-level p_T bin i.

The precision of the unfolding technique is assessed using a data-driven closure test [20, 62]. The particle-level p_T spectrum in the MC simulation is reweighted such that the reweighted reconstructed spectrum and the data agree. The reconstructed spectrum in this reweighted MC simulation is then unfolded using the same procedure as for the data. The ratio of the unfolded spectrum to the reweighted particle-level spectrum provides an estimate of the unfolding bias. The residual bias is taken into account as a systematic uncertainty. After one IDS iteration, this uncertainty is of the order of a few per mille in the whole phase-space region, except for the very high p_T bins in each of the rapidity bins, where it grows to a few percent (up to 15% in certain cases).

The statistical and systematic uncertainties are evaluated by repeating the unfolding as explained in section 8.

8   Propagation of the statistical and systematic uncertainties

The statistical uncertainties are propagated through the unfolding procedure using an ensemble of pseudo-experiments. For each pseudo-experiment in the ensemble, a weight fluctuated according to a Poisson distribution with a mean value equal to one is applied to each event in data and simulation. This procedure takes into account the correlation between jets produced in the same event. The unfolding is performed for each pseudo-experiment. An ensemble of 10000 pseudo-experiments is used to calculate a covariance matrix for the cross-section in each jet rapidity bin. The total statistical uncertainty is obtained from the covariance matrix, where bin-to-bin correlations are also encoded. The separate contributions from the data and from the MC statistics are obtained from the same procedure by fluctuating only either the data or the simulated events. Furthermore, an overall covariance matrix is constructed to describe the full statistical covariance among all analysis bins.

To propagate the JES uncertainties to the measurement, the jet p_T is scaled up and down by one standard deviation of each of the components (see section 6) in the MC simulation. The resulting p_T spectra are unfolded for detector effects using the nominal unfolding matrix. The difference between the nominal unfolded cross-section and the one with the jet p_T scaled up and down is taken as a systematic uncertainty.

The uncertainty in the JER is the second largest individual source of systematic uncertainty. The effect of each of the 11 JER systematic uncertainty components is evaluated by smearing the energy of the reconstructed jets in the MC simulation such that the resolution is degraded by the size of each uncertainty component. A new transfer matrix is constructed using the smeared jets and is used to unfold the data spectra. The difference of the cross-sections unfolded with the jet-energy-smeared transfer matrix and the nominal transfer matrix is taken as a systematic uncertainty. The JER uncertainty is applied symmetrically as an upward and downward variation.

The JAR is propagated to the cross-section in the same way as for the JER.

The uncertainty associated with the residual model dependence in the unfolding procedure is described in section 7. The systematic uncertainties propagated through the

unfolding are evaluated using a set of pseudo-experiments for each component, as in the evaluation of the statistical uncertainties.

The use of pseudo-experiments for the evaluation of the systematic uncertainties allows an evaluation of the statistical fluctuations. The statistical fluctuations of the systematic uncertainties are reduced using a smoothing procedure. For each component, the p_T bins are combined until the propagated uncertainty value in the bin has a Poisson statistical significance larger than two standard deviations. A Gaussian kernel smoothing [50] is used to restore the original fine bins.

An uncertainty for the jet cleaning procedure described in section 5 is estimated from the relative difference between the efficiencies obtained from the distributions with and without the jet quality cut in data and simulation.

The uncertainty in the luminosity measurement of 1.9% [29] is propagated as being correlated across all measurement bins.

An uncertainty in the beam energy of 0.1% [63] is considered when comparing data with the theory prediction at a fixed beam energy. The induced uncertainty at the cross-section level is evaluated by comparing the theory predictions at the nominal and shifted beam energies. It amounts for 0.2% at low p_T and 1% at high p_T in the central region and rises up to 3% at highest p_T and high rapidity. This uncertainty is similar for jets with $R = 0.4$ and $R = 0.6$.

The individual systematic uncertainty sources are treated as uncorrelated with each other for the quantitative comparison of the data and the theory prediction. When shown in figures the individual uncertainties are added in quadrature to obtain the total systematic uncertainty. The shape of the systematic uncertainties follows a log-normal distribution, as in the analysis of inclusive jet production at 7 TeV [19]. The systematic uncertainties in the inclusive jet cross-section measurement are shown in figure 1 for representative rapidity regions for anti-k_t jets with $R = 0.4$ and $R = 0.6$. In the central (forward) region the total uncertainty is about 5% (10%) at medium p_T of 300–600 GeV. The uncertainty increases towards both lower and higher p_T reaching to 15% at low p_T and 50% at high p_T. The JES and JER uncertainties for jets with different sizes are rather similar at the jet level. However, at the cross-section level differences occur due to the different slopes of the distributions.

The dominant systematic uncertainty source for the measurement of the inclusive jet cross-sections is related to the jet energy measurement. The jet energy scale uncertainty is larger than the jet energy resolution uncertainty.

9 Theoretical predictions

9.1 Next-to-leading-order QCD calculation

The NLOJet++ [64] (v4.1.3) software program is used to calculate the NLO QCD predictions for the $2 \to 2$ processes for the inclusive jet cross-sections. The renormalisation and factorisation scales are set to the p_T of the leading jet in the event, i.e. $\mu_R = \mu_F = p_T^{\text{jet,max}}$. For fast and flexible calculations with various PDFs as well as different renormalisation and factorisation scales, the APPLGRID software [65] is interfaced with NLOJet++.
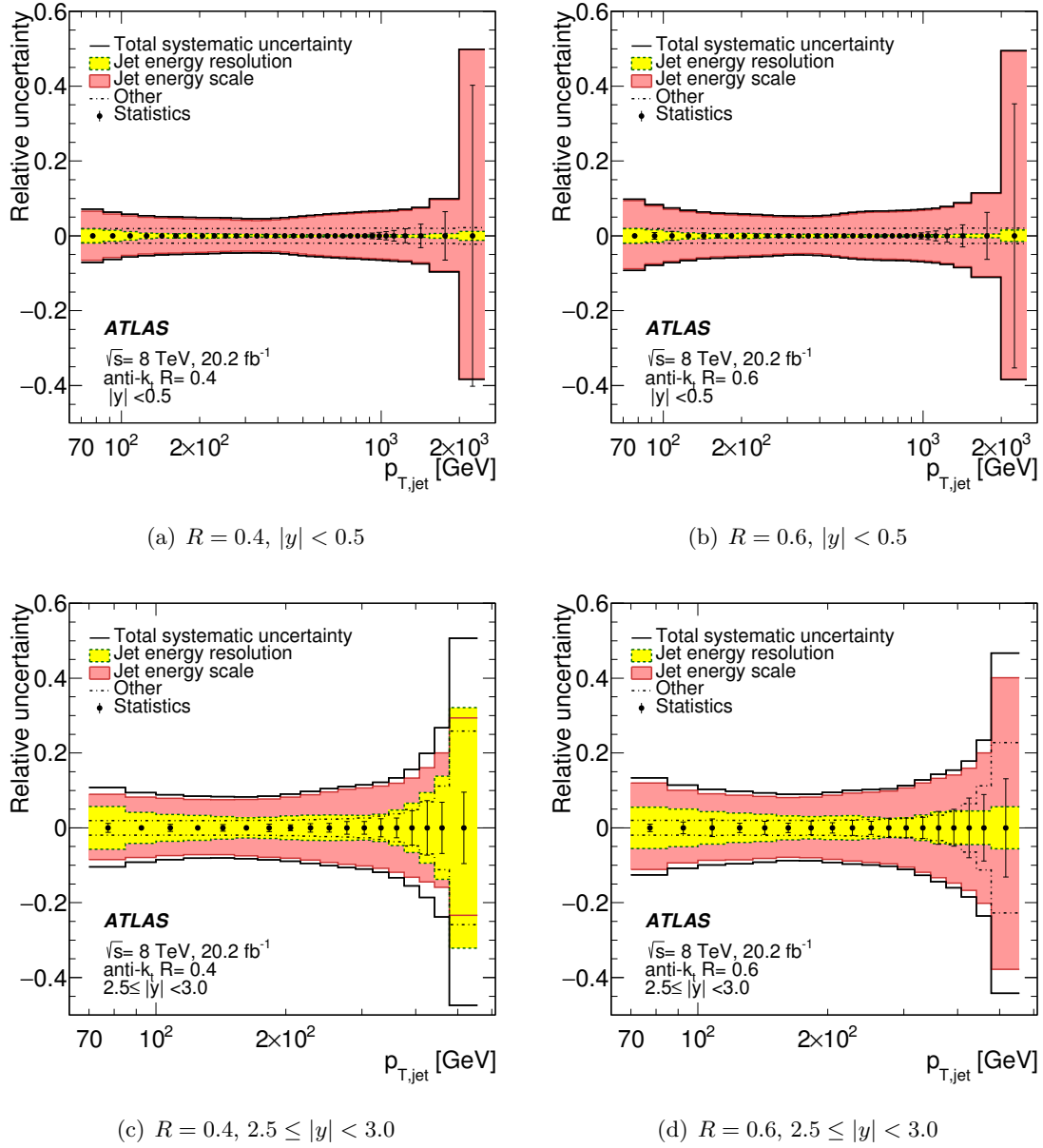
Figure 1. Relative systematic uncertainty for the inclusive jet cross-section as a function of the jet transverse momentum $p_{\text{T,jet}}$. The total systematic uncertainty is shown by the black line. The individual uncertainties are shown in colours: the jet energy scale (red), jet energy resolution (yellow) and the other uncertainties (JAR, jet selection, luminosity and unfolding bias) added in quadrature. The results are shown for the (a,b) first and (c,d) last jet rapidity bins and for anti-k_t jets with (a,c) $R = 0.4$ and (b,d) $R = 0.6$. The statistical uncertainty is shown by the vertical error bar on each point.

The inclusive jet cross-sections are presented for the CT14 [66], MMHT2014 [67], NNPDF3.0 [68], HERAPDF2.0 [69] PDF sets provided by the LHAPDF6 [70] library. The value for the strong coupling constant α_s is taken from the corresponding PDF set.

Three sources of uncertainty in the NLO QCD calculation are considered: the PDFs, the choice of renormalisation and factorisation scales, and the value of α_s. The PDF uncertainty is defined at 68% confidence level (CL) and is evaluated following the prescriptions given for each PDF set, as recommended by the PDF4LHC group for PDF-sensitive analyses [71]. The scale uncertainty is evaluated by varying the renormalisation and factorisation scales by a factor of two with respect to the original choice in the calculation. The envelope of the cross-sections with all possible combinations of the scale variations, except the ones when the two scales are varied in opposite directions, is considered as a systematic uncertainty. An alternative scale choice, $\mu_R = \mu_F = p_T^{\rm jet}$, the p_T of each individual jet that enters the cross-section calculation, is also considered. This scale choice is proposed in ref. [72]. The difference with respect to the prediction obtained for the $p_T^{\rm jet,max}$ scale choice is treated as an additional uncertainty. The uncertainty from α_s is evaluated by calculating the cross-sections using two PDF sets determined with two different values of α_s and then scaling the cross-section difference corresponding to an α_s uncertainty $\Delta\alpha_s = 0.0015$ as recommended in ref. [71].

The uncertainties in the NLO QCD cross-section predictions obtained with the CT14 PDF set are shown in figure 2 for representative phase-space regions. The renormalisation and factorisation scale uncertainty is the dominant uncertainty in most phase-space regions, rising from around $5-10\%$ at low p_T in the central rapidity bin to about 50% in the highest p_T bins in the most forward rapidity region. This uncertainty is asymmetric and it is larger for anti-k_t jets with $R = 0.6$ than for jets with $R = 0.4$. The alternative scale choice, $p_T^{\rm jet}$, leads to a similar inclusive jet cross-section at the highest jet p_T, but gives an increasingly higher cross-section when the jet p_T decreases. For $p_T = 70\,{\rm GeV}$ this difference is about 10%. The PDF uncertainties vary from 5% to 50% depending on the jet p_T and rapidity. The α_s uncertainty is about 3% and is rather constant in the considered phase-space regions.

9.2   Electroweak corrections

The NLO QCD predictions are corrected for electroweak effects derived using an NLO calculation in the electroweak coupling (α) and based on a LO QCD calculation [73]. The CTEQ6L1 PDF set is used [74]. This calculation includes tree-level effects on the cross-section of $O(\alpha\alpha_S, \alpha^2)$ as well as effects of loops of weak interactions at $O(\alpha\alpha_s^2)$. Effects of photon or W/Z radiation are not included in the corrections. Real W/Z radiation may affect the cross-section by a few percent at $p_T \sim 1\,{\rm TeV}$ [75].

The correction factors were derived in the phase space considered for the measurement presented here and are provided by the authors of ref. [73] through a private communication. No uncertainty associated with these corrections is presently estimated.

Figure 3 shows the electroweak corrections for jets with $R = 0.4$ and $R = 0.6$. The correction reaches more than 10% for the highest p_T in the lowest rapidity bin, but decreases rapidly as the rapidity increases. It is less than 3% for jets with $|y| > 1$.

9.3   Non-perturbative corrections

In order to compare the fixed-order NLO QCD calculations to the measured inclusive jet cross-sections, corrections for non-perturbative (NP) effects need to be applied. Each
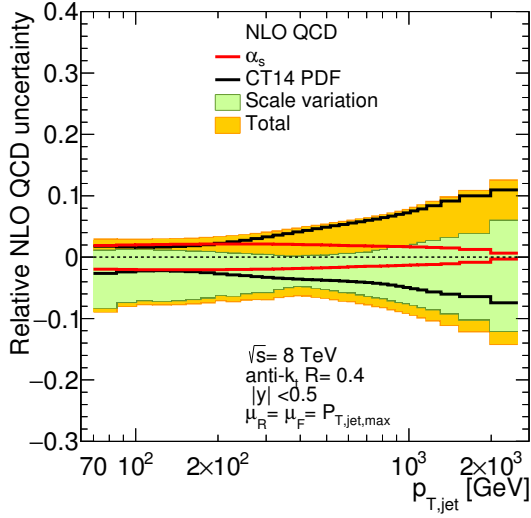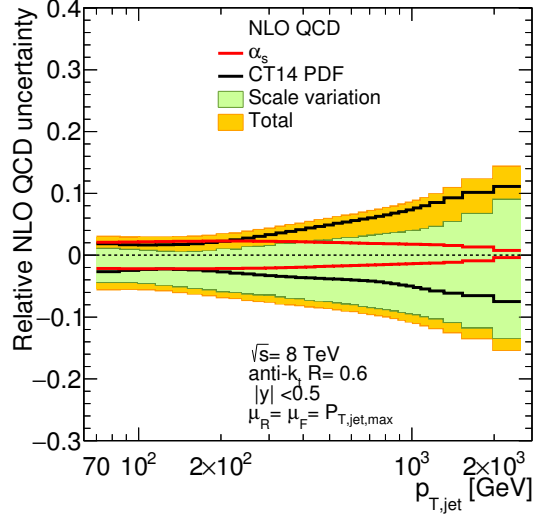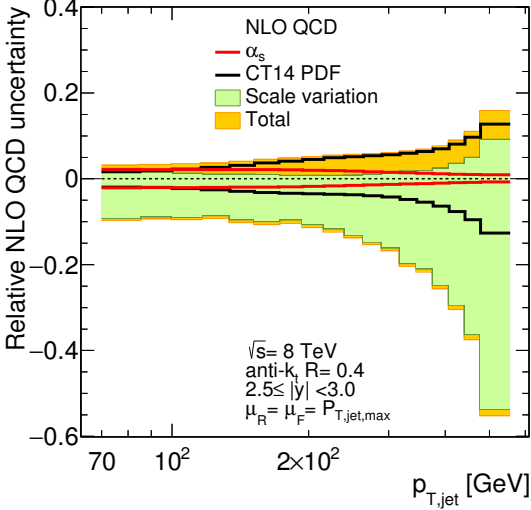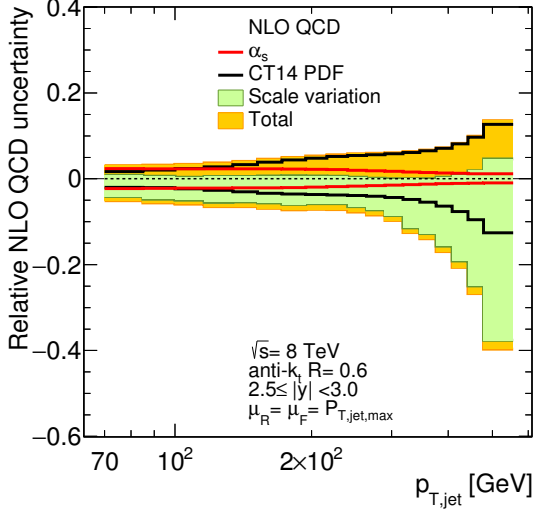
Figure 2. Relative NLO QCD uncertainties for the inclusive jet cross-section calculated for the CT14 PDF set in the (a,b) central and (c,d) forward region for anti-k_t jets with (a,c) $R = 0.4$ and (b,d) $R = 0.6$. Shown are the uncertainties due to the renormalisation and factorisation scales, the α_s, the PDF and the total uncertainty. The default scale choice $p_\mathrm{T}^{\mathrm{jet,max}}$ is used.

bin of the NLO QCD cross-section is multiplied by the corresponding correction for non-perturbative effects.

The corrections are derived using LO Monte Carlo event generators complemented by the leading-logarithmic parton shower by evaluating the bin-wise ratio of the cross-section with and without the hadronisation and the underlying event processes.

(a) $R = 0.4$ (b) $R = 0.6$
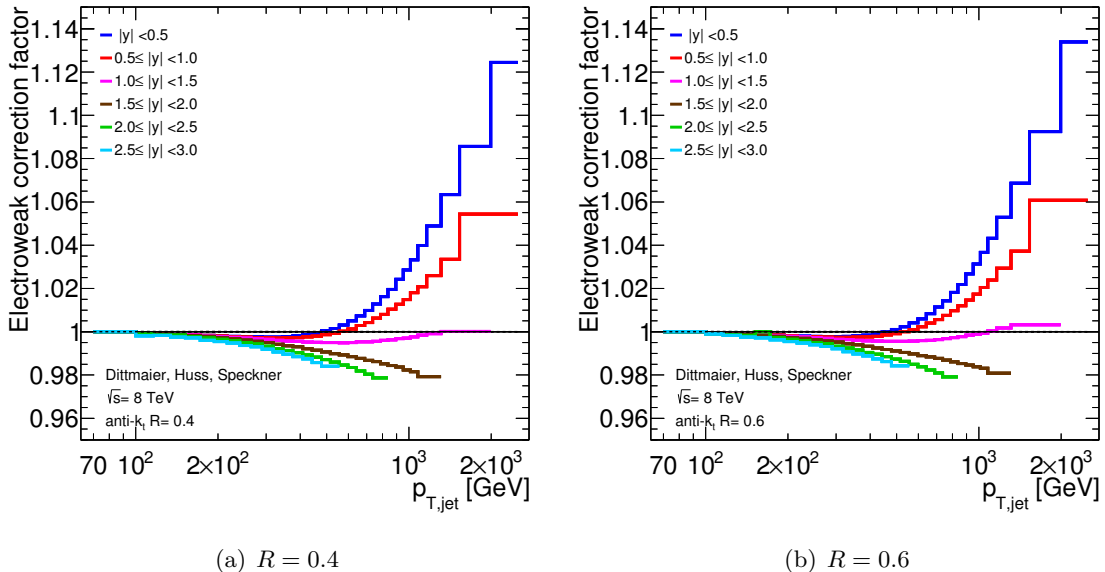
Figure 3. Electroweak correction factors for the inclusive jet cross-section as a function of the jet p_{T} for all jet rapidity bins for anti-k_t jets with (a) $R = 0.4$ and (b) $R = 0.6$.

The MC event generators are run twice, once with the hadronisation and underlying event switched on and again with these two processes switched off. The inclusive jet cross-sections are built either from the stable particles or from the last partons in the event record, i.e. the partons after the parton showers finished and before the hadronisation process starts. These partons are the ones that are used in the Lund string model and the cluster fragmentation model to form the final-state hadrons. The bin-by-bin ratios of the inclusive jet cross-sections are taken as an estimate for the non-perturbative corrections.

The nominal correction is obtained from the Pythia 8 event generator [30] with the AU2 tune using the CT10 PDF [35], i.e. the same configuration as used to correct the data for detector effects (see section 3). The uncertainty is estimated as the envelope of the corrections obtained from a series of alternative Monte Carlo event generator configurations as shown in table 1.

The correction factors are shown in figure 4 in representative rapidity bins for anti-k_t jets with $R = 0.4$ and $R = 0.6$ as a function of the jet p_{T}.

The nominal correction increases the cross-section by 4% (15%) for $p_{\mathrm{T}} = 70\,\mathrm{GeV}$ for anti-k_t jets with $R = 0.4$ ($R = 0.6$). The large differences between the two jet sizes result from the different interplay of hadronisation and underlying-event effects. While for anti-k_t jets with $R = 0.4$ the contribution from the hadronisation tends to cancel with the one from the underlying event, for anti-k_t jets with $R = 0.6$ the effect from the underlying event becomes dominant. At large p_{T} the non-perturbative correction factor is close to 1. There is only a small dependence of the non-perturbative corrections on the jet rapidity.

Generator	Tune	PDF
Pythia 8	4C [78]	CTEQ6L [74]
	Monash [76]	NNPDF2.3L [79, 80]
	AU2 [34]	CT10 [35]
	AU2 [34]	CTEQ6L [74]
	A14 [77]	NNPDF2.3L [79, 80]
	A14 [77]	MRSTW2008lo** [81]
	A14 [77]	CTEQ6L [74]
Herwig++	UE-EE-5 [82, 83]	CTEQ6L [74]
	UE-EE-5 [82, 83]	MRSTW2008lo** [81]
	UE-EE-4 [82, 83]	CTEQ6L [74]

Table 1. Summary of Monte Carlo generator configurations used for the evaluation of the non-perturbative corrections. The name of the generator and the soft physics model tune as well as the PDF set used when deriving the tune is specified.

The nominal correction is larger than the correction from other MC configurations. The corrections based on Pythia 8 with the Monash [76] or the A14 [77] tunes give correction factors that are closer to 1. The corrections based on Herwig++ give corrections that are much lower than the one based on Pythia 8. The correction based on Herwig++ is -10% (1%) for $p_\mathrm{T} = 70\,\mathrm{GeV}$ for anti-k_t jets with $R = 0.4$ ($R = 0.6$).

9.4 NLO QCD matched with parton showers and hadronisation

The measured inclusive jet cross-section can be directly compared to predictions based on the Powheg Monte Carlo generator where an NLO QCD calculation for the hard scattering $2 \rightarrow 2$ process is matched to parton showers, hadronisation and underlying event.

A procedure to estimate the effect of the matching of the hard scattering and the parton shower is not yet well established. Therefore, no uncertainties are shown for the Powheg predictions. The Powheg prediction's uncertainty due to PDF is expected to be similar to that in fixed-order NLO calculations, whereas the uncertainty due to α_s is expected to be larger, and the uncertainty due to the renormalisation and factorisation scales smaller.

The simulation using a matched parton shower has a more coherent treatment of the effect of parton showers and hadronisation than the approach using a fixed-order NLO QCD calculation corrected for non-perturbative effects. However, ambiguities in the matching procedure and the tuning of the parton shower parameters based on processes simulated only at leading order by Pythia 8 may introduce additional theoretical uncertainties. Therefore, quantitative comparisons using theoretical uncertainties based on Powheg are not performed in this paper.

(a) $R = 0.4$, $|y| < 0.5$

(b) $R = 0.6$, $|y| < 0.5$

(c) $R = 0.4$, $2.5 \leq |y| < 3.0$

(d) $R = 0.6$, $2.5 \leq |y| < 3.0$
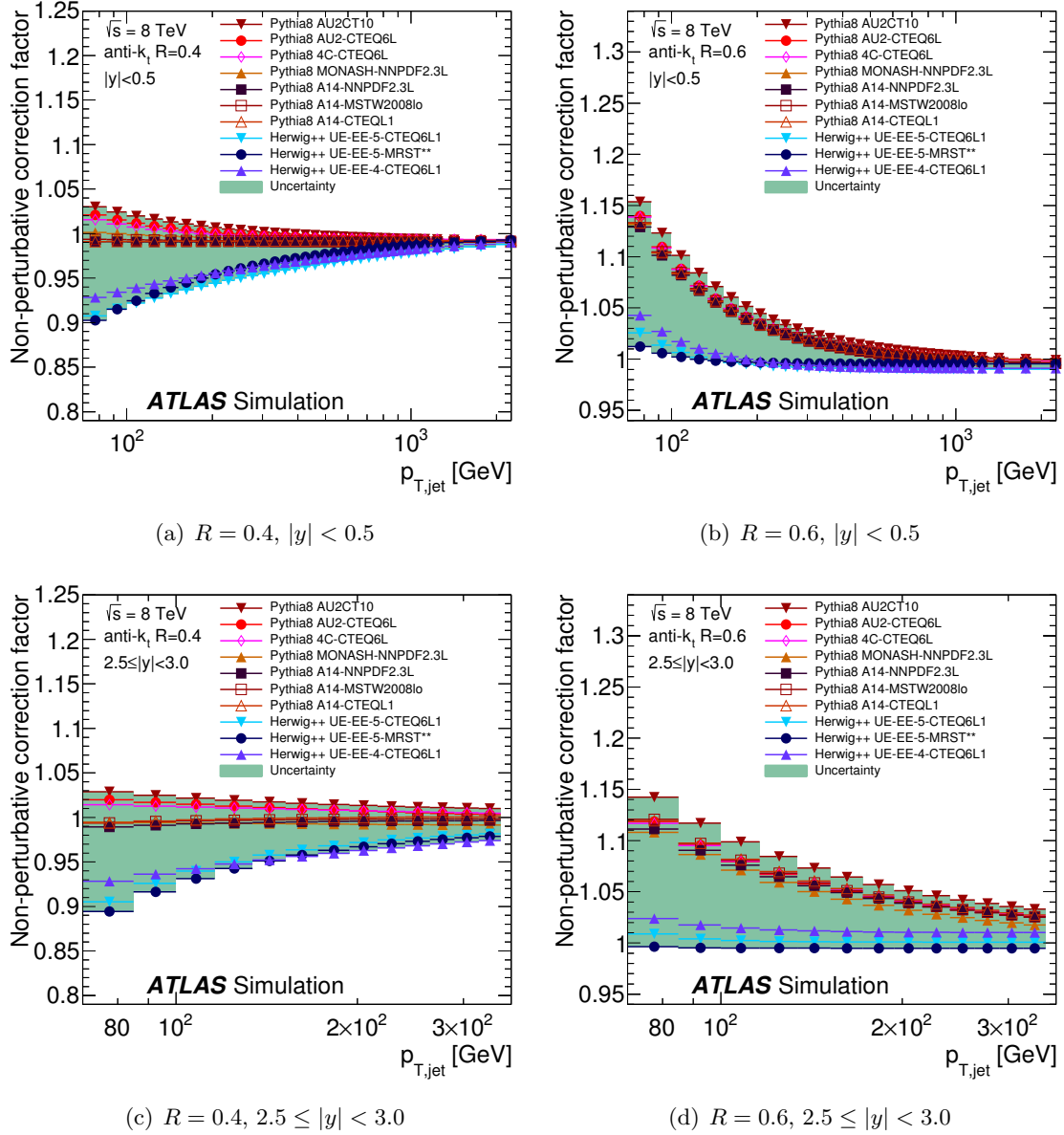
Figure 4. Non-perturbative correction factors as a function of jet p_{T} for (a,b) the most central and (c,d) most forward region, for jets defined by the anti-k_t algorithm with (a,c) $R = 0.4$ and (b,d) $R = 0.6$. The corrections are derived using Pythia 8 and Herwig++ with several soft physics tunes. The envelope of all MC configuration variations is shown as a band.

10 Results

10.1 Qualitative comparisons of data to NLO QCD calculations

The measured double-differential inclusive jet cross-sections are shown in figure 5 and figure 6 as a function of the jet p_{T} for anti-k_t jets with $R = 0.4$ and $R = 0.6$ for each jet rapidity bin. The cross-section covers 11 orders of magnitude in the central rapidity region and 9 orders of magnitude in the forward region. Jet transverse momenta above $p_{\mathrm{T}} = 2\,\mathrm{TeV}$
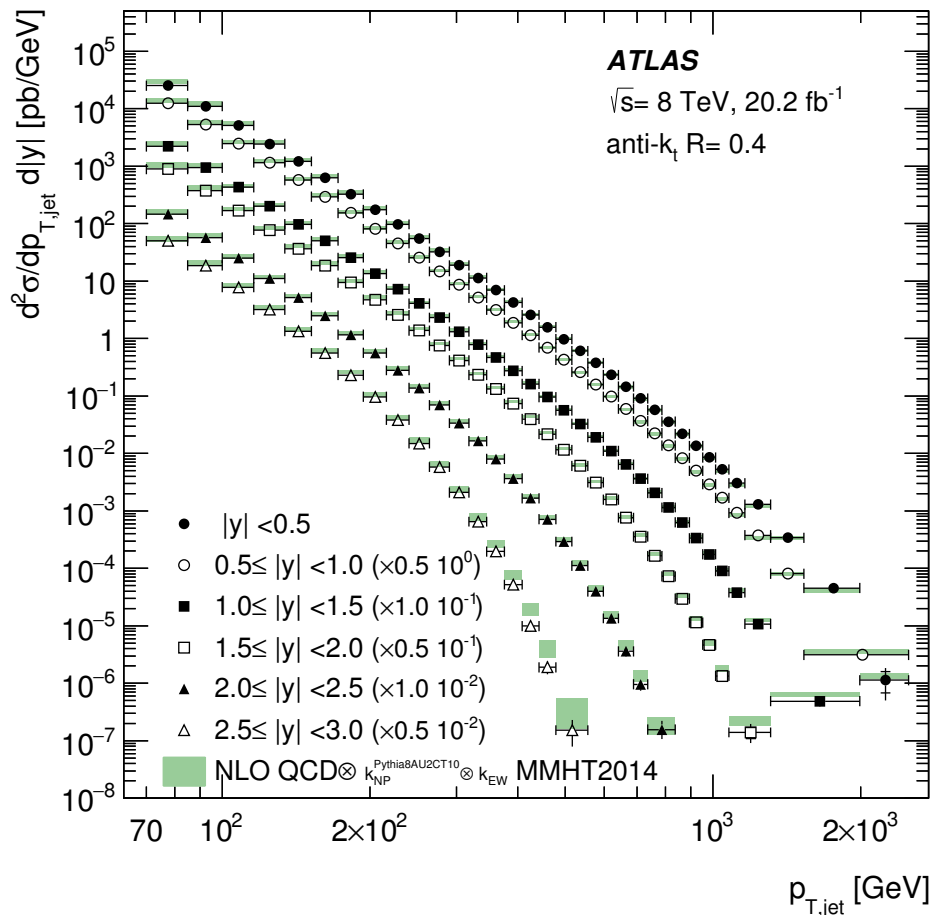
Figure 5. Inclusive jet cross-section as a function of jet p_T in bins of jet rapidity. The results are shown for jets identified using the anti-k_t algorithm with $R = 0.4$. For better visibility the cross-sections are multiplied by the factors indicated in the legend. The data are compared to the NLO QCD prediction with the MMHT2014 PDF set corrected for non-perturbative and electroweak effects. The error bars indicate the statistical uncertainty and the systematic uncertainty in the measurement added in quadrature. The statistical uncertainty is shown separately by the inner vertical line.

are observed. In the most forward region the jet p_T reaches about 500 GeV. Tabulated values of all observed results, with full details of uncertainties and their correlations, are also provided in the Durham HEP database [84].

The measurement is compared to an NLO QCD prediction using the MMHT2014 PDF set [67] based on NLOJet++ corrected for non-perturbative and electroweak effects. The shaded band shows the total theory uncertainty as explained in section 9.1. This theory prediction describes the gross features in the data.

The ratio of NLO QCD calculations to data corrected for non-perturbative and electroweak effects for various PDF sets is shown in figure 7 and figure 8 for anti-k_t jets $R = 0.4$ and $R = 0.6$, respectively. At low p_T the level of agreement is very sensitive to
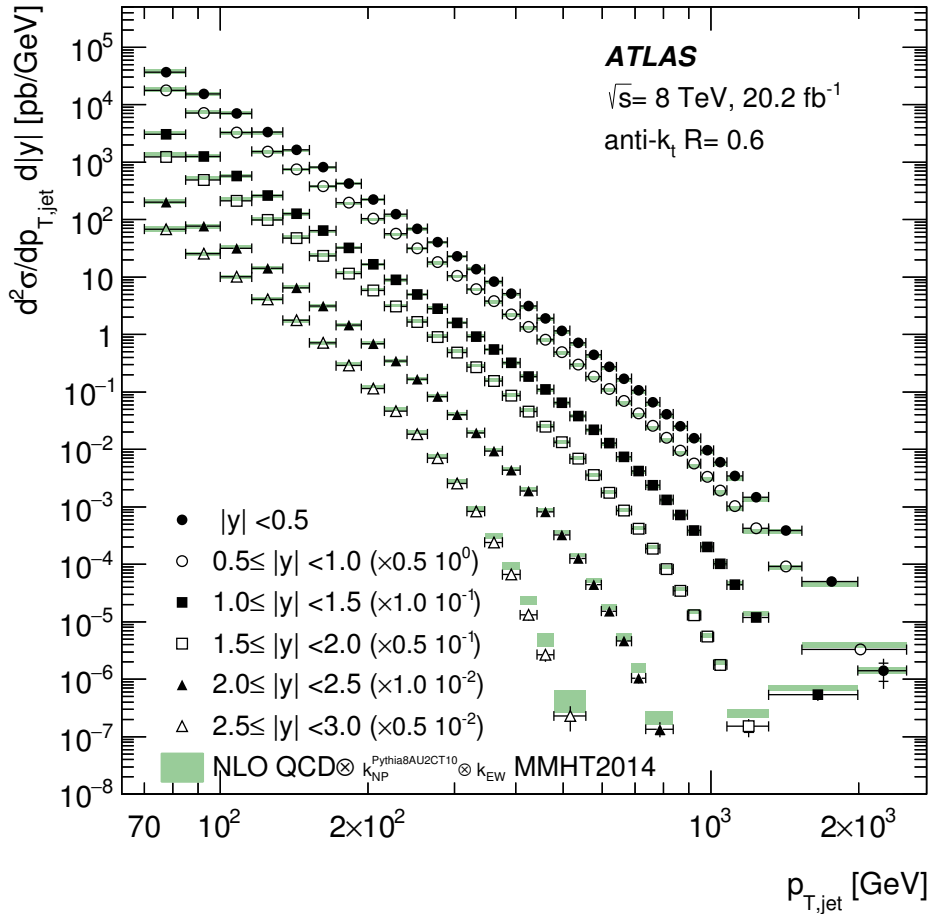
Figure 6. Inclusive jet cross-section as a function of jet p_T in bins of jet rapidity. The results are shown for jets identified using the anti-k_t algorithm with $R = 0.6$. For better visibility the cross-sections are multiplied by the factors indicated in the legend. The data are compared to the NLO QCD prediction with the MMHT2014 PDF set corrected for non-perturbative and electroweak effects. The error bars indicate the statistical uncertainty and the systematic uncertainty in the measurement added in quadrature. The statistical uncertainty is shown separately by the inner vertical line.

non-perturbative effects. When using Pythia 8 as the nominal non-perturbative correction, the NLO QCD prediction is typically about 10–20% above the data at low p_T, whereas the NLO QCD prediction corrected with Herwig++ follows the data well for anti-k_t jets with $R = 0.4$, while it is 5–10% below the data for anti-k_t jets with $R = 0.6$.

The comparison is also influenced by the nominal choice of renormalisation and factorisation scales in the NLO QCD calculation. Setting the scale to p_T^{jet} instead of $p_T^{jet,max}$ (see section 9.1) leads to an NLO QCD prediction that is at low jet p_T higher than the prediction using the $p_T^{jet,max}$ scale (about 8% at $p_T = 100\,\text{GeV}$ for all pseudorapidity regions). With this scale setting the deviation from the data at low p_T is larger.
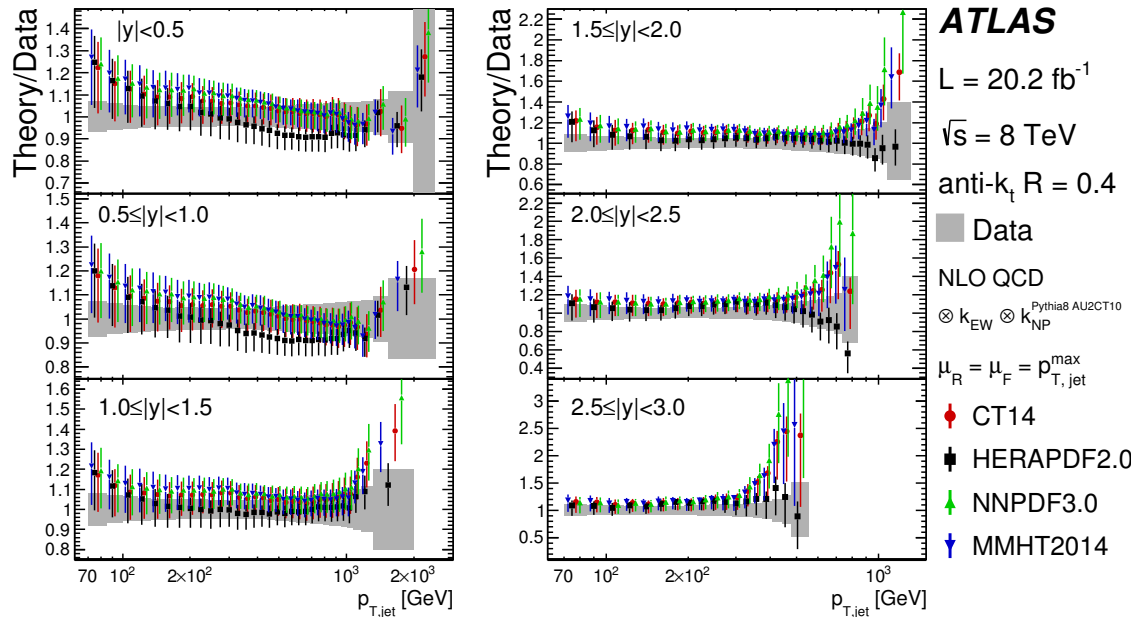
Figure 7. Ratio of the inclusive jet cross-section predicted by NLO QCD corrected for non-perturbative and electroweak effects to the cross-section in data as a function of the jet p_T in each jet rapidity bin. Shown are the predictions for various PDF sets for anti-k_t jets with $R = 0.4$. The points are offset in jet p_T for better visibility. The error bars indicate the total theory uncertainty. The grey band shows the total uncertainty in the measurement.

The recent calculation of NNLO QCD inclusive jet cross-sections at $\sqrt{s} = 7\,\text{TeV}$ is higher than in NLO QCD at low jet p_T for all jet rapidity regions [12]. For instance, for $p_T = 100\,\text{GeV}$ the increase from NLO to NNLO is about 10%. For both the NNLO and the NLO QCD calculations the $p_T^{\text{jet,max}}$ scale is used. Therefore, it is expected that the NNLO QCD prediction at $\sqrt{s} = 8\,\text{TeV}$ would deviate from the data more strongly than the NLO QCD calculation. This deviation might need to be accommodated by an adjustment of the PDFs.

Towards higher p_T the NLO QCD predictions get closer to the data while for $p_T > 1\,\text{TeV}$ they rise with respect to the data. For the highest p_T at central rapidities they are typically up to 10–20% higher than data. The behaviour of the CT14, NNPDF3.0 and MMHT2014 PDF sets is similar. The NLO QCD predictions based on the HERA-PDF2.0, however, are significantly lower than data in the region $300 < p_T < 1000\,\text{GeV}$.

In the most forward region, $|y| > 2$, all PDF sets give predictions close to the data at low p_T for anti-k_t jets with $R = 0.4$ and $R = 0.6$. However, towards higher p_T and in particular for $p_T > 400\,\text{GeV}$ the CT14, NNPDF3.0 and MMHT2014 PDF sets give predictions much higher than the data. The prediction for the HERAPDF2.0 is lower than for the other PDF sets and also falls below the data. In this region, both the experimental and the theoretical uncertainties become large.

Overall, the NLO QCD prediction based on the CT14 PDF set gives the best qualitative agreement, while HERAPDF2.0 gives the worst agreement over a wide jet p_T range.
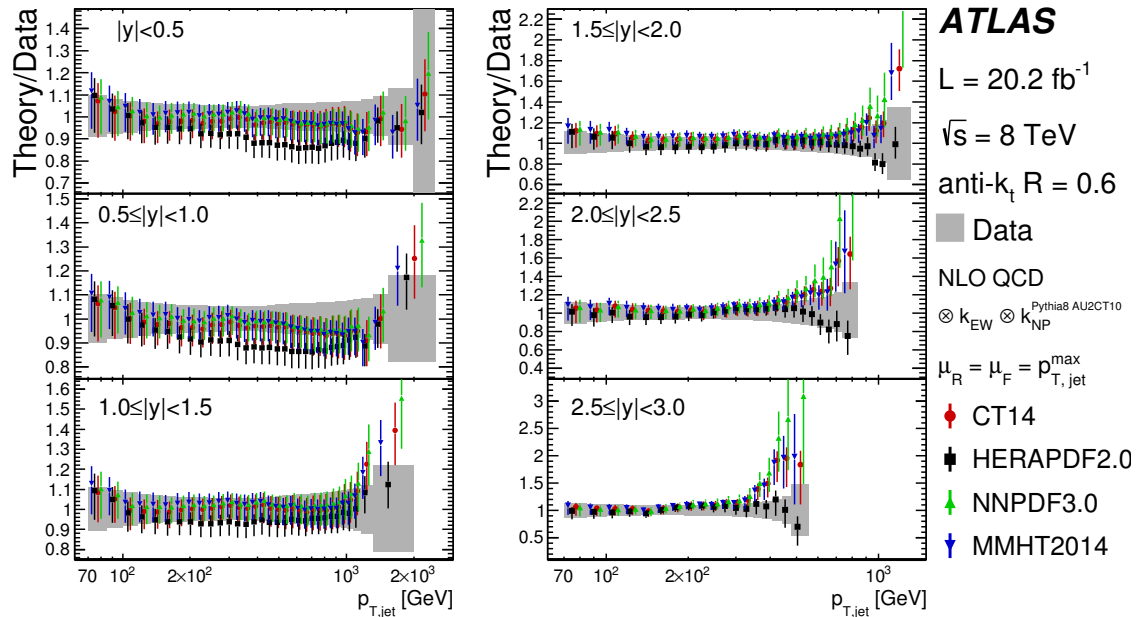
Figure 8. Ratio of the inclusive jet cross-section predicted by NLO QCD corrected for non-perturbative and electroweak effects to the cross-section in data as a function of the jet p_T in each jet rapidity bin. Shown are the predictions for various PDF sets for anti-k_t jets with $R = 0.6$. The points are offset in jet p_T for better visibility. The error bars indicate the total theory uncertainty. The grey band shows the total uncertainty in the measurement.

However, the central values from the HERAPDF2.0 PDF set are more consistent with the data in the forward region at high p_T. This indicates that this measurement has sensitivity to constrain PDFs.

10.2 Quantitative comparison of data to NLO QCD calculations

A quantitative comparison of the NLO QCD predictions, corrected for non-perturbative and electroweak effects, to the measurement is performed using the method described in ref. [85]. The χ^2 value and the corresponding observed p-value, P_{obs}, are computed taking into account the asymmetries and the correlations of the experimental and theoretical uncertainties. The individual experimental and theoretical uncertainty components are assumed to be uncorrelated among one another and fully correlated across the p_T and y bins. The correlation of the statistical uncertainties across p_T and rapidity bins are taken into account using covariance matrices derived from 10000 pseudo-experiments obtained by fluctuating the data and the MC simulation (see section 7).

For the theoretical prediction, the uncertainties related to the scale variations, the alternative scale choice, the PDF eigenvectors, the non-perturbative corrections and the strong coupling constant are treated as separate uncertainty components. In the case of the NNPDF3.0 PDF set, the replicas are used to evaluate a covariance matrix, from which the eigenvectors are then determined.

Table 2 shows the evaluated P_{obs} for the NLO QCD predictions corrected for non-perturbative and electroweak effects for each rapidity bin considered individually. In this

Rapidity ranges	P_{obs}			
	CT14	MMHT2014	NNPDF3.0	HERAPDF2.0
Anti-k_t jets $R = 0.4$				
$|y| < 0.5$	44%	28%	25%	16%
$0.5 \leq |y| < 1.0$	43%	29%	18%	18%
$1.0 \leq |y| < 1.5$	44%	47%	46%	69%
$1.5 \leq |y| < 2.0$	3.7%	4.6%	7.7%	7.0%
$2.0 \leq |y| < 2.5$	92%	89%	89%	35%
$2.5 \leq |y| < 3.0$	4.5%	6.2%	16%	9.6%
Anti-k_t jets $R = 0.6$				
$|y| < 0.5$	6.7%	4.9%	4.6%	1.1%
$0.5 \leq |y| < 1.0$	1.3%	0.7%	0.4%	0.2%
$1.0 \leq |y| < 1.5$	30%	33%	47%	67%
$1.5 \leq |y| < 2.0$	12%	16%	15%	3.1%
$2.0 \leq |y| < 2.5$	94%	94%	91%	38%
$2.5 \leq |y| < 3.0$	13%	15%	20%	8.6%

Table 2. Observed P_{obs} values evaluated for the NLO QCD predictions corrected for non-perturbative and electroweak effects and the measured inclusive jet cross-section of anti-k_t jets with $R = 0.4$ and $R = 0.6$. Only measurements with $p_T > 100\,\text{GeV}$ are included. The predictions are evaluated for various PDF sets. The default scale choice $p_T^{\text{jet,max}}$ is used.

case, only cross-section measurements with $p_T > 100\,\text{GeV}$ are included in the quantitative comparison of data and theory to reduce the influence of non-perturbative corrections.

For anti-k_t jets with $R = 0.4$, P_{obs} values larger than about 4% are found for all cross-sections and PDF sets. This indicates a satisfactory description of the data by the theory. The lowest P_{obs} values are found in the jet rapidity region $1.5 \leq |y| < 2.0$ and $2.5 \leq |y| < 3.0$. For anti-k_t jets with $R = 0.6$ good agreement is found in the regions with $|y| > 1$. Here, the P_{obs} values are larger than about 10%. However, in the central region $|y| < 1$ the agreement is worse than for jets with $R = 0.4$ resulting in P_{obs} values of the order of a percent or lower.

Similar studies were performed, for each rapidity bin, in various p_T ranges: $p_T > 70\,\text{GeV}$, $100 < p_T < 900\,\text{GeV}$, $100 < p_T < 400\,\text{GeV}$. In all these cases, a similar level of agreement is observed between the measurement and the theory prediction, with a general trend of P_{obs} values decreasing with the increasing number of bins (i.e. when considering wider phase-space regions).

In addition to the quantitative comparisons of the theory and data cross-sections in individual jet rapidity bins, all data points can be considered together. Table 3 shows the χ^2 values for each PDF set, R value and scale choice, when using all the $|y|$ bins together. Various p_T ranges are tested. All the corresponding P_{obs} are much smaller than 10^{-3}. If the statistical uncertainty of the η-intercalibration were treated as a single component (see section 6), the χ^2 values computed in table 3 would be strongly enhanced (by even more than 200 units for some configurations).

χ^2/ndf	$p_{\mathrm{T}}^{\mathrm{jet,max}}$		$p_{\mathrm{T}}^{\mathrm{jet}}$	
	$R = 0.4$	$R = 0.6$	$R = 0.4$	$R = 0.6$
$p_{\mathrm{T}} > 70\,\mathrm{GeV}$				
CT14	349/171	398/171	340/171	392/171
HERAPDF2.0	415/171	424/171	405/171	418/171
NNPDF3.0	351/171	393/171	350/171	393/171
MMHT2014	356/171	400/171	354/171	399/171
$p_{\mathrm{T}} > 100\,\mathrm{GeV}$				
CT14	321/159	360/159	313/159	356/159
HERAPDF2.0	385/159	374/159	377/159	370/159
NNPDF3.0	333/159	356/159	331/159	356/159
MMHT2014	335/159	364/159	333/159	362/159
$100 < p_{\mathrm{T}} < 900\,\mathrm{GeV}$				
CT14	272/134	306/134	262/134	301/134
HERAPDF2.0	350/134	331/134	340/134	326/134
NNPDF3.0	289/134	300/134	285/134	299/134
MMHT2014	292/134	311/134	284/134	308/134
$100 < p_{\mathrm{T}} < 400\,\mathrm{GeV}$				
CT14	128/72	149/72	118/72	145/72
HERAPDF2.0	148/72	175/72	141/72	170/72
NNPDF3.0	119/72	141/72	115/72	139/72
MMHT2014	132/72	143/72	122/72	140/72

Table 3. Summary of χ^2/ndf obtained from the comparison of the inclusive jet cross-section and the NLO QCD prediction for various PDF sets and scale choices for anti-k_t jets with $R = 0.4$ and $R = 0.6$, for several p_{T} cuts, using all $|y|$ bins. All the corresponding p-values are $\ll 10^{-3}$.

Further quantitative comparisons using all the $|y|$ bins together were performed in more restricted p_{T} ranges ($70 < p_{\mathrm{T}} < 100\,\mathrm{GeV}$, $100 < p_{\mathrm{T}} < 240\,\mathrm{GeV}$, $240 < p_{\mathrm{T}} < 408\,\mathrm{GeV}$, $408 < p_{\mathrm{T}} < 642\,\mathrm{GeV}$, $642 < p_{\mathrm{T}} < 952\,\mathrm{GeV}$ and $p_{\mathrm{T}} > 952\,\mathrm{GeV}$), for the CT14 PDF set. While good agreement is observed in the range $70 < p_{\mathrm{T}} < 100\,\mathrm{GeV}$, for both jet radii R values, the P_{obs} values for the other ranges are small (often below 0.1%). For the same five restricted p_{T} ranges above $100\,\mathrm{GeV}$, considering this time pairs of consecutive $|y|$ bins, good agreement between data and theory is observed in most cases. Good agreement is also observed when considering pairs of one central and one forward (i.e. first-last) $|y|$ bins. These tests show that the source of the low P_{obs} values discussed above is not localised in a single rapidity bin, nor due to some possible tension between the central and the forward regions.

Since the difference between the non-perturbative corrections with two Monte Carlo generators is taken as a systematic uncertainty, the result of the quantitative comparison has little sensitivity to which correction is chosen as the nominal one. Even using the correction that brings the fixed-order NLO QCD to the Powheg prediction, i.e. including an additional correction for parton shower effects, does not alter the P_{obs} values. It is therefore expected that an explicit correction of parton shower effects as suggested in

ref. [86] has a similar effect. The quantitative comparison is also not very sensitive to the choice of nominal renormalisation and factorisation scales in the NLO calculations.

A set of χ^2 values were also evaluated for the ABM11 PDF set [87], for $R = 0.4$ and $R = 0.6$, for the $p_T^{\text{jet,max}}$ and p_T^{jet} scale choices, in the full p_T range, for individual $|y|$ bins, as well as all the $|y|$ bins together. In this case, tension between data and the theory prediction is observed even in individual $|y|$ bins, with P_{obs} values below 10^{-3} for both $|y| < 0.5$ and $0.5 \leq |y| < 1.0$. When using all the $|y|$ bins together, the χ^2 is significantly larger than for other PDF sets, by up to 152–232 units compared to the results obtained for CT14.

10.3 Quantitative comparison of data to NLO QCD calculations with alternative correlation scenarios

Considering all data points together requires a good understanding of the correlations of the experimental and theoretical systematic uncertainties in jet p_T and rapidity. In the ATLAS JES uncertainty correlation model [50, 51, 56] the correlations of most uncertainties in the jet energy measurement are generally well known.

Where this is not the case, alternative correlation scenarios are provided alongside the default scenario: the "weaker" correlation scenario proposed in ref. [56] was tested, and found to yield χ^2 reductions by up to about 12 units for some phase-space regions.

Correlations of the uncertainties that are based on simple comparisons between two options (two-point systematic uncertainties), e.g. systematic uncertainties due to differences between the fragmentation models in Pythia [30] and Herwig++ [39], are not well defined and therefore different levels of correlations can in principle be used. Concerning the theoretical prediction, the correlations are not well defined for the uncertainty related to the scale variations, the uncertainty related to the alternative scale choice and the uncertainty due to the non-perturbative corrections. For this reason, this analysis investigated in detail the impact of alternative correlation scenarios for the largest sources of two-point experimental uncertainties, as well as for the theoretical uncertainties.

The impact of fully decorrelating (in both p_T and $|y|$) any of those two-point systematic uncertainties was checked. Potentially important effects are observed when fully decorrelating the uncertainty due to the response difference between quark- and gluon-induced jets (JES Flavour Response), the jet fragmentation uncertainty in the multijet balance (JES MJB Fragmentation) and the uncertainty in the density of pile-up activity in a given event (ρ) (JES Pile-up Rho topology) (see ref. [56] for more details). However, even if the exact correlations are not known, one must keep in mind that this potential χ^2 reduction is far too optimistic, since some non-negligible level of correlation, in both p_T and $|y|$, is expected for these uncertainties. This motivated some tests using more realistic decorrelation models for these uncertainties. These experimental systematic uncertainties are split into sub-components whose size varies with jet rapidity and p_T. While the sub-components are independent of each other, each of them is fully correlated between different phase-space regions and their sum in quadrature equals the original uncertainty. A series of 18 different splitting options into two or three sub-components, with various smooth p_T and $|y|$ dependences, were studied for both $R = 0.4$ and $R = 0.6$, using the CT14 PDF set and the

$p_{\mathrm{T}}^{\mathrm{jet,max}}$ scale choice. While many of these decorrelation options have little impact on the χ^2, some of them induce a χ^2 reduction by up to 33 units. When applying various splitting options (the ones yielding the largest χ^2 reductions when splitting one single component) to the JES Flavour Response, JES MJB Fragmentation and JES Pile-up Rho topology uncertainties simultaneously, the χ^2 is reduced by up to 51 units compared to the nominal JES configuration. For all these variations of the correlations, the corresponding P_{obs} values are $\ll 10^{-3}$.

For the theoretical uncertainties, in addition to the 18 options discussed above, 3 other splitting options based on the ones discussed in ref. [88] were tested. These additional options consist in splitting a given uncertainty component into six sub-components. Many of these decorrelation options have little impact on the χ^2, but some of them induce a χ^2 reduction by up to 60 units. Still, all the corresponding P_{obs} values are $\ll 10^{-3}$. When applying various splitting options (the ones yielding the largest χ^2 reductions when splitting one single component) to the scale variations, the alternative scale choice and the non-perturbative corrections uncertainties simultaneously, the χ^2 is reduced by up to 87 units compared to the nominal configuration, but the corresponding P_{obs} values are still $\ll 10^{-3}$.

The various splitting options yielding the largest χ^2 reductions when splitting either the experimental or the theoretical uncertainties were applied to both the experimental (JES Flavour Response, the JES MJB Fragmentation, JES Pile-up Rho topology) and theoretical uncertainties (the scale variations, the alternative scale choice and the non-perturbative corrections uncertainties) simultaneously. In this case the χ^2 evaluated for CT14 is reduced by up to 96 units compared to the nominal configuration, but the corresponding P_{obs} values are still below 10^{-3}. Similar reductions of the χ^2 values are observed for NNPDF3.0.

In summary, all the tested JES uncertainty decorrelation scenarios that could be judged as justifiable from the performance point of view yield small P_{obs} values. The same is true when using similar decorrelation scenarios for the theoretical uncertainties. When decorrelating the JES uncertainty components and the theoretical uncertainties simultaneously, values of χ^2/ndf down to $256/159$ are obtained. Furthermore, it should be noted that for the experimental and theoretical systematic uncertainties that are based on simple comparisons between two options (e.g. the renormalisation and factorisation scale uncertainties), even the notion of a standard deviation (i.e. the size of the uncertainty itself) in different phase-space regions is not well defined. Since, in addition to the correlations, the phase-space dependence of the size of the uncertainties is a key ingredient in the χ^2 evaluation, this second aspect may also explain part of the observed tension between the measurement and the theory.

10.4 Comparisons with NLO QCD calculation including parton showers and fragmentation

The comparisons of the Powheg predictions with the measurement for jets with $R = 0.4$ and $R = 0.6$ are shown in figure 9 and figure 10 as a function of the jet p_{T} in bins of the jet rapidity. The measurements are also compared to the NLO QCD prediction
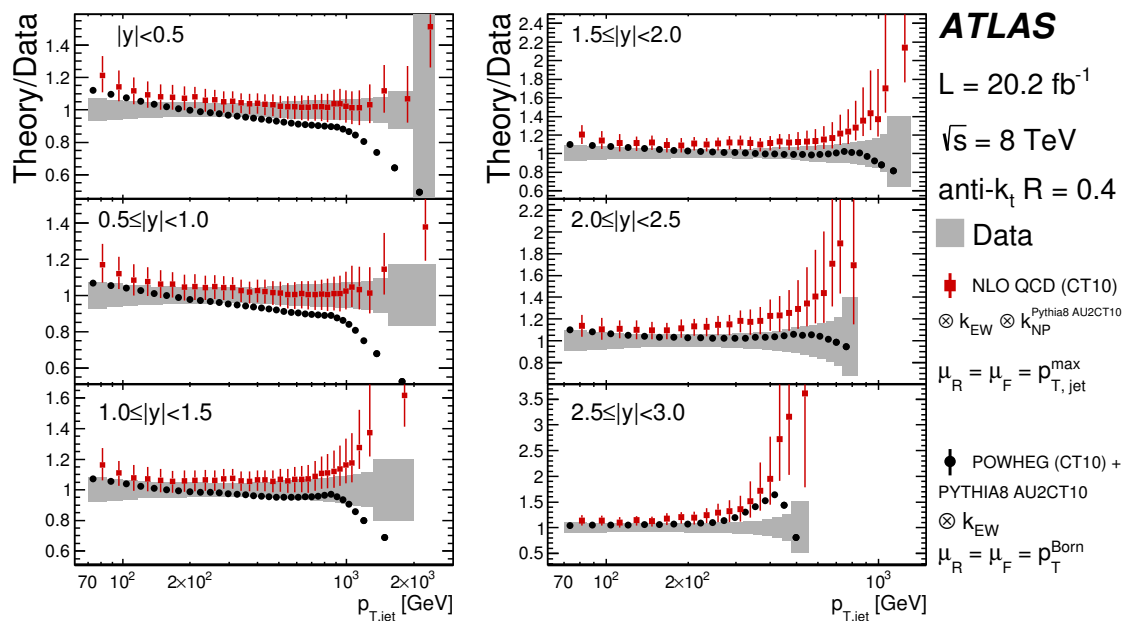
Figure 9. Ratio of the inclusive jet cross-section predicted by the Powheg Monte Carlo event generator with respect to the cross-section in data as a function of the jet p_T in each jet rapidity bin for anti-k_t jets with $R = 0.4$. Only the nominal values of this ratio are indicated. Also shown is the prediction by NLO QCD corrected for non-perturbative effects, where the error bars indicate the total theory uncertainty. Electroweak corrections are applied for both theory predictions and the CT10 PDF set is used. The points are offset in jet p_T for better visibility. The grey band shows the total uncertainty in the measurement.

using the CT10 PDF set and corrected for non-perturbative effects with the same MC generator configuration as was used for Powheg. Electroweak corrections are also applied in both cases.

For anti-k_t jets with $R = 0.4$ the Powheg prediction is lower than the one from fixed-order NLO QCD corrected for non-perturbative effects. This difference increases towards high-p_T and decreases with jet rapidity. In the most forward rapidity region the two predictions are similar. For anti-k_t jets with $R = 0.6$ the Powheg prediction is higher than the fixed-order NLO QCD prediction at low p_T and lower at high p_T. In the most forward rapidity region the two predictions are similar.

The ratio of the Powheg prediction to data is less dependent on the jet radius than the same ratio using the fixed-order NLO QCD prediction corrected for non-perturbative effects. The theory to data ratio for anti-k_t jets with $R = 0.6$ and the same ratio for anti-k_t jets with $R = 0.4$ is unity within 5% for all jet p_T and rapidities while the fixed-order calculation shows deviations of up to 15% for low p_T jets in the central region. This indicates the importance of parton shower effects in correctly describing the jet radius dependence.
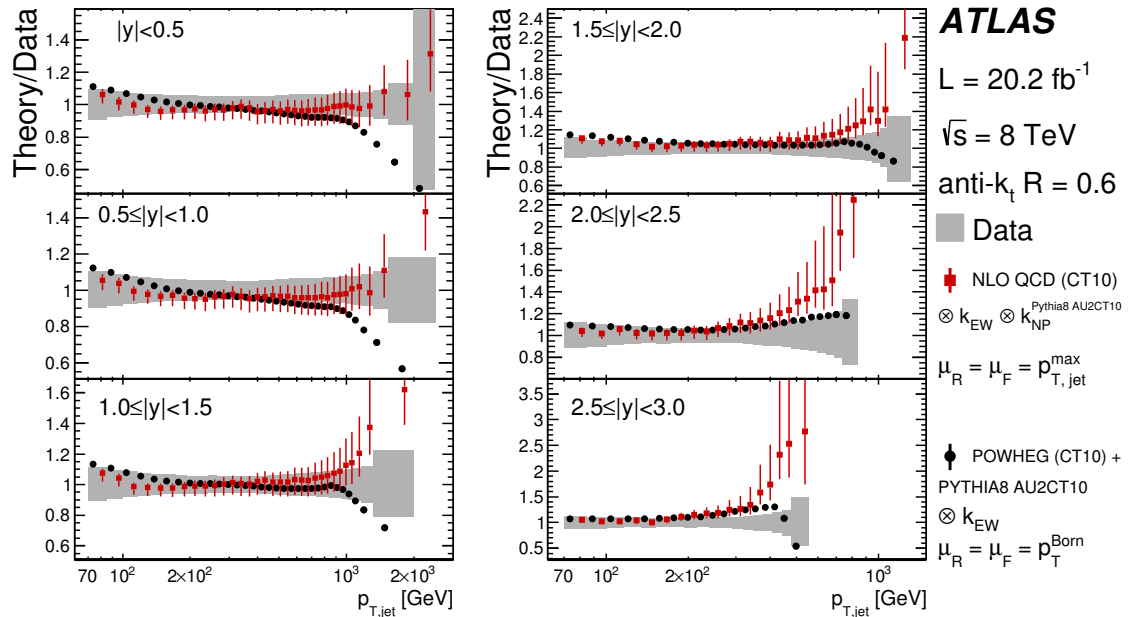
Figure 10. Ratio of the inclusive jet cross-section predicted by the Powheg Monte Carlo event generator with respect to the cross-section in data as a function of the jet p_T in each jet rapidity bin for anti-k_t jets with $R = 0.6$. Only the nominal values of this ratio are indicated. Also shown is the prediction by NLO QCD corrected for non-perturbative effects, where the error bars indicate the total theory uncertainty. Electroweak corrections are applied for both theory predictions and the CT10 PDF set is used. The points are offset in jet p_T for better visibility. The grey band shows the total uncertainty in the measurement.

11 Conclusion

The double-differential inclusive jet cross-sections in proton-proton collisions at $\sqrt{s} = 8\,\text{TeV}$ are measured for jets reconstructed with the anti-k_t algorithm with jet radius parameter values of $R = 0.4$ and $R = 0.6$ in the kinematic region of the jet transverse momentum from $p_T = 70\,\text{GeV}$ to about 2.5 TeV and jet rapidities $|y| < 3$. The measurement is based on the data collected with the ATLAS detector during LHC operation in 2012, corresponding to an integrated luminosity of $20.2\,\text{fb}^{-1}$. The cross-sections are measured double-differentially in the jet transverse momentum and rapidity.

The dominant systematic uncertainty arises from the jet energy calibration. Compared to previous jet cross-section measurements a significant reduction of the uncertainties is achieved.

The publication of all observed results, including uncertainties and correlations, in the Durham HEP database allows further quantitative comparisons of data and theory.

A quantitative comparison of the measurement to fixed-order NLO QCD calculations, corrected for non-perturbative and electroweak effects, shows overall fair agreement (with p-values in the percent range) when considering jet cross-sections in individual jet rapidity bins treated independently. Some tension between data and theory is observed in the central rapidity region for anti-k_t jets with $R = 0.6$. Strong tension between data and

theory is observed when considering data points from all jet transverse momentum and rapidity regions, with a full treatment of the correlations. This tension can be reduced, but not completely resolved, using alternative correlation scenarios for the experimental and theoretical two-point systematic uncertainties. The remaining tension could be due either to the breakdown of the assumptions that need to be made in the treatment of two-point systematic uncertainty components, or to an incomplete theoretical description, such as missing higher-order corrections.

Acknowledgments

A Quantitative comparison of data to NLO QCD calculations with alternate correlation scenarios

Alternative correlation scenarios for experimental and theoretical uncertainties

In order to test in a realistic way the sensitivity of the results to the correlations for two-point systematic uncertainties, 18 different options for splitting into sub-components (see table 4) were studied for experimental and theoretical uncertaitablenties. The options 1–12 (13–18) correspond to a splitting into two (three) sub-components, of which one (two) are explicitly listed in table 4. An extra (complementary) sub-component completes them, such that the sum in quadrature of all the sub-components in each splitting option equals the original uncertainty. These sub-components are defined as fractions of the original uncertainty. The actual fractions are functions with various p_{T} and $|y|$ dependences. They depend only on p_{T} for options 1–6, only on $|y|$ for options 7–8 and on both p_{T} and $|y|$ for the other options. The functions used for the splitting are defined using the linear function $L(x, \mathrm{min}, \mathrm{max}) = (x - \mathrm{min})/(\mathrm{max} - \mathrm{min})$, for x in the range $[\mathrm{min}, \mathrm{max}]$. This function is set to $L(x, \mathrm{min}, \mathrm{max}) = 0$ for $x < \mathrm{min}$ and to $L(x, \mathrm{min}, \mathrm{max}) = 1$ for $x > \mathrm{max}$ respectively. For options 2, 4, 6, 11 and 12, the factor 0.5 included for the listed component induces a reduction of its size, hence the enhancement of the complementary component.

Three additional splitting options (19-21), based on the ones discussed in ref. [88], were tested for the theoretical uncertainties. These options consist in splitting a given uncertainty component into six sub-components,[2] with the following p_{T} and y dependencies indicated in eq. (A.1):

$$
\begin{aligned}
f_1(p_{\mathrm{T}}, y) &= C(p_{\mathrm{T}}, y) \cdot c_1 / \log\left(M(y)/p_{\mathrm{T}}\right), \\
f_2(p_{\mathrm{T}}, y) &= C(p_{\mathrm{T}}, y) \cdot c_2 \cdot y^2 / \log\left(M(y)/p_{\mathrm{T}}\right), \\
f_3(p_{\mathrm{T}}, y) &= C(p_{\mathrm{T}}, y) \cdot c_3, \\
f_4(p_{\mathrm{T}}, y) &= C(p_{\mathrm{T}}, y) \cdot c_4 \cdot y^2, \\
f_5(p_{\mathrm{T}}, y) &= C(p_{\mathrm{T}}, y) \cdot c_5 \cdot \log\left(15 p_{\mathrm{T}}/M(y)\right), \\
f_6(p_{\mathrm{T}}, y) &= C(p_{\mathrm{T}}, y) \cdot c_6 \cdot y^2 \cdot \log\left(15 p_{\mathrm{T}}/M(y)\right),
\end{aligned}
\tag{A.1}
$$

where $M(y) = \sqrt{s} \cdot e^{-y}$. The coefficients $(c_1$–$c_6)$ are (4.56, 1.24, 5.36, 0.536, 1.07, 0.214) for option 19, (9.62, 2.89, 8.42, 0.842, 1.68, 0.336) for option 20 and (5.0, 1.5, 5.7, 0.57, 1.15, 0.24) for option 21 respectively. The normalisation coefficient $C(p_{\mathrm{T}}, y)$ is adjusted in each bin, such that the sum in quadrature of the 6 components is equal to the original uncertainty that is split.

When studying the correlations of the uncertainty related to the scale variations, this uncertainty is first split into three independent sub-components, matching the variation factors of the (renormalisation; factorisation) scales, for the "Up" and "Down" components, as follows: (Up (0.5; 0.5), Down (2; 2)), (Up (0.5; 1), Down (2; 1)) and (Up (1; 0.5),

---

[2]A 7th component is described in ref. [88], corresponding to the uncertainty associated with the non-perturbative correction. The present analysis does not include this 7th component in these splitting options, since the non-perturbative uncertainty is treated differently in our study.

Splitting option	Sub-component(s) definition(s), completed by complementary
1	$L(\ln(p_{\mathrm{T}}[\mathrm{TeV}]), \ln(0.1), \ln(2.5))\cdot$ uncertainty
2	$L(\ln(p_{\mathrm{T}}[\mathrm{TeV}]), \ln(0.1), \ln(2.5)) \cdot 0.5\cdot$ uncertainty
3	$L(p_{\mathrm{T}}[\mathrm{TeV}], 0.1, 2.5)\cdot$ uncertainty
4	$L(p_{\mathrm{T}}[\mathrm{TeV}], 0.1, 2.5) \cdot 0.5\cdot$ uncertainty
5	$L((\ln(p_{\mathrm{T}}[\mathrm{TeV}]))^2, (\ln(0.1))^2, (\ln(2.5))^2)\cdot$ uncertainty
6	$L((\ln(p_{\mathrm{T}}[\mathrm{TeV}]))^2, (\ln(0.1))^2, (\ln(2.5))^2) \cdot 0.5\cdot$ uncertainty
7	$L(|y|, 0, 3)\cdot$ uncertainty
8	$L(|y|, 0, 3) \cdot 0.5\cdot$ uncertainty
9	$L(\ln(p_{\mathrm{T}}[\mathrm{TeV}]), \ln(0.1), \ln(2.5)) \cdot L(|y|, 0, 3)\cdot$ uncertainty
10	$L(\ln(p_{\mathrm{T}}[\mathrm{TeV}]), \ln(0.1), \ln(2.5)) \cdot \sqrt{1 - L(|y|, 0, 3)^2}\cdot$ uncertainty
11	$L(\ln(p_{\mathrm{T}}[\mathrm{TeV}]), \ln(0.1), \ln(2.5)) \cdot L(|y|, 0, 3) \cdot 0.5\cdot$ uncertainty
12	$L(\ln(p_{\mathrm{T}}[\mathrm{TeV}]), \ln(0.1), \ln(2.5)) \cdot \sqrt{1 - L(|y|, 0, 3)^2} \cdot 0.5\cdot$ uncertainty
13	$L(\ln(p_{\mathrm{T}}[\mathrm{TeV}]), \ln(0.1), \ln(2.5)) \cdot \sqrt{1 - L(|y|, 0, 1.5)^2}\cdot$ uncertainty
	$L(\ln(p_{\mathrm{T}}[\mathrm{TeV}]), \ln(0.1), \ln(2.5)) \cdot L(|y|, 1.5, 3)\cdot$ uncertainty
14	$L(\ln(p_{\mathrm{T}}[\mathrm{TeV}]), \ln(0.1), \ln(2.5)) \cdot \sqrt{1 - L(|y|, 0, 1)^2}\cdot$ uncertainty
	$L(\ln(p_{\mathrm{T}}[\mathrm{TeV}]), \ln(0.1), \ln(2.5)) \cdot L(|y|, 1, 3)\cdot$ uncertainty
15	$L(\ln(p_{\mathrm{T}}[\mathrm{TeV}]), \ln(0.1), \ln(2.5)) \cdot \sqrt{1 - L(|y|, 0, 2)^2}\cdot$ uncertainty
	$L(\ln(p_{\mathrm{T}}[\mathrm{TeV}]), \ln(0.1), \ln(2.5)) \cdot L(|y|, 2, 3)\cdot$ uncertainty
16	$\sqrt{1 - L(\ln(p_{\mathrm{T}}[\mathrm{TeV}]), \ln(0.1), \ln(2.5))^2} \cdot \sqrt{1 - L(|y|, 0, 1.5)^2}\cdot$ uncertainty
	$\sqrt{1 - L(\ln(p_{\mathrm{T}}[\mathrm{TeV}]), \ln(0.1), \ln(2.5))^2} \cdot L(|y|, 1.5, 3)\cdot$ uncertainty
17	$\sqrt{1 - L(\ln(p_{\mathrm{T}}[\mathrm{TeV}]), \ln(0.1), \ln(2.5))^2} \cdot \sqrt{1 - L(|y|, 0, 1)^2}\cdot$ uncertainty
	$\sqrt{1 - L(\ln(p_{\mathrm{T}}[\mathrm{TeV}]), \ln(0.1), \ln(2.5))^2} \cdot L(|y|, 1, 3)\cdot$ uncertainty
18	$\sqrt{1 - L(\ln(p_{\mathrm{T}}[\mathrm{TeV}]), \ln(0.1), \ln(2.5))^2} \cdot \sqrt{1 - L(|y|, 0, 2)^2}\cdot$ uncertainty
	$\sqrt{1 - L(\ln(p_{\mathrm{T}}[\mathrm{TeV}]), \ln(0.1), \ln(2.5))^2} \cdot L(|y|, 2, 3)\cdot$ uncertainty

Table 4. Summary of the 18 options for splitting the two-point systematic uncertainties into two (first 12 options) or three (last 6 options) sub-components. One or two sub-components are defined in the table, as fractions of the original uncertainty. An extra (complementary) sub-component completes them, such that the sum in quadrature of all the sub-components in each splitting option equals the original uncertainty. $L(x, \min, \max) = (x - \min)/(\max - \min)$, for x in the range $[\min, \max]$, $L(x, \min, \max) = 0$ for $x < \min$, $L(x, \min, \max) = 1$ for $x > \max$.

Down $(1; 2))$ respectively. These matching options allow minimisation of the phase space where for some component(s) the "Up" and the "Down" variations have the same sign. These three sub-components are then further decorrelated using one of the 21 splitting options discussed above.

Tables 5 and 6 show the χ^2 obtained when applying various splitting options[3] to both the experimental (JES Flavour Response, the JES MJB Fragmentation, JES Pile-up Rho

---

[3]The splitting options shown here are restricted to the ones yielding the largest χ^2 reductions when splitting either the experimental or the theoretical uncertainties.

Splitting options for $R = 0.4$	CT14	NNPDF3.0
JES Flavour Response Opt 7		
JES MJB Fragmentation Opt 17		
JES Pile-up Rho topology Opt 18		
Scale variations Opt 17		
Alternative scale choice Opt 7		
Non-perturbative corrections Opt 7	268/159	257/159
JES Flavour Response Opt 7		
JES MJB Fragmentation Opt 17		
JES Pile-up Rho topology Opt 18		
Scale variations Opt 20		
Alternative scale choice Opt 17		
Non-perturbative corrections Opt 7	261/159	260/159

Table 5. Summary of χ^2/ndf obtained from the comparison of the inclusive jet cross-section and the NLO QCD prediction for the CT14 and the NNPDF30 PDF sets and the $p_{\mathrm{T}}^{\mathrm{jet,max}}$ scale choice for anti-k_t jets with $R = 0.4$, for $p_{\mathrm{T}} > 100\,\mathrm{GeV}$ and various de-correlation options (see text) of the JES Flavour Response, the JES MJB Fragmentation, JES Pile-up Rho topology, the uncertainty related to the scale variations, the uncertainty related to the alternative scale choice and the uncertainty related to the non-perturbative corrections. All the p-values corresponding to the χ^2/ndf in the table are $\ll 10^{-3}$.

Splitting options for $R = 0.6$	CT14	NNPDF3.0
JES Flavour Response Opt 14		
JES MJB Fragmentation Opt 17		
JES Pile-up Rho topology Opt 16		
Scale variations Opt 17		
Alternative scale choice Opt 16		
Non-perturbative corrections Opt 18	266/159	258/159
JES Flavour Response Opt 7		
JES MJB Fragmentation Opt 17		
JES Pile-up Rho topology Opt 16		
Scale variations Opt 17		
Alternative scale choice Opt 16		
Non-perturbative corrections Opt 18	264/159	256/159

Table 6. Summary of χ^2/ndf obtained from the comparison of the inclusive jet cross-section and the NLO QCD prediction for the CT14 and the NNPDF30 PDF sets and the $p_{\mathrm{T}}^{\mathrm{jet,max}}$ scale choice for anti-k_t jets with $R = 0.6$, for $p_{\mathrm{T}} > 100\,\mathrm{GeV}$ and various de-correlation options (see text) of the JES Flavour Response, the JES MJB Fragmentation, JES Pile-up Rho topology, the uncertainty related to the scale variations, the uncertainty related to the alternative scale choice and the uncertainty related to the non-perturbative corrections. All the p-values corresponding to the χ^2/ndf in the table are $\ll 10^{-3}$.

topology) and theoretical uncertainties (the scale variations, the alternative scale choice and the non-perturbative corrections uncertainties) simultaneously. Results are shown for both the CT14 and the NNPDF3.0 pdf sets.

References

[1] L. Evans and P. Bryant, *LHC Machine*, 2008 *JINST* **3** S08001 [ɪɴSPIRE].

[2] S.D. Ellis, Z. Kunszt and D.E. Soper, *Two jet production in hadron collisions at order alpha-S³ in QCD*, *Phys. Rev. Lett.* **69** (1992) 1496 [ɪɴSPIRE].

[3] W.T. Giele, E.W.N. Glover and D.A. Kosower, *The Two-Jet Differential Cross Section at $\mathcal{O}(\alpha_s^3)$ in Hadron Collisions*, *Phys. Rev. Lett.* **73** (1994) 2019 [hep-ph/9403347] [ɪɴSPIRE].

[4] E.W.N. Glover, C. Oleari and M.E. Tejeda-Yeomans, *Two loop QCD corrections to gluon-gluon scattering*, *Nucl. Phys.* **B 605** (2001) 467 [hep-ph/0102201] [ɪɴSPIRE].

[5] E.W.N. Glover and M.E. Tejeda-Yeomans, *One loop QCD corrections to gluon-gluon scattering at NNLO*, *JHEP* **05** (2001) 010 [hep-ph/0104178] [ɪɴSPIRE].

[6] Z. Bern, A. De Freitas and L.J. Dixon, *Two loop helicity amplitudes for quark gluon scattering in QCD and gluino gluon scattering in supersymmetric Yang-Mills theory*, *JHEP* **06** (2003) 028 [*Erratum ibid.* **1404** (2014) 112] [hep-ph/0304168] [ɪɴSPIRE].

[7] C. Anastasiou, E.W.N. Glover, C. Oleari and M.E. Tejeda-Yeomans, *Two loop QCD corrections to massless quark gluon scattering*, *Nucl. Phys.* **B 605** (2001) 486 [hep-ph/0101304] [ɪɴSPIRE].

[8] Z. Bern, L.J. Dixon, D.C. Dunbar and D.A. Kosower, *One loop n point gauge theory amplitudes, unitarity and collinear limits*, *Nucl. Phys.* **B 425** (1994) 217 [hep-ph/9403226] [ɪɴSPIRE].

[9] Z. Bern, L.J. Dixon and D.A. Kosower, *One loop corrections to two quark three gluon amplitudes*, *Nucl. Phys.* **B 437** (1995) 259 [hep-ph/9409393] [ɪɴSPIRE].

[10] A. Gehrmann-De Ridder, T. Gehrmann, E.W.N. Glover and J. Pires, *Second order QCD corrections to jet production at hadron colliders: the all-gluon contribution*, *Phys. Rev. Lett.* **110** (2013) 162003 [arXiv:1301.7310] [ɪɴSPIRE].

[11] J. Currie, A. Gehrmann-De Ridder, E.W.N. Glover and J. Pires, *NNLO QCD corrections to jet production at hadron colliders from gluon scattering*, *JHEP* **01** (2014) 110 [arXiv:1310.3993] [ɪɴSPIRE].

[12] J. Currie, E.W.N. Glover and J. Pires, *Next-to-Next-to Leading Order QCD Predictions for Single Jet Inclusive Production at the LHC*, *Phys. Rev. Lett.* **118** (2017) 072002 [arXiv:1611.01460] [ɪɴSPIRE].

[13] A. Buckley et al., *General-purpose event generators for LHC physics*, *Phys. Rept.* **504** (2011) 145 [arXiv:1101.2599] [ɪɴSPIRE].

[14] CDF collaboration, T. Aaltonen et al., *Measurement of the Inclusive Jet Cross Section at the Fermilab Tevatron $p\bar{p}$ Collider Using a Cone-Based Jet Algorithm*, *Phys. Rev.* **D 78** (2008) 052006 [*Erratum ibid.* **D 79** (2009) 119902] [arXiv:0807.2204] [ɪɴSPIRE].

[15] D0 collaboration, V.M. Abazov et al., *Measurement of the inclusive jet cross section in $p\bar{p}$ collisions at $\sqrt{s} = 1.96\,TeV$*, *Phys. Rev.* **D 85** (2012) 052006 [arXiv:1110.3771] [ɪɴSPIRE].

[16] ALICE collaboration, *Measurement of the inclusive differential jet cross section in pp collisions at $\sqrt{s} = 2.76\,TeV$*, *Phys. Lett.* **B 722** (2013) 262 [`arXiv:1301.3475`] [INSPIRE].

[17] ATLAS collaboration, *Measurement of the inclusive jet cross section in pp collisions at $\sqrt{s} = 2.76\,TeV$ and comparison to the inclusive jet cross section at $\sqrt{s} = 7\,TeV$ using the ATLAS detector*, *Eur. Phys. J.* **C 73** (2013) 2509 [`arXiv:1304.4739`] [INSPIRE].

[18] CMS collaboration, *Measurement of the inclusive jet cross section in pp collisions at $\sqrt{s} = 2.76\,TeV$*, *Eur. Phys. J.* **C 76** (2016) 265 [`arXiv:1512.06212`] [INSPIRE].

[19] ATLAS collaboration, *Measurement of the inclusive jet cross-section in proton-proton collisions at $\sqrt{s} = 7\,TeV$ using $4.5\,fb^{-1}$ of data with the ATLAS detector*, *JHEP* **02** (2015) 153 [*Erratum ibid.* **1509** (2015) 141] [`arXiv:1410.8857`] [INSPIRE].

[20] ATLAS collaboration, *Measurement of inclusive jet and dijet production in pp collisions at $\sqrt{s} = 7\,TeV$ using the ATLAS detector*, *Phys. Rev.* **D 86** (2012) 014022 [`arXiv:1112.6297`] [INSPIRE].

[21] CMS collaboration, *Measurements of differential jet cross sections in proton-proton collisions at $\sqrt{s} = 7\,TeV$ with the CMS detector*, *Phys. Rev.* **D 87** (2013) 112002 [`arXiv:1212.6660`] [INSPIRE].

[22] ATLAS collaboration, *Measurement of inclusive jet and dijet cross sections in proton-proton collisions at $7\,TeV$ centre-of-mass energy with the ATLAS detector*, *Eur. Phys. J.* **C 71** (2011) 1512 [`arXiv:1009.5908`] [INSPIRE].

[23] CMS collaboration, *Measurement of the Inclusive Jet Cross Section in pp Collisions at $\sqrt{s} = 7\,TeV$*, *Phys. Rev. Lett.* **107** (2011) 132001 [`arXiv:1106.0208`] [INSPIRE].

[24] CMS collaboration, *Measurement and QCD analysis of double-differential inclusive jet cross sections in pp collisions at $\sqrt{s} = 8\,TeV$ and cross section ratios to 2.76 and $7\,TeV$*, *JHEP* **03** (2017) 156 [`arXiv:1609.05331`] [INSPIRE].

[25] CMS collaboration, *Measurement of the double-differential inclusive jet cross section in proton-proton collisions at $\sqrt{s} = 13\,TeV$*, *Eur. Phys. J.* **C 76** (2016) 451 [`arXiv:1605.04436`] [INSPIRE].

[26] M. Cacciari, G.P. Salam and G. Soyez, *The Anti-k_t jet clustering algorithm*, *JHEP* **04** (2008) 063 [`arXiv:0802.1189`] [INSPIRE].

[27] ATLAS collaboration, *The ATLAS Experiment at the CERN Large Hadron Collider*, 2008 *JINST* **3** S08003 [INSPIRE].

[28] ATLAS collaboration, *The performance of the jet trigger for the ATLAS detector during 2011 data taking*, *Eur. Phys. J.* **C 76** (2016) 526 [`arXiv:1606.07759`] [INSPIRE].

[29] ATLAS collaboration, *Luminosity determination in pp collisions at $\sqrt{s} = 8\,TeV$ using the ATLAS detector at the LHC*, *Eur. Phys. J.* **C 76** (2016) 653 [`arXiv:1608.03953`] [INSPIRE].

[30] T. Sjöstrand, S. Mrenna and P.Z. Skands, *A Brief Introduction to PYTHIA 8.1*, *Comput. Phys. Commun.* **178** (2008) 852 [`arXiv:0710.3820`] [INSPIRE].

[31] T. Sjöstrand and P.Z. Skands, *Transverse-momentum-ordered showers and interleaved multiple interactions*, *Eur. Phys. J.* **C 39** (2005) 129 [`hep-ph/0408302`] [INSPIRE].

[32] T. Sjöstrand and P.Z. Skands, *Multiple interactions and the structure of beam remnants*, *JHEP* **03** (2004) 053 [`hep-ph/0402078`] [INSPIRE].

[33] B. Andersson, G. Gustafson, G. Ingelman and T. Sjöstrand, *Parton Fragmentation and String Dynamics*, *Phys. Rept.* **97** (1983) 31 [INSPIRE].

[34] ATLAS collaboration, *Summary of ATLAS PYTHIA 8 tunes*, ATL-PHYS-PUB-2012-003 (2012).

[35] H.-L. Lai et al., *New parton distributions for collider physics*, *Phys. Rev.* **D 82** (2010) 074024 [arXiv:1007.2241] [ɪɴSPIRE].

[36] ATLAS collaboration, *The ATLAS Simulation Infrastructure*, *Eur. Phys. J.* **C 70** (2010) 823 [arXiv:1005.4568] [ɪɴSPIRE].

[37] GEANT4 collaboration, S. Agostinelli et al., *GEANT4: A Simulation toolkit*, *Nucl. Instrum. Meth.* **A 506** (2003) 250 [ɪɴSPIRE].

[38] A.D. Martin, W.J. Stirling, R.S. Thorne and G. Watt, *Parton distributions for the LHC*, *Eur. Phys. J.* **C 63** (2009) 189 [arXiv:0901.0002] [ɪɴSPIRE].

[39] M. Bahr et al., *HERWIG++ Physics and Manual*, *Eur. Phys. J.* **C 58** (2008) 639 [arXiv:0803.0883] [ɪɴSPIRE].

[40] J. Bellm et al., *HERWIG++ 2.7 Release Note*, arXiv:1310.6877 [ɪɴSPIRE].

[41] S. Gieseke, P. Stephens and B. Webber, *New formalism for QCD parton showers*, *JHEP* **12** (2003) 045 [hep-ph/0310083] [ɪɴSPIRE].

[42] M. Bahr, S. Gieseke and M.H. Seymour, *Simulation of multiple partonic interactions in HERWIG++*, *JHEP* **07** (2008) 076 [arXiv:0803.3633] [ɪɴSPIRE].

[43] B.R. Webber, *A QCD Model for Jet Fragmentation Including Soft Gluon Interference*, *Nucl. Phys.* **B 238** (1984) 492 [ɪɴSPIRE].

[44] P. Nason, *A New method for combining NLO QCD with shower Monte Carlo algorithms*, *JHEP* **11** (2004) 040 [hep-ph/0409146] [ɪɴSPIRE].

[45] S. Frixione, P. Nason and C. Oleari, *Matching NLO QCD computations with Parton Shower simulations: the POWHEG method*, *JHEP* **11** (2007) 070 [arXiv:0709.2092] [ɪɴSPIRE].

[46] S. Alioli, K. Hamilton, P. Nason, C. Oleari and E. Re, *Jet pair production in POWHEG*, *JHEP* **04** (2011) 081 [arXiv:1012.3380] [ɪɴSPIRE].

[47] S. Alioli, P. Nason, C. Oleari and E. Re, *A general framework for implementing NLO calculations in shower Monte Carlo programs: the POWHEG BOX*, *JHEP* **06** (2010) 043 [arXiv:1002.2581] [ɪɴSPIRE].

[48] M. Cacciari, G.P. Salam and G. Soyez, *FastJet User Manual*, *Eur. Phys. J.* **C 72** (2012) 1896 [arXiv:1111.6097] [ɪɴSPIRE].

[49] ATLAS collaboration, *Proposal for truth particle observable definitions in physics measurements*, ATL-PHYS-PUB-2015-013 (2015).

[50] ATLAS collaboration, *Jet energy measurement and its systematic uncertainty in proton-proton collisions at $\sqrt{s} = 7$ TeV with the ATLAS detector*, *Eur. Phys. J.* **C 75** (2015) 17 [arXiv:1406.0076] [ɪɴSPIRE].

[51] ATLAS collaboration, *Jet energy measurement with the ATLAS detector in proton-proton collisions at $\sqrt{s} = 7$ TeV*, *Eur. Phys. J.* **C 73** (2013) 2304 [arXiv:1112.6426] [ɪɴSPIRE].

[52] ATLAS collaboration, *Topological cell clustering in the ATLAS calorimeters and its performance in LHC Run 1*, *Eur. Phys. J.* **C 77** (2017) 490 [arXiv:1603.02934] [ɪɴSPIRE].

[53] ATLAS collaboration, *Performance of pile-up mitigation techniques for jets in pp collisions at $\sqrt{s} = 8$ TeV using the ATLAS detector*, *Eur. Phys. J.* **C 76** (2016) 581 [arXiv:1510.03823] [ɪɴSPIRE].

[54] M. Cacciari and G.P. Salam, *Pileup subtraction using jet areas*, *Phys. Lett.* **B 659** (2008) 119 [`arXiv:0707.1378`] [INSPIRE].

[55] M. Cacciari and G.P. Salam, *Dispelling the N^3 myth for the k_t jet-finder*, *Phys. Lett.* **B 641** (2006) 57 [`hep-ph/0512210`] [INSPIRE].

[56] ATLAS collaboration, *Monte Carlo Calibration and Combination of In-situ Measurements of Jet Energy Scale, Jet Energy Resolution and Jet Mass in ATLAS*, ATLAS-CONF-2015-037 (2015).

[57] ATLAS collaboration, *Jet global sequential corrections with the ATLAS detector in proton-proton collisions at $\sqrt{s} = 8$ TeV*, ATLAS-CONF-2015-002 (2015).

[58] ATLAS collaboration, *Data-driven determination of the energy scale and resolution of jets reconstructed in the ATLAS calorimeters using dijet and multijet events at $\sqrt{s} = 8$ TeV*, ATLAS-CONF-2015-017 (2015).

[59] ATLAS collaboration, *Determination of the jet energy scale and resolution at ATLAS using Z/γ-jet events in data at $\sqrt{s} = 13$ TeV*, ATLAS-CONF-2015-057 (2015).

[60] ATLAS collaboration, *Single hadron response measurement and calorimeter jet energy scale uncertainty with the ATLAS detector at the LHC*, *Eur. Phys. J.* **C 73** (2013) 2305 [`arXiv:1203.1302`] [INSPIRE].

[61] ATLAS collaboration, *A measurement of the calorimeter response to single hadrons and determination of the jet energy scale uncertainty using LHC Run-1 pp-collision data with the ATLAS detector*, *Eur. Phys. J.* **C 77** (2017) 26 [`arXiv:1607.08842`] [INSPIRE].

[62] B. Malaescu, *An Iterative, Dynamically Stabilized(IDS) Method of Data Unfolding*, `arXiv:1106.3107` [INSPIRE].

[63] J. Wenninger and E. Todesco, *Large Hadron Collider momentum calibration and accuracy*, CERN-ATS-2017-0007 (2017).

[64] Z. Nagy, *Next-to-leading order calculation of three jet observables in hadron hadron collision*, *Phys. Rev.* **D 68** (2003) 094002 [`hep-ph/0307268`] [INSPIRE].

[65] T. Carli et al., *A posteriori inclusion of parton density functions in NLO QCD final-state calculations at hadron colliders: The APPLGRID Project*, *Eur. Phys. J.* **C 66** (2010) 503 [`arXiv:0911.2985`] [INSPIRE].

[66] S. Dulat et al., *New parton distribution functions from a global analysis of quantum chromodynamics*, *Phys. Rev.* **D 93** (2016) 033006 [`arXiv:1506.07443`] [INSPIRE].

[67] L.A. Harland-Lang, A.D. Martin, P. Motylinski and R.S. Thorne, *Parton distributions in the LHC era: MMHT 2014 PDFs*, *Eur. Phys. J.* **C 75** (2015) 204 [`arXiv:1412.3989`] [INSPIRE].

[68] NNPDF collaboration, R.D. Ball et al., *Parton distributions for the LHC Run II*, *JHEP* **04** (2015) 040 [`arXiv:1410.8849`] [INSPIRE].

[69] ZEUS, H1 collaboration, Z. Zhang et al., *HERA Inclusive Neutral and Charged Current Cross Sections and a New PDF Fit, HERAPDF 2.0*, *Acta Phys. Polon. Supp.* **8** (2015) 957 [`arXiv:1511.05402`] [INSPIRE].

[70] A. Buckley et al., *LHAPDF6: parton density access in the LHC precision era*, *Eur. Phys. J.* **C 75** (2015) 132 [`arXiv:1412.7420`] [INSPIRE].

[71] J. Butterworth et al., *PDF4LHC recommendations for LHC Run II*, *J. Phys.* **G 43** (2016) 023001 [`arXiv:1510.03865`] [INSPIRE].

[72] S. Carrazza and J. Pires, *Perturbative QCD description of jet data from LHC Run-I and TeVatron Run-II*, *JHEP* **10** (2014) 145 [arXiv:1407.7031] [ɪɴSPIRE].

[73] S. Dittmaier, A. Huss and C. Speckner, *Weak radiative corrections to dijet production at hadron colliders*, *JHEP* **11** (2012) 095 [arXiv:1210.0438] [ɪɴSPIRE].

[74] J. Pumplin, D.R. Stump, J. Huston, H.L. Lai, P.M. Nadolsky and W.K. Tung, *New generation of parton distributions with uncertainties from global QCD analysis*, *JHEP* **07** (2002) 012 [hep-ph/0201195] [ɪɴSPIRE].

[75] U. Baur, *Weak Boson Emission in Hadron Collider Processes*, *Phys. Rev.* **D 75** (2007) 013005 [hep-ph/0611241] [ɪɴSPIRE].

[76] P. Skands, S. Carrazza and J. Rojo, *Tuning PYTHIA 8.1: the Monash 2013 Tune*, *Eur. Phys. J.* **C 74** (2014) 3024 [arXiv:1404.5630] [ɪɴSPIRE].

[77] ATLAS collaboration, *ATLAS Pythia 8 tunes to 7 TeV data*, ATL-PHYS-PUB-2014-021 (2014).

[78] R. Corke and T. Sjöstrand, *Interleaved Parton Showers and Tuning Prospects*, *JHEP* **03** (2011) 032 [arXiv:1011.1759] [ɪɴSPIRE].

[79] NNPDF collaboration, R.D. Ball et al., *Unbiased global determination of parton distributions and their uncertainties at NNLO and at LO*, *Nucl. Phys.* **B 855** (2012) 153 [arXiv:1107.2652] [ɪɴSPIRE].

[80] NNPDF collaboration, R.D. Ball et al., *Parton distributions with QED corrections*, *Nucl. Phys.* **B 877** (2013) 290 [arXiv:1308.0598] [ɪɴSPIRE].

[81] A. Sherstnev and R.S. Thorne, *Parton Distributions for LO Generators*, *Eur. Phys. J.* **C 55** (2008) 553 [arXiv:0711.2473] [ɪɴSPIRE].

[82] S. Gieseke, C. Rohr and A. Siodmok, *Colour reconnections in HERWIG++*, *Eur. Phys. J.* **C 72** (2012) 2225 [arXiv:1206.0041] [ɪɴSPIRE].

[83] M.H. Seymour and A. Siodmok, *Constraining MPI models using σ_{eff} and recent TeVatron and LHC Underlying Event data*, *JHEP* **10** (2013) 113 [arXiv:1307.5015] [ɪɴSPIRE].

[84] A complete set of tables with the full results are available at the Durham HepData repository, https://hepdata.net.

[85] ATLAS collaboration, *Measurement of dijet cross sections in pp collisions at 7 TeV centre-of-mass energy using the ATLAS detector*, *JHEP* **05** (2014) 059 [arXiv:1312.3524] [ɪɴSPIRE].

[86] S. Dooling, P. Gunnellini, F. Hautmann and H. Jung, *Longitudinal momentum shifts, showering and nonperturbative corrections in matched next-to-leading-order shower event generators*, *Phys. Rev.* **D 87** (2013) 094009 [arXiv:1212.6164] [ɪɴSPIRE].

[87] S. Alekhin, J. Blumlein and S.O. Moch, *ABM11 PDFs and the cross section benchmarks in NNLO*, arXiv:1302.1516 [ɪɴSPIRE].

[88] F.I. Olness and D.E. Soper, *Correlated theoretical uncertainties for the one-jet inclusive cross section*, *Phys. Rev.* **D 81** (2010) 035018 [arXiv:0907.5052] [ɪɴSPIRE].

[89] ATLAS collaboration, *ATLAS Computing Acknowledgements 2016-2017*, ATL-GEN-PUB-2016-002 (2016).

The ATLAS collaboration

M. Aaboud[137d], G. Aad[88], B. Abbott[115], J. Abdallah[8], O. Abdinov[12,*], B. Abeloos[119],
S.H. Abidi[161], O.S. AbouZeid[139], N.L. Abraham[151], H. Abramowicz[155], H. Abreu[154], R. Abreu[118],
Y. Abulaiti[148a,148b], B.S. Acharya[167a,167b,a], S. Adachi[157], L. Adamczyk[41a], J. Adelman[110],
M. Adersberger[102], T. Adye[133], A.A. Affolder[139], T. Agatonovic-Jovin[14], C. Agheorghiesei[28c],
J.A. Aguilar-Saavedra[128a,128f], S.P. Ahlen[24], F. Ahmadov[68,b], G. Aielli[135a,135b], S. Akatsuka[71],
H. Akerstedt[148a,148b], T.P.A. Åkesson[84], A.V. Akimov[98], G.L. Alberghi[22a,22b], J. Albert[172],
M.J. Alconada Verzini[74], M. Aleksa[32], I.N. Aleksandrov[68], C. Alexa[28b], G. Alexander[155],
T. Alexopoulos[10], M. Alhroob[115], B. Ali[130], M. Aliev[76a,76b], G. Alimonti[94a], J. Alison[33],
S.P. Alkire[38], B.M.M. Allbrooke[151], B.W. Allen[118], P.P. Allport[19], A. Aloisio[106a,106b],
A. Alonso[39], F. Alonso[74], C. Alpigiani[140], A.A. Alshehri[56], M. Alstaty[88], B. Alvarez Gonzalez[32],
D. Álvarez Piqueras[170], M.G. Alviggi[106a,106b], B.T. Amadio[16], Y. Amaral Coutinho[26a],
C. Amelung[25], D. Amidei[92], S.P. Amor Dos Santos[128a,128c], A. Amorim[128a,128b], S. Amoroso[32],
G. Amundsen[25], C. Anastopoulos[141], L.S. Ancu[52], N. Andari[19], T. Andeen[11], C.F. Anders[60b],
J.K. Anders[77], K.J. Anderson[33], A. Andreazza[94a,94b], V. Andrei[60a], S. Angelidakis[9],
I. Angelozzi[109], A. Angerami[38], F. Anghinolfi[32], A.V. Anisenkov[111,c], N. Anjos[13],
A. Annovi[126a,126b], C. Antel[60a], M. Antonelli[50], A. Antonov[100,*], D.J. Antrim[166], F. Anulli[134a],
M. Aoki[69], L. Aperio Bella[32], G. Arabidze[93], Y. Arai[69], J.P. Araque[128a], V. Araujo Ferraz[26a],
A.T.H. Arce[48], R.E. Ardell[80], F.A. Arduh[74], J-F. Arguin[97], S. Argyropoulos[66], M. Arik[20a],
A.J. Armbruster[145], L.J. Armitage[79], O. Arnaez[32], H. Arnold[51], M. Arratia[30], O. Arslan[23],
A. Artamonov[99], G. Artoni[122], S. Artz[86], S. Asai[157], N. Asbah[45], A. Ashkenazi[155], L. Asquith[151],
K. Assamagan[27], R. Astalos[146a], M. Atkinson[169], N.B. Atlay[143], K. Augsten[130], G. Avolio[32],
B. Axen[16], M.K. Ayoub[119], G. Azuelos[97,d], A.E. Baas[60a], M.J. Baca[19], H. Bachacou[138],
K. Bachas[76a,76b], M. Backes[122], M. Backhaus[32], P. Bagiacchi[134a,134b], P. Bagnaia[134a,134b],
H. Bahrasemani[144], J.T. Baines[133], M. Bajic[39], O.K. Baker[179], E.M. Baldin[111,c], P. Balek[175],
T. Balestri[150], F. Balli[138], W.K. Balunas[124], E. Banas[42], Sw. Banerjee[176,e], A.A.E. Bannoura[178],
L. Barak[32], E.L. Barberio[91], D. Barberis[53a,53b], M. Barbero[88], T. Barillari[103], M-S Barisits[32],
T. Barklow[145], N. Barlow[30], S.L. Barnes[36c], B.M. Barnett[133], R.M. Barnett[16],
Z. Barnovska-Blenessy[36a], A. Baroncelli[136a], G. Barone[25], A.J. Barr[122], L. Barranco Navarro[170],
F. Barreiro[85], J. Barreiro Guimarães da Costa[35a], R. Bartoldus[145], A.E. Barton[75], P. Bartos[146a],
A. Basalaev[125], A. Bassalat[119,f], R.L. Bates[56], S.J. Batista[161], J.R. Batley[30], M. Battaglia[139],
M. Bauce[134a,134b], F. Bauer[138], H.S. Bawa[145,g], J.B. Beacham[113], M.D. Beattie[75], T. Beau[83],
P.H. Beauchemin[165], P. Bechtle[23], H.P. Beck[18,h], K. Becker[122], M. Becker[86], M. Beckingham[173],
C. Becot[112], A.J. Beddall[20e], A. Beddall[20b], V.A. Bednyakov[68], M. Bedognetti[109], C.P. Bee[150],
T.A. Beermann[32], M. Begalli[26a], M. Begel[27], J.K. Behr[45], A.S. Bell[81], G. Bella[155],
L. Bellagamba[22a], A. Bellerive[31], M. Bellomo[154], K. Belotskiy[100], O. Beltramello[32],
N.L. Belyaev[100], O. Benary[155,*], D. Benchekroun[137a], M. Bender[102], K. Bendtz[148a,148b],
N. Benekos[10], Y. Benhammou[155], E. Benhar Noccioli[179], J. Benitez[66], D.P. Benjamin[48],
M. Benoit[52], J.R. Bensinger[25], S. Bentvelsen[109], L. Beresford[122], M. Beretta[50], D. Berge[109],
E. Bergeaas Kuutmann[168], N. Berger[5], J. Beringer[16], S. Berlendis[58], N.R. Bernard[89],
G. Bernardi[83], C. Bernius[145], F.U. Bernlochner[23], T. Berry[80], P. Berta[131], C. Bertella[35a],
G. Bertoli[148a,148b], F. Bertolucci[126a,126b], I.A. Bertram[75], C. Bertsche[45], D. Bertsche[115],
G.J. Besjes[39], O. Bessidskaia Bylund[148a,148b], M. Bessner[45], N. Besson[138], C. Betancourt[51],
A. Bethani[87], S. Bethke[103], A.J. Bevan[79], R.M. Bianchi[127], O. Biebel[102], D. Biedermann[17],
R. Bielski[87], N.V. Biesuz[126a,126b], M. Biglietti[136a], J. Bilbao De Mendizabal[52], T.R.V. Billoud[97],
H. Bilokon[50], M. Bindi[57], A. Bingul[20b], C. Bini[134a,134b], S. Biondi[22a,22b], T. Bisanz[57],
C. Bittrich[47], D.M. Bjergaard[48], C.W. Black[152], J.E. Black[145], K.M. Black[24], D. Blackburn[140],

R.E. Blair[6], T. Blazek[146a], I. Bloch[45], C. Blocker[25], A. Blue[56], W. Blum[86,*], U. Blumenschein[79],
S. Blunier[34a], G.J. Bobbink[109], V.S. Bobrovnikov[111,c], S.S. Bocchetta[84], A. Bocci[48], C. Bock[102],
M. Boehler[51], D. Boerner[178], D. Bogavac[102], A.G. Bogdanchikov[111], C. Bohm[148a], V. Boisvert[80],
P. Bokan[168,i], T. Bold[41a], A.S. Boldyrev[101], M. Bomben[83], M. Bona[79], M. Boonekamp[138],
A. Borisov[132], G. Borissov[75], J. Bortfeldt[32], D. Bortoletto[122], V. Bortolotto[62a,62b,62c],
D. Boscherini[22a], M. Bosman[13], J.D. Bossio Sola[29], J. Boudreau[127], J. Bouffard[2],
E.V. Bouhova-Thacker[75], D. Boumediene[37], C. Bourdarios[119], S.K. Boutle[56], A. Boveia[113],
J. Boyd[32], I.R. Boyko[68], J. Bracinik[19], A. Brandt[8], G. Brandt[57], O. Brandt[60a], U. Bratzler[158],
B. Brau[89], J.E. Brau[118], W.D. Breaden Madden[56], K. Brendlinger[45], A.J. Brennan[91],
L. Brenner[109], R. Brenner[168], S. Bressler[175], D.L. Briglin[19], T.M. Bristow[49], D. Britton[56],
D. Britzger[45], F.M. Brochu[30], I. Brock[23], R. Brock[93], G. Brooijmans[38], T. Brooks[80],
W.K. Brooks[34b], J. Brosamer[16], E. Brost[110], J.H Broughton[19], P.A. Bruckman de Renstrom[42],
D. Bruncko[146b], A. Bruni[22a], G. Bruni[22a], L.S. Bruni[109], BH Brunt[30], M. Bruschi[22a],
N. Bruscino[23], P. Bryant[33], L. Bryngemark[84], T. Buanes[15], Q. Buat[144], P. Buchholz[143],
A.G. Buckley[56], I.A. Budagov[68], F. Buehrer[51], M.K. Bugge[121], O. Bulekov[100], D. Bullock[8],
H. Burckhart[32], S. Burdin[77], C.D. Burgard[51], A.M. Burger[5], B. Burghgrave[110], K. Burka[42],
S. Burke[133], I. Burmeister[46], J.T.P. Burr[122], E. Busato[37], D. Büscher[51], V. Büscher[86],
P. Bussey[56], J.M. Butler[24], C.M. Buttar[56], J.M. Butterworth[81], P. Butti[32], W. Buttinger[27],
A. Buzatu[35c], A.R. Buzykaev[111,c], S. Cabrera Urbán[170], D. Caforio[130], V.M. Cairo[40a,40b],
O. Cakir[4a], N. Calace[52], P. Calafiura[16], A. Calandri[88], G. Calderini[83], P. Calfayan[64],
G. Callea[40a,40b], L.P. Caloba[26a], S. Calvente Lopez[85], D. Calvet[37], S. Calvet[37], T.P. Calvet[88],
R. Camacho Toro[33], S. Camarda[32], P. Camarri[135a,135b], D. Cameron[121],
R. Caminal Armadans[169], C. Camincher[58], S. Campana[32], M. Campanelli[81], A. Camplani[94a,94b],
A. Campoverde[143], V. Canale[106a,106b], M. Cano Bret[36c], J. Cantero[116], T. Cao[155],
M.D.M. Capeans Garrido[32], I. Caprini[28b], M. Caprini[28b], M. Capua[40a,40b], R.M. Carbone[38],
R. Cardarelli[135a], F. Cardillo[51], I. Carli[131], T. Carli[32], G. Carlino[106a], B.T. Carlson[127],
L. Carminati[94a,94b], R.M.D. Carney[148a,148b], S. Caron[108], E. Carquin[34b], G.D. Carrillo-Montoya[32],
J. Carvalho[128a,128c], D. Casadei[19], M.P. Casado[13,j], M. Casolino[13], D.W. Casper[166],
R. Castelijn[109], A. Castelli[109], V. Castillo Gimenez[170], N.F. Castro[128a,k], A. Catinaccio[32],
J.R. Catmore[121], A. Cattai[32], J. Caudron[23], V. Cavaliere[169], E. Cavallaro[13], D. Cavalli[94a],
M. Cavalli-Sforza[13], V. Cavasinni[126a,126b], E. Celebi[20a], F. Ceradini[136a,136b], L. Cerda Alberich[170],
A.S. Cerqueira[26b], A. Cerri[151], L. Cerrito[135a,135b], F. Cerutti[16], A. Cervelli[18], S.A. Cetin[20d],
A. Chafaq[137a], D. Chakraborty[110], S.K. Chan[59], W.S. Chan[109], Y.L. Chan[62a], P. Chang[169],
J.D. Chapman[30], D.G. Charlton[19], A. Chatterjee[52], C.C. Chau[161], C.A. Chavez Barajas[151],
S. Che[113], S. Cheatham[167a,167c], A. Chegwidden[93], S. Chekanov[6], S.V. Chekulaev[163a],
G.A. Chelkov[68,l], M.A. Chelstowska[32], C. Chen[67], H. Chen[27], S. Chen[35b], S. Chen[157],
X. Chen[35c,m], Y. Chen[70], H.C. Cheng[92], H.J. Cheng[35a], Y. Cheng[33], A. Cheplakov[68],
E. Cheremushkina[132], R. Cherkaoui El Moursli[137e], V. Chernyatin[27,*], E. Cheu[7], L. Chevalier[138],
V. Chiarella[50], G. Chiarelli[126a,126b], G. Chiodini[76a], A.S. Chisholm[32], A. Chitan[28b], Y.H. Chiu[172],
M.V. Chizhov[68], K. Choi[64], A.R. Chomont[37], S. Chouridou[9], B.K.B. Chow[102],
V. Christodoulou[81], D. Chromek-Burckhart[32], M.C. Chu[62a], J. Chudoba[129], A.J. Chuinard[90],
J.J. Chwastowski[42], L. Chytka[117], A.K. Ciftci[4a], D. Cinca[46], V. Cindro[78], I.A. Cioara[23],
C. Ciocca[22a,22b], A. Ciocio[16], F. Cirotto[106a,106b], Z.H. Citron[175], M. Citterio[94a], M. Ciubancan[28b],
A. Clark[52], B.L. Clark[59], M.R. Clark[38], P.J. Clark[49], R.N. Clarke[16], C. Clement[148a,148b],
Y. Coadou[88], M. Cobal[167a,167c], A. Coccaro[52], J. Cochran[67], L. Colasurdo[108], B. Cole[38],
A.P. Colijn[109], J. Collot[58], T. Colombo[166], P. Conde Muiño[128a,128b], E. Coniavitis[51],
S.H. Connell[147b], I.A. Connelly[87], V. Consorti[51], S. Constantinescu[28b], G. Conti[32],
F. Conventi[106a,n], M. Cooke[16], B.D. Cooper[81], A.M. Cooper-Sarkar[122], F. Cormier[171],

K.J.R. Cormier[161], M. Corradi[134a,134b], F. Corriveau[90,o], A. Cortes-Gonzalez[32], G. Cortiana[103], G. Costa[94a], M.J. Costa[170], D. Costanzo[141], G. Cottin[30], G. Cowan[80], B.E. Cox[87], K. Cranmer[112], S.J. Crawley[56], R.A. Creager[124], G. Cree[31], S. Crépé-Renaudin[58], F. Crescioli[83], W.A. Cribbs[148a,148b], M. Crispin Ortuzar[122], M. Cristinziani[23], V. Croft[108], G. Crosetti[40a,40b], A. Cueto[85], T. Cuhadar Donszelmann[141], A.R. Cukierman[145], J. Cummings[179], M. Curatolo[50], J. Cúth[86], H. Czirr[143], P. Czodrowski[32], G. D'amen[22a,22b], S. D'Auria[56], M. D'Onofrio[77], M.J. Da Cunha Sargedas De Sousa[128a,128b], C. Da Via[87], W. Dabrowski[41a], T. Dado[146a], T. Dai[92], O. Dale[15], F. Dallaire[97], C. Dallapiccola[89], M. Dam[39], J.R. Dandoy[124], N.P. Dang[51], A.C. Daniells[19], N.S. Dann[87], M. Danninger[171], M. Dano Hoffmann[138], V. Dao[150], G. Darbo[53a], S. Darmora[8], J. Dassoulas[3], A. Dattagupta[118], T. Daubney[45], W. Davey[23], C. David[45], T. Davidek[131], M. Davies[155], P. Davison[81], E. Dawe[91], I. Dawson[141], K. De[8], R. de Asmundis[106a], A. De Benedetti[115], S. De Castro[22a,22b], S. De Cecco[83], N. De Groot[108], P. de Jong[109], H. De la Torre[93], F. De Lorenzi[67], A. De Maria[57], D. De Pedis[134a], A. De Salvo[134a], U. De Sanctis[135a,135b], A. De Santo[151], K. De Vasconcelos Corga[88], J.B. De Vivie De Regie[119], W.J. Dearnaley[75], R. Debbe[27], C. Debenedetti[139], D.V. Dedovich[68], N. Dehghanian[3], I. Deigaard[109], M. Del Gaudio[40a,40b], J. Del Peso[85], T. Del Prete[126a,126b], D. Delgove[119], F. Deliot[138], C.M. Delitzsch[52], A. Dell'Acqua[32], L. Dell'Asta[24], M. Dell'Orso[126a,126b], M. Della Pietra[106a,106b], D. della Volpe[52], M. Delmastro[5], C. Delporte[119], P.A. Delsart[58], D.A. DeMarco[161], S. Demers[179], M. Demichev[68], A. Demilly[83], S.P. Denisov[132], D. Denysiuk[138], D. Derendarz[42], J.E. Derkaoui[137d], F. Derue[83], P. Dervan[77], K. Desch[23], C. Deterre[45], K. Dette[46], P.O. Deviveiros[32], A. Dewhurst[133], S. Dhaliwal[25], A. Di Ciaccio[135a,135b], L. Di Ciaccio[5], W.K. Di Clemente[124], C. Di Donato[106a,106b], A. Di Girolamo[32], B. Di Girolamo[32], B. Di Micco[136a,136b], R. Di Nardo[32], K.F. Di Petrillo[59], A. Di Simone[51], R. Di Sipio[161], D. Di Valentino[31], C. Diaconu[88], M. Diamond[161], F.A. Dias[49], M.A. Diaz[34a], E.B. Diehl[92], J. Dietrich[17], S. Díez Cornell[45], A. Dimitrievska[14], J. Dingfelder[23], P. Dita[28b], S. Dita[28b], F. Dittus[32], F. Djama[88], T. Djobava[54b], J.I. Djuvsland[60a], M.A.B. do Vale[26c], D. Dobos[32], M. Dobre[28b], C. Doglioni[84], J. Dolejsi[131], Z. Dolezal[131], M. Donadelli[26d], S. Donati[126a,126b], P. Dondero[123a,123b], J. Donini[37], J. Dopke[133], A. Doria[106a], M.T. Dova[74], A.T. Doyle[56], E. Drechsler[57], M. Dris[10], Y. Du[36b], J. Duarte-Campderros[155], E. Duchovni[175], G. Duckeck[102], A. Ducourthial[83], O.A. Ducu[97,p], D. Duda[109], A. Dudarev[32], A.Chr. Dudder[86], E.M. Duffield[16], L. Duflot[119], M. Dührssen[32], M. Dumancic[175], A.E. Dumitriu[28b], A.K. Duncan[56], M. Dunford[60a], H. Duran Yildiz[4a], M. Düren[55], A. Durglishvili[54b], D. Duschinger[47], B. Dutta[45], M. Dyndal[45], C. Eckardt[45], K.M. Ecker[103], R.C. Edgar[92], T. Eifert[32], G. Eigen[15], K. Einsweiler[16], T. Ekelof[168], M. El Kacimi[137c], R. El Kosseifi[88], V. Ellajosyula[88], M. Ellert[168], S. Elles[5], F. Ellinghaus[178], A.A. Elliot[172], N. Ellis[32], J. Elmsheuser[27], M. Elsing[32], D. Emeliyanov[133], Y. Enari[157], O.C. Endner[86], J.S. Ennis[173], J. Erdmann[46], A. Ereditato[18], G. Ernis[178], M. Ernst[27], S. Errede[169], E. Ertel[86], M. Escalier[119], H. Esch[46], C. Escobar[127], B. Esposito[50], O. Estrada Pastor[170], A.I. Etienvre[138], E. Etzion[155], H. Evans[64], A. Ezhilov[125], M. Ezzi[137e], F. Fabbri[22a,22b], L. Fabbri[22a,22b], G. Facini[33], R.M. Fakhrutdinov[132], S. Falciano[134a], R.J. Falla[81], J. Faltova[32], Y. Fang[35a], M. Fanti[94a,94b], A. Farbin[8], A. Farilla[136a], C. Farina[127], E.M. Farina[123a,123b], T. Farooque[93], S. Farrell[16], S.M. Farrington[173], P. Farthouat[32], F. Fassi[137e], P. Fassnacht[32], D. Fassouliotis[9], M. Faucci Giannelli[80], A. Favareto[53a,53b], W.J. Fawcett[122], L. Fayard[119], O.L. Fedin[125,q], W. Fedorko[171], S. Feigl[121], L. Feligioni[88], C. Feng[36b], E.J. Feng[32], H. Feng[92], A.B. Fenyuk[132], L. Feremenga[8], P. Fernandez Martinez[170], S. Fernandez Perez[13], J. Ferrando[45], A. Ferrari[168], P. Ferrari[109], R. Ferrari[123a], D.E. Ferreira de Lima[60b], A. Ferrer[170], D. Ferrere[52], C. Ferretti[92], F. Fiedler[86], A. Filipčič[78], M. Filipuzzi[45], F. Filthaut[108], M. Fincke-Keeler[172], K.D. Finelli[152], M.C.N. Fiolhais[128a,128c,r], L. Fiorini[170], A. Fischer[2], C. Fischer[13], J. Fischer[178], W.C. Fisher[93], N. Flaschel[45], I. Fleck[143], P. Fleischmann[92],

R.R.M. Fletcher[124], T. Flick[178], B.M. Flierl[102], L.R. Flores Castillo[62a], M.J. Flowerdew[103],
G.T. Forcolin[87], A. Formica[138], F.A. Förster[13], A. Forti[87], A.G. Foster[19], D. Fournier[119],
H. Fox[75], S. Fracchia[141], P. Francavilla[83], M. Franchini[22a,22b], S. Franchino[60a], D. Francis[32],
L. Franconi[121], M. Franklin[59], M. Frate[166], M. Fraternali[123a,123b], D. Freeborn[81],
S.M. Fressard-Batraneanu[32], B. Freund[97], D. Froidevaux[32], J.A. Frost[122],
E. Fullana Torregrosa[86], C. Fukunaga[158], T. Fusayasu[104], J. Fuster[170], C. Gabaldon[58],
O. Gabizon[154], A. Gabrielli[22a,22b], A. Gabrielli[16], G.P. Gach[41a], S. Gadatsch[32], S. Gadomski[80],
G. Gagliardi[53a,53b], L.G. Gagnon[97], P. Gagnon[64], C. Galea[108], B. Galhardo[128a,128c],
E.J. Gallas[122], B.J. Gallop[133], P. Gallus[130], G. Galster[39], K.K. Gan[113], S. Ganguly[37], J. Gao[36a],
Y. Gao[77], Y.S. Gao[145,g], F.M. Garay Walls[49], C. García[170], J.E. García Navarro[170],
M. Garcia-Sciveres[16], R.W. Gardner[33], N. Garelli[145], V. Garonne[121], A. Gascon Bravo[45],
K. Gasnikova[45], C. Gatti[50], A. Gaudiello[53a,53b], G. Gaudio[123a], I.L. Gavrilenko[98], C. Gay[171],
G. Gaycken[23], E.N. Gazis[10], C.N.P. Gee[133], M. Geisen[86], M.P. Geisler[60a], K. Gellerstedt[148a,148b],
C. Gemme[53a], M.H. Genest[58], C. Geng[36a,s], S. Gentile[134a,134b], C. Gentsos[156], S. George[80],
D. Gerbaudo[13], A. Gershon[155], S. Ghasemi[143], M. Ghneimat[23], B. Giacobbe[22a], S. Giagu[134a,134b],
P. Giannetti[126a,126b], S.M. Gibson[80], M. Gignac[171], M. Gilchriese[16], D. Gillberg[31], G. Gilles[178],
D.M. Gingrich[3,d], N. Giokaris[9,*], M.P. Giordani[167a,167c], F.M. Giorgi[22a], P.F. Giraud[138],
P. Giromini[59], D. Giugni[94a], F. Giuli[122], C. Giuliani[103], M. Giulini[60b], B.K. Gjelsten[121],
S. Gkaitatzis[156], I. Gkialas[9], E.L. Gkougkousis[139], L.K. Gladilin[101], C. Glasman[85], J. Glatzer[13],
P.C.F. Glaysher[45], A. Glazov[45], M. Goblirsch-Kolb[25], J. Godlewski[42], S. Goldfarb[91], T. Golling[52],
D. Golubkov[132], A. Gomes[128a,128b,128d], R. Gonçalo[128a], R. Goncalves Gama[26a],
J. Goncalves Pinto Firmino Da Costa[138], G. Gonella[51], L. Gonella[19], A. Gongadze[68],
S. González de la Hoz[170], S. Gonzalez-Sevilla[52], L. Goossens[32], P.A. Gorbounov[99],
H.A. Gordon[27], I. Gorelov[107], B. Gorini[32], E. Gorini[76a,76b], A. Gorišek[78], A.T. Goshaw[48],
C. Gössling[46], M.I. Gostkin[68], C.R. Goudet[119], D. Goujdami[137c], A.G. Goussiou[140],
N. Govender[147b,t], E. Gozani[154], L. Graber[57], I. Grabowska-Bold[41a], P.O.J. Gradin[168],
J. Gramling[52], E. Gramstad[121], S. Grancagnolo[17], V. Gratchev[125], P.M. Gravila[28f], C. Gray[56],
H.M. Gray[32], Z.D. Greenwood[82,u], C. Grefe[23], K. Gregersen[81], I.M. Gregor[45], P. Grenier[145],
K. Grevtsov[5], J. Griffiths[8], A.A. Grillo[139], K. Grimm[75], S. Grinstein[13,v], Ph. Gris[37],
J.-F. Grivaz[119], S. Groh[86], E. Gross[175], J. Grosse-Knetter[57], G.C. Grossi[82], Z.J. Grout[81],
A. Grummer[107], L. Guan[92], W. Guan[176], J. Guenther[65], F. Guescini[163a], D. Guest[166],
O. Gueta[155], B. Gui[113], E. Guido[53a,53b], T. Guillemin[5], S. Guindon[2], U. Gul[56], C. Gumpert[32],
J. Guo[36c], W. Guo[92], Y. Guo[36a], R. Gupta[43], S. Gupta[122], G. Gustavino[134a,134b], P. Gutierrez[115],
N.G. Gutierrez Ortiz[81], C. Gutschow[81], C. Guyot[138], M.P. Guzik[41a], C. Gwenlan[122],
C.B. Gwilliam[77], A. Haas[112], C. Haber[16], H.K. Hadavand[8], N. Haddad[137e], A. Hadef[88],
S. Hageböck[23], M. Hagihara[164], H. Hakobyan[180,*], M. Haleem[45], J. Haley[116], G. Halladjian[93],
G.D. Hallewell[88], K. Hamacher[178], P. Hamal[117], K. Hamano[172], A. Hamilton[147a],
G.N. Hamity[141], P.G. Hamnett[45], L. Han[36a], S. Han[35a], K. Hanagaki[69,w], K. Hanawa[157],
M. Hance[139], B. Haney[124], P. Hanke[60a], J.B. Hansen[39], J.D. Hansen[39], M.C. Hansen[23],
P.H. Hansen[39], K. Hara[164], A.S. Hard[176], T. Harenberg[178], F. Hariri[119], S. Harkusha[95],
R.D. Harrington[49], P.F. Harrison[173], N.M. Hartmann[102], M. Hasegawa[70], Y. Hasegawa[142],
A. Hasib[49], S. Hassani[138], S. Haug[18], R. Hauser[93], L. Hauswald[47], L.B. Havener[38],
M. Havranek[130], C.M. Hawkes[19], R.J. Hawkings[32], D. Hayakawa[159], D. Hayden[93], C.P. Hays[122],
J.M. Hays[79], H.S. Hayward[77], S.J. Haywood[133], S.J. Head[19], T. Heck[86], V. Hedberg[84],
L. Heelan[8], K.K. Heidegger[51], S. Heim[45], T. Heim[16], B. Heinemann[45,x], J.J. Heinrich[102],
L. Heinrich[112], C. Heinz[55], J. Hejbal[129], L. Helary[32], A. Held[171], S. Hellman[148a,148b],
C. Helsens[32], J. Henderson[122], R.C.W. Henderson[75], Y. Heng[176], S. Henkelmann[171],
A.M. Henriques Correia[32], S. Henrot-Versille[119], G.H. Herbert[17], H. Herde[25], V. Herget[177],

Y. Hernández Jiménez[147c], G. Herten[51], R. Hertenberger[102], L. Hervas[32], T.C. Herwig[124], G.G. Hesketh[81], N.P. Hessey[163a], J.W. Hetherly[43], S. Higashino[69], E. Higón-Rodriguez[170], E. Hill[172], J.C. Hill[30], K.H. Hiller[45], S.J. Hillier[19], I. Hinchliffe[16], M. Hirose[51], D. Hirschbuehl[178], B. Hiti[78], O. Hladik[129], X. Hoad[49], J. Hobbs[150], N. Hod[163a], M.C. Hodgkinson[141], P. Hodgson[141], A. Hoecker[32], M.R. Hoeferkamp[107], F. Hoenig[102], D. Hohn[23], T.R. Holmes[16], M. Homann[46], S. Honda[164], T. Honda[69], T.M. Hong[127], B.H. Hooberman[169], W.H. Hopkins[118], Y. Horii[105], A.J. Horton[144], J-Y. Hostachy[58], S. Hou[153], A. Hoummada[137a], J. Howarth[45], J. Hoya[74], M. Hrabovsky[117], I. Hristova[17], J. Hrivnac[119], T. Hryn'ova[5], A. Hrynevich[96], P.J. Hsu[63], S.-C. Hsu[140], Q. Hu[36a], S. Hu[36c], Y. Huang[35a], Z. Hubacek[130], F. Hubaut[88], F. Huegging[23], T.B. Huffman[122], E.W. Hughes[38], G. Hughes[75], M. Huhtinen[32], P. Huo[150], N. Huseynov[68,b], J. Huston[93], J. Huth[59], G. Iacobucci[52], G. Iakovidis[27], I. Ibragimov[143], L. Iconomidou-Fayard[119], Z. Idrissi[137e], P. Iengo[32], O. Igonkina[109,y], T. Iizawa[174], Y. Ikegami[69], M. Ikeno[69], Y. Ilchenko[11,z], D. Iliadis[156], N. Ilic[145], G. Introzzi[123a,123b], P. Ioannou[9,*], M. Iodice[136a], K. Iordanidou[38], V. Ippolito[59], N. Ishijima[120], M. Ishino[157], M. Ishitsuka[159], C. Issever[122], S. Istin[20a], F. Ito[164], J.M. Iturbe Ponce[87], R. Iuppa[162a,162b], H. Iwasaki[69], J.M. Izen[44], V. Izzo[106a], S. Jabbar[3], P. Jackson[1], V. Jain[2], K.B. Jakobi[86], K. Jakobs[51], S. Jakobsen[32], T. Jakoubek[129], D.O. Jamin[116], D.K. Jana[82], R. Jansky[65], J. Janssen[23], M. Janus[57], P.A. Janus[41a], G. Jarlskog[84], N. Javadov[68,b], T. Javůrek[51], M. Javurkova[51], F. Jeanneau[138], L. Jeanty[16], J. Jejelava[54a,aa], A. Jelinskas[173], P. Jenni[51,ab], C. Jeske[173], S. Jézéquel[5], H. Ji[176], J. Jia[150], H. Jiang[67], Y. Jiang[36a], Z. Jiang[145], S. Jiggins[81], J. Jimenez Pena[170], S. Jin[35a], A. Jinaru[28b], O. Jinnouchi[159], H. Jivan[147c], P. Johansson[141], K.A. Johns[7], C.A. Johnson[64], W.J. Johnson[140], K. Jon-And[148a,148b], R.W.L. Jones[75], S.D. Jones[151], S. Jones[7], T.J. Jones[77], J. Jongmanns[60a], P.M. Jorge[128a,128b], J. Jovicevic[163a], X. Ju[176], A. Juste Rozas[13,v], M.K. Köhler[175], A. Kaczmarska[42], M. Kado[119], H. Kagan[113], M. Kagan[145], S.J. Kahn[88], T. Kaji[174], E. Kajomovitz[48], C.W. Kalderon[84], A. Kaluza[86], S. Kama[43], A. Kamenshchikov[132], N. Kanaya[157], S. Kaneti[30], L. Kanjir[78], V.A. Kantserov[100], J. Kanzaki[69], B. Kaplan[112], L.S. Kaplan[176], D. Kar[147c], K. Karakostas[10], N. Karastathis[10], M.J. Kareem[57], E. Karentzos[10], S.N. Karpov[68], Z.M. Karpova[68], K. Karthik[112], V. Kartvelishvili[75], A.N. Karyukhin[132], K. Kasahara[164], L. Kashif[176], R.D. Kass[113], A. Kastanas[149], Y. Kataoka[157], C. Kato[157], A. Katre[52], J. Katzy[45], K. Kawade[105], K. Kawagoe[73], T. Kawamoto[157], G. Kawamura[57], E.F. Kay[77], V.F. Kazanin[111,c], R. Keeler[172], R. Kehoe[43], J.S. Keller[45], J.J. Kempster[80], H. Keoshkerian[161], O. Kepka[129], B.P. Kerševan[78], S. Kersten[178], R.A. Keyes[90], M. Khader[169], F. Khalil-zada[12], A. Khanov[116], A.G. Kharlamov[111,c], T. Kharlamova[111,c], A. Khodinov[160], T.J. Khoo[52], V. Khovanskiy[99,*], E. Khramov[68], J. Khubua[54b,ac], S. Kido[70], C.R. Kilby[80], H.Y. Kim[8], S.H. Kim[164], Y.K. Kim[33], N. Kimura[156], O.M. Kind[17], B.T. King[77], D. Kirchmeier[47], J. Kirk[133], A.E. Kiryunin[103], T. Kishimoto[157], D. Kisielewska[41a], K. Kiuchi[164], O. Kivernyk[5], E. Kladiva[146b], T. Klapdor-Kleingrothaus[51], M.H. Klein[38], M. Klein[77], U. Klein[77], K. Kleinknecht[86], P. Klimek[110], A. Klimentov[27], R. Klingenberg[46], T. Klingl[23], T. Klioutchnikova[32], E.-E. Kluge[60a], P. Kluit[109], S. Kluth[103], J. Knapik[42], E. Kneringer[65], E.B.F.G. Knoops[88], A. Knue[103], A. Kobayashi[157], D. Kobayashi[159], T. Kobayashi[157], M. Kobel[47], M. Kocian[145], P. Kodys[131], T. Koffas[31], E. Koffeman[109], N.M. Köhler[103], T. Koi[145], M. Kolb[60b], I. Koletsou[5], A.A. Komar[98,*], Y. Komori[157], T. Kondo[69], N. Kondrashova[36c], K. Köneke[51], A.C. König[108], T. Kono[69,ad], R. Konoplich[112,ae], N. Konstantinidis[81], R. Kopeliansky[64], S. Koperny[41a], A.K. Kopp[51], K. Korcyl[42], K. Kordas[156], A. Korn[81], A.A. Korol[111,c], I. Korolkov[13], E.V. Korolkova[141], O. Kortner[103], S. Kortner[103], T. Kosek[131], V.V. Kostyukhin[23], A. Kotwal[48], A. Koulouris[10], A. Kourkoumeli-Charalampidi[123a,123b], C. Kourkoumelis[9], E. Kourlitis[141], V. Kouskoura[27], A.B. Kowalewska[42], R. Kowalewski[172], T.Z. Kowalski[41a], C. Kozakai[157], W. Kozanecki[138], A.S. Kozhin[132], V.A. Kramarenko[101], G. Kramberger[78], D. Krasnopevtsev[100], M.W. Krasny[83],

A. Krasznahorkay[32], D. Krauss[103], A. Kravchenko[27], J.A. Kremer[41a], M. Kretz[60c],
J. Kretzschmar[77], K. Kreutzfeldt[55], P. Krieger[161], K. Krizka[33], K. Kroeninger[46], H. Kroha[103],
J. Kroll[129], J. Kroll[124], J. Kroseberg[23], J. Krstic[14], U. Kruchonak[68], H. Krüger[23], N. Krumnack[67],
M.C. Kruse[48], M. Kruskal[24], T. Kubota[91], H. Kucuk[81], S. Kuday[4b], J.T. Kuechler[178], S. Kuehn[32],
A. Kugel[60c], F. Kuger[177], T. Kuhl[45], V. Kukhtin[68], R. Kukla[88], Y. Kulchitsky[95], S. Kuleshov[34b],
Y.P. Kulinich[169], M. Kuna[134a,134b], T. Kunigo[71], A. Kupco[129], O. Kuprash[155], H. Kurashige[70],
L.L. Kurchaninov[163a], Y.A. Kurochkin[95], M.G. Kurth[35a], V. Kus[129], E.S. Kuwertz[172],
M. Kuze[159], J. Kvita[117], T. Kwan[172], D. Kyriazopoulos[141], A. La Rosa[103],
J.L. La Rosa Navarro[26d], L. La Rotonda[40a,40b], C. Lacasta[170], F. Lacava[134a,134b], J. Lacey[45],
H. Lacker[17], D. Lacour[83], E. Ladygin[68], R. Lafaye[5], B. Laforge[83], T. Lagouri[179], S. Lai[57],
S. Lammers[64], W. Lampl[7], E. Lançon[27], U. Landgraf[51], M.P.J. Landon[79], M.C. Lanfermann[52],
V.S. Lang[60a], J.C. Lange[13], A.J. Lankford[166], F. Lanni[27], K. Lantzsch[23], A. Lanza[123a],
A. Lapertosa[53a,53b], S. Laplace[83], J.F. Laporte[138], T. Lari[94a], F. Lasagni Manghi[22a,22b],
M. Lassnig[32], P. Laurelli[50], W. Lavrijsen[16], A.T. Law[139], P. Laycock[77], T. Lazovich[59],
M. Lazzaroni[94a,94b], B. Le[91], O. Le Dortz[83], E. Le Guirriec[88], E.P. Le Quilleuc[138], M. LeBlanc[172],
T. LeCompte[6], F. Ledroit-Guillon[58], C.A. Lee[27], G.R. Lee[133,af], S.C. Lee[153], L. Lee[59],
B. Lefebvre[90], G. Lefebvre[83], M. Lefebvre[172], F. Legger[102], C. Leggett[16], A. Lehan[77],
G. Lehmann Miotto[32], X. Lei[7], W.A. Leight[45], M.A.L. Leite[26d], R. Leitner[131], D. Lellouch[175],
B. Lemmer[57], K.J.C. Leney[81], T. Lenz[23], B. Lenzi[32], R. Leone[7], S. Leone[126a,126b],
C. Leonidopoulos[49], G. Lerner[151], C. Leroy[97], A.A.J. Lesage[138], C.G. Lester[30], M. Levchenko[125],
J. Levêque[5], D. Levin[92], L.J. Levinson[175], M. Levy[19], D. Lewis[79], B. Li[36a,s], C. Li[36a], H. Li[150],
L. Li[36c], Q. Li[35a], S. Li[48], X. Li[36c], Y. Li[143], Z. Liang[35a], B. Liberti[135a], A. Liblong[161], K. Lie[169],
J. Liebal[23], W. Liebig[15], A. Limosani[152], S.C. Lin[153,ag], T.H. Lin[86], B.E. Lindquist[150],
A.E. Lionti[52], E. Lipeles[124], A. Lipniacka[15], M. Lisovyi[60b], T.M. Liss[169], A. Lister[171],
A.M. Litke[139], B. Liu[153,ah], H. Liu[92], H. Liu[27], J.K.K. Liu[122], J. Liu[36b], J.B. Liu[36a], K. Liu[88],
L. Liu[169], M. Liu[36a], Y.L. Liu[36a], Y. Liu[36a], M. Livan[123a,123b], A. Lleres[58], J. Llorente Merino[35a],
S.L. Lloyd[79], C.Y. Lo[62b], F. Lo Sterzo[153], E.M. Lobodzinska[45], P. Loch[7], F.K. Loebinger[87],
K.M. Loew[25], A. Loginov[179,*], T. Lohse[17], K. Lohwasser[45], M. Lokajicek[129], B.A. Long[24],
J.D. Long[169], R.E. Long[75], L. Longo[76a,76b], K.A. Looper[113], J.A. Lopez[34b], D. Lopez Mateos[59],
I. Lopez Paz[13], A. Lopez Solis[83], J. Lorenz[102], N. Lorenzo Martinez[5], M. Losada[21], P.J. Lösel[102],
X. Lou[35a], A. Lounis[119], J. Love[6], P.A. Love[75], H. Lu[62a], N. Lu[92], Y.J. Lu[63], H.J. Lubatti[140],
C. Luci[134a,134b], A. Lucotte[58], C. Luedtke[51], F. Luehring[64], W. Lukas[65], L. Luminari[134a],
O. Lundberg[148a,148b], B. Lund-Jensen[149], P.M. Luzi[83], D. Lynn[27], R. Lysak[129], E. Lytken[84],
V. Lyubushkin[68], H. Ma[27], L.L. Ma[36b], Y. Ma[36b], G. Maccarrone[50], A. Macchiolo[103],
C.M. Macdonald[141], B. Maček[78], J. Machado Miguens[124,128b], D. Madaffari[88], R. Madar[37],
H.J. Maddocks[168], W.F. Mader[47], A. Madsen[45], J. Maeda[70], S. Maeland[15], T. Maeno[27],
A.S. Maevskiy[101], E. Magradze[57], J. Mahlstedt[109], C. Maiani[119], C. Maidantchik[26a],
A.A. Maier[103], T. Maier[102], A. Maio[128a,128b,128d], S. Majewski[118], Y. Makida[69], N. Makovec[119],
B. Malaescu[83], Pa. Malecki[42], V.P. Maleev[125], F. Malek[58], U. Mallik[66], D. Malon[6], C. Malone[30],
S. Maltezos[10], S. Malyukov[32], J. Mamuzic[170], G. Mancini[50], L. Mandelli[94a], I. Mandić[78],
J. Maneira[128a,128b], L. Manhaes de Andrade Filho[26b], J. Manjarres Ramos[163b], A. Mann[102],
A. Manousos[32], B. Mansoulie[138], J.D. Mansour[35a], R. Mantifel[90], M. Mantoani[57],
S. Manzoni[94a,94b], L. Mapelli[32], G. Marceca[29], L. March[52], L. Marchese[122], G. Marchiori[83],
M. Marcisovsky[129], M. Marjanovic[37], D.E. Marley[92], F. Marroquim[26a], S.P. Marsden[87],
Z. Marshall[16], M.U.F Martensson[168], S. Marti-Garcia[170], C.B. Martin[113], T.A. Martin[173],
V.J. Martin[49], B. Martin dit Latour[15], M. Martinez[13,v], V.I. Martinez Outschoorn[169],
S. Martin-Haugh[133], V.S. Martoiu[28b], A.C. Martyniuk[81], A. Marzin[32], L. Masetti[86],
T. Mashimo[157], R. Mashinistov[98], J. Masik[87], A.L. Maslennikov[111,c], L. Massa[135a,135b],

P. Mastrandrea[5], A. Mastroberardino[40a,40b], T. Masubuchi[157], P. Mättig[178], J. Maurer[28b],
S.J. Maxfield[77], D.A. Maximov[111,c], R. Mazini[153], I. Maznas[156], S.M. Mazza[94a,94b],
N.C. Mc Fadden[107], G. Mc Goldrick[161], S.P. Mc Kee[92], A. McCarn[92], R.L. McCarthy[150],
T.G. McCarthy[103], L.I. McClymont[81], E.F. McDonald[91], J.A. Mcfayden[81], G. Mchedlidze[57],
S.J. McMahon[133], P.C. McNamara[91], R.A. McPherson[172,o], S. Meehan[140], T.J. Megy[51],
S. Mehlhase[102], A. Mehta[77], T. Meideck[58], K. Meier[60a], C. Meineck[102], B. Meirose[44],
D. Melini[170,ai], B.R. Mellado Garcia[147c], M. Melo[146a], F. Meloni[18], S.B. Menary[87], L. Meng[77],
X.T. Meng[92], A. Mengarelli[22a,22b], S. Menke[103], E. Meoni[40a,40b], S. Mergelmeyer[17], P. Mermod[52],
L. Merola[106a,106b], C. Meroni[94a], F.S. Merritt[33], A. Messina[134a,134b], J. Metcalfe[6], A.S. Mete[166],
C. Meyer[124], J-P. Meyer[138], J. Meyer[109], H. Meyer Zu Theenhausen[60a], F. Miano[151],
R.P. Middleton[133], S. Miglioranzi[53a,53b], L. Mijović[49], G. Mikenberg[175], M. Mikestikova[129],
M. Mikuž[78], M. Milesi[91], A. Milic[27], D.W. Miller[33], C. Mills[49], A. Milov[175],
D.A. Milstead[148a,148b], A.A. Minaenko[132], Y. Minami[157], I.A. Minashvili[68], A.I. Mincer[112],
B. Mindur[41a], M. Mineev[68], Y. Minegishi[157], Y. Ming[176], L.M. Mir[13], K.P. Mistry[124],
T. Mitani[174], J. Mitrevski[102], V.A. Mitsou[170], A. Miucci[18], P.S. Miyagawa[141], A. Mizukami[69],
J.U. Mjörnmark[84], M. Mlynarikova[131], T. Moa[148a,148b], K. Mochizuki[97], P. Mogg[51],
S. Mohapatra[38], S. Molander[148a,148b], R. Moles-Valls[23], R. Monden[71], M.C. Mondragon[93],
K. Mönig[45], J. Monk[39], E. Monnier[88], A. Montalbano[150], J. Montejo Berlingen[32], F. Monticelli[74],
S. Monzani[94a,94b], R.W. Moore[3], N. Morange[119], D. Moreno[21], M. Moreno Llácer[57],
P. Morettini[53a], S. Morgenstern[32], D. Mori[144], T. Mori[157], M. Morii[59], M. Morinaga[157],
V. Morisbak[121], A.K. Morley[152], G. Mornacchi[32], J.D. Morris[79], L. Morvaj[150], P. Moschovakos[10],
M. Mosidze[54b], H.J. Moss[141], J. Moss[145,aj], K. Motohashi[159], R. Mount[145], E. Mountricha[27],
E.J.W. Moyse[89], S. Muanza[88], R.D. Mudd[19], F. Mueller[103], J. Mueller[127], R.S.P. Mueller[102],
D. Muenstermann[75], P. Mullen[56], G.A. Mullier[18], F.J. Munoz Sanchez[87], W.J. Murray[173,133],
H. Musheghyan[57], M. Muškinja[78], A.G. Myagkov[132,ak], M. Myska[130], B.P. Nachman[16],
O. Nackenhorst[52], K. Nagai[122], R. Nagai[69,ad], K. Nagano[69], Y. Nagasaka[61], K. Nagata[164],
M. Nagel[51], E. Nagy[88], A.M. Nairz[32], Y. Nakahama[105], K. Nakamura[69], T. Nakamura[157],
I. Nakano[114], R.F. Naranjo Garcia[45], R. Narayan[11], D.I. Narrias Villar[60a], I. Naryshkin[125],
T. Naumann[45], G. Navarro[21], R. Nayyar[7], H.A. Neal[92], P.Yu. Nechaeva[98], T.J. Neep[138],
A. Negri[123a,123b], M. Negrini[22a], S. Nektarijevic[108], C. Nellist[119], A. Nelson[166], M.E. Nelson[122],
S. Nemecek[129], P. Nemethy[112], A.A. Nepomuceno[26a], M. Nessi[32,al], M.S. Neubauer[169],
M. Neumann[178], P.R. Newman[19], T.Y. Ng[62c], T. Nguyen Manh[97], R.B. Nickerson[122],
R. Nicolaidou[138], J. Nielsen[139], V. Nikolaenko[132,ak], I. Nikolic-Audit[83], K. Nikolopoulos[19],
J.K. Nilsen[121], P. Nilsson[27], Y. Ninomiya[157], A. Nisati[134a], N. Nishu[35c], R. Nisius[103], T. Nobe[157],
Y. Noguchi[71], M. Nomachi[120], I. Nomidis[31], M.A. Nomura[27], T. Nooney[79], M. Nordberg[32],
N. Norjoharuddeen[122], O. Novgorodova[47], S. Nowak[103], M. Nozaki[69], L. Nozka[117], K. Ntekas[166],
E. Nurse[81], F. Nuti[91], K. O'connor[25], D.C. O'Neil[144], A.A. O'Rourke[45], V. O'Shea[56],
F.G. Oakham[31,d], H. Oberlack[103], T. Obermann[23], J. Ocariz[83], A. Ochi[70], I. Ochoa[38],
J.P. Ochoa-Ricoux[34a], S. Oda[73], S. Odaka[69], H. Ogren[64], A. Oh[87], S.H. Oh[48], C.C. Ohm[16],
H. Ohman[168], H. Oide[53a,53b], H. Okawa[164], Y. Okumura[157], T. Okuyama[69], A. Olariu[28b],
L.F. Oleiro Seabra[128a], S.A. Olivares Pino[49], D. Oliveira Damazio[27], A. Olszewski[42],
J. Olszowska[42], A. Onofre[128a,128e], K. Onogi[105], P.U.E. Onyisi[11,z], M.J. Oreglia[33], Y. Oren[155],
D. Orestano[136a,136b], N. Orlando[62b], R.S. Orr[161], B. Osculati[53a,53b,*], R. Ospanov[87],
G. Otero y Garzon[29], H. Otono[73], M. Ouchrif[137d], F. Ould-Saada[121], A. Ouraou[138],
K.P. Oussoren[109], Q. Ouyang[35a], M. Owen[56], R.E. Owen[19], V.E. Ozcan[20a], N. Ozturk[8],
K. Pachal[144], A. Pacheco Pages[13], L. Pacheco Rodriguez[138], C. Padilla Aranda[13],
S. Pagan Griso[16], M. Paganini[179], F. Paige[27], P. Pais[89], G. Palacino[64], S. Palazzo[40a,40b],
S. Palestini[32], M. Palka[41b], D. Pallin[37], E.St. Panagiotopoulou[10], I. Panagoulias[10],

C.E. Pandini[83], J.G. Panduro Vazquez[80], P. Pani[32], S. Panitkin[27], D. Pantea[28b], L. Paolozzi[52],
Th.D. Papadopoulou[10], K. Papageorgiou[9], A. Paramonov[6], D. Paredes Hernandez[179],
A.J. Parker[75], M.A. Parker[30], K.A. Parker[45], F. Parodi[53a,53b], J.A. Parsons[38], U. Parzefall[51],
V.R. Pascuzzi[161], J.M. Pasner[139], E. Pasqualucci[134a], S. Passaggio[53a], Fr. Pastore[80],
S. Pataraia[178], J.R. Pater[87], T. Pauly[32], J. Pearce[172], B. Pearson[103], S. Pedraza Lopez[170],
R. Pedro[128a,128b], S.V. Peleganchuk[111,c], O. Penc[129], C. Peng[35a], H. Peng[36a], J. Penwell[64],
B.S. Peralva[26b], M.M. Perego[138], D.V. Perepelitsa[27], L. Perini[94a,94b], H. Pernegger[32],
S. Perrella[106a,106b], R. Peschke[45], V.D. Peshekhonov[68,*], K. Peters[45], R.F.Y. Peters[87],
B.A. Petersen[32], T.C. Petersen[39], E. Petit[58], A. Petridis[1], C. Petridou[156], P. Petroff[119],
E. Petrolo[134a], M. Petrov[122], F. Petrucci[136a,136b], N.E. Pettersson[89], A. Peyaud[138], R. Pezoa[34b],
P.W. Phillips[133], G. Piacquadio[150], E. Pianori[173], A. Picazio[89], E. Piccaro[79], M.A. Pickering[122],
R. Piegaia[29], J.E. Pilcher[33], A.D. Pilkington[87], A.W.J. Pin[87], M. Pinamonti[167a,167c,am],
J.L. Pinfold[3], H. Pirumov[45], M. Pitt[175], L. Plazak[146a], M.-A. Pleier[27], V. Pleskot[86],
E. Plotnikova[68], D. Pluth[67], P. Podberezko[111], R. Poettgen[148a,148b], R. Poggi[123a,123b],
L. Poggioli[119], D. Pohl[23], G. Polesello[123a], A. Poley[45], A. Policicchio[40a,40b], R. Polifka[32],
A. Polini[22a], C.S. Pollard[56], V. Polychronakos[27], K. Pommès[32], D. Ponomarenko[100],
L. Pontecorvo[134a], B.G. Pope[93], G.A. Popeneciu[28d], A. Poppleton[32], S. Pospisil[130],
K. Potamianos[16], I.N. Potrap[68], C.J. Potter[30], G. Poulard[32], J. Poveda[32],
M.E. Pozo Astigarraga[32], P. Pralavorio[88], A. Pranko[16], S. Prell[67], D. Price[87], L.E. Price[6],
M. Primavera[76a], S. Prince[90], N. Proklova[100], K. Prokofiev[62c], F. Prokoshin[34b],
S. Protopopescu[27], J. Proudfoot[6], M. Przybycien[41a], D. Puddu[136a,136b], A. Puri[169], P. Puzo[119],
J. Qian[92], G. Qin[56], Y. Qin[87], A. Quadt[57], M. Queitsch-Maitland[45], D. Quilty[56], S. Raddum[121],
V. Radeka[27], V. Radescu[122], S.K. Radhakrishnan[150], P. Radloff[118], P. Rados[91], F. Ragusa[94a,94b],
G. Rahal[182], J.A. Raine[87], S. Rajagopalan[27], C. Rangel-Smith[168], M.G. Ratti[94a,94b],
D.M. Rauch[45], F. Rauscher[102], S. Rave[86], T. Ravenscroft[56], I. Ravinovich[175], J.H. Rawling[87],
M. Raymond[32], A.L. Read[121], N.P. Readioff[77], M. Reale[76a,76b], D.M. Rebuzzi[123a,123b],
A. Redelbach[177], G. Redlinger[27], R. Reece[139], R.G. Reed[147c], K. Reeves[44], L. Rehnisch[17],
J. Reichert[124], A. Reiss[86], C. Rembser[32], H. Ren[35a], M. Rescigno[134a], S. Resconi[94a],
E.D. Resseguie[124], S. Rettie[171], E. Reynolds[19], O.L. Rezanova[111,c], P. Reznicek[131], R. Rezvani[97],
R. Richter[103], S. Richter[81], E. Richter-Was[41b], O. Ricken[23], M. Ridel[83], P. Rieck[103],
C.J. Riegel[178], J. Rieger[57], O. Rifki[115], M. Rijssenbeek[150], A. Rimoldi[123a,123b], M. Rimoldi[18],
L. Rinaldi[22a], B. Ristić[52], E. Ritsch[32], I. Riu[13], F. Rizatdinova[116], E. Rizvi[79], C. Rizzi[13],
R.T. Roberts[87], S.H. Robertson[90,o], A. Robichaud-Veronneau[90], D. Robinson[30],
J.E.M. Robinson[45], A. Robson[56], E. Rocco[86], C. Roda[126a,126b], Y. Rodina[88,an],
S. Rodriguez Bosca[170], A. Rodriguez Perez[13], D. Rodriguez Rodriguez[170], S. Roe[32], C.S. Rogan[59],
O. Røhne[121], J. Roloff[59], A. Romaniouk[100], M. Romano[22a,22b], S.M. Romano Saez[37],
E. Romero Adam[170], N. Rompotis[77], M. Ronzani[51], L. Roos[83], S. Rosati[134a], K. Rosbach[51],
P. Rose[139], N.-A. Rosien[57], V. Rossetti[148a,148b], E. Rossi[106a,106b], L.P. Rossi[53a], J.H.N. Rosten[30],
R. Rosten[140], M. Rotaru[28b], I. Roth[175], J. Rothberg[140], D. Rousseau[119], A. Rozanov[88],
Y. Rozen[154], X. Ruan[147c], F. Rubbo[145], F. Rühr[51], A. Ruiz-Martinez[31], Z. Rurikova[51],
N.A. Rusakovich[68], H.L. Russell[140], J.P. Rutherfoord[7], N. Ruthmann[32], Y.F. Ryabov[125],
M. Rybar[169], G. Rybkin[119], S. Ryu[6], A. Ryzhov[132], G.F. Rzehorz[57], A.F. Saavedra[152],
G. Sabato[109], S. Sacerdoti[29], H.F-W. Sadrozinski[139], R. Sadykov[68], F. Safai Tehrani[134a],
P. Saha[110], M. Sahinsoy[60a], M. Saimpert[45], M. Saito[157], T. Saito[157], H. Sakamoto[157],
Y. Sakurai[174], G. Salamanna[136a,136b], J.E. Salazar Loyola[34b], D. Salek[109], P.H. Sales De Bruin[168],
D. Salihagic[103], A. Salnikov[145], J. Salt[170], D. Salvatore[40a,40b], F. Salvatore[151],
A. Salvucci[62a,62b,62c], A. Salzburger[32], D. Sammel[51], D. Sampsonidis[156], J. Sánchez[170],
V. Sanchez Martinez[170], A. Sanchez Pineda[167a,167c], H. Sandaker[121], R.L. Sandbach[79],

C.O. Sander[45], M. Sandhoff[178], C. Sandoval[21], D.P.C. Sankey[133], M. Sannino[53a,53b], A. Sansoni[50],
C. Santoni[37], R. Santonico[135a,135b], H. Santos[128a], I. Santoyo Castillo[151], K. Sapp[127],
A. Sapronov[68], J.G. Saraiva[128a,128d], B. Sarrazin[23], O. Sasaki[69], K. Sato[164], E. Sauvan[5],
G. Savage[80], P. Savard[161,d], N. Savic[103], C. Sawyer[133], L. Sawyer[82,u], J. Saxon[33], C. Sbarra[22a],
A. Sbrizzi[22a,22b], T. Scanlon[81], D.A. Scannicchio[166], M. Scarcella[152], V. Scarfone[40a,40b],
J. Schaarschmidt[140], P. Schacht[103], B.M. Schachtner[102], D. Schaefer[32], L. Schaefer[124],
R. Schaefer[45], J. Schaeffer[86], S. Schaepe[23], S. Schaetzel[60b], U. Schäfer[86], A.C. Schaffer[119],
D. Schaile[102], R.D. Schamberger[150], V. Scharf[60a], V.A. Schegelsky[125], D. Scheirich[131],
M. Schernau[166], C. Schiavi[53a,53b], S. Schier[139], L.K. Schildgen[23], C. Schillo[51], M. Schioppa[40a,40b],
S. Schlenker[32], K.R. Schmidt-Sommerfeld[103], K. Schmieden[32], C. Schmitt[86], S. Schmitt[45],
S. Schmitz[86], U. Schnoor[51], L. Schoeffel[138], A. Schoening[60b], B.D. Schoenrock[93], E. Schopf[23],
M. Schott[86], J.F.P. Schouwenberg[108], J. Schovancova[181], S. Schramm[52], N. Schuh[86], A. Schulte[86],
M.J. Schultens[23], H.-C. Schultz-Coulon[60a], H. Schulz[17], M. Schumacher[51], B.A. Schumm[139],
Ph. Schune[138], A. Schwartzman[145], T.A. Schwarz[92], H. Schweiger[87], Ph. Schwemling[138],
R. Schwienhorst[93], J. Schwindling[138], T. Schwindt[23], A. Sciandra[23], G. Sciolla[25], F. Scuri[126a,126b],
F. Scutti[91], J. Searcy[92], P. Seema[23], S.C. Seidel[107], A. Seiden[139], J.M. Seixas[26a],
G. Sekhniaidze[106a], K. Sekhon[92], S.J. Sekula[43], N. Semprini-Cesari[22a,22b], C. Serfon[121],
L. Serin[119], L. Serkin[167a,167b], M. Sessa[136a,136b], R. Seuster[172], H. Severini[115], T. Sfiligoj[78],
F. Sforza[32], A. Sfyrla[52], E. Shabalina[57], N.W. Shaikh[148a,148b], L.Y. Shan[35a], R. Shang[169],
J.T. Shank[24], M. Shapiro[16], P.B. Shatalov[99], K. Shaw[167a,167b], S.M. Shaw[87],
A. Shcherbakova[148a,148b], C.Y. Shehu[151], Y. Shen[115], P. Sherwood[81], L. Shi[153,ao], S. Shimizu[70],
C.O. Shimmin[179], M. Shimojima[104], I.P.J. Shipsey[122], S. Shirabe[73], M. Shiyakova[68,ap],
J. Shlomi[175], A. Shmeleva[98], D. Shoaleh Saadi[97], M.J. Shochet[33], S. Shojaii[94a], D.R. Shope[115],
S. Shrestha[113], E. Shulga[100], M.A. Shupe[7], P. Sicho[129], A.M. Sickles[169], P.E. Sidebo[149],
E. Sideras Haddad[147c], O. Sidiropoulou[177], D. Sidorov[116], A. Sidoti[22a,22b], F. Siegert[47],
Dj. Sijacki[14], J. Silva[128a,128d], S.B. Silverstein[148a], V. Simak[130], Lj. Simic[14], S. Simion[119],
E. Simioni[86], B. Simmons[81], M. Simon[86], P. Sinervo[161], N.B. Sinev[118], M. Sioli[22a,22b],
G. Siragusa[177], I. Siral[92], S.Yu. Sivoklokov[101], J. Sjölin[148a,148b], M.B. Skinner[75], P. Skubic[115],
M. Slater[19], T. Slavicek[130], M. Slawinska[109], K. Sliwa[165], R. Slovak[131], V. Smakhtin[175],
B.H. Smart[5], J. Smiesko[146a], N. Smirnov[100], S.Yu. Smirnov[100], Y. Smirnov[100],
L.N. Smirnova[101,aq], O. Smirnova[84], J.W. Smith[57], M.N.K. Smith[38], R.W. Smith[38],
M. Smizanska[75], K. Smolek[130], A.A. Snesarev[98], I.M. Snyder[118], S. Snyder[27], R. Sobie[172,o],
F. Socher[47], A. Soffer[155], D.A. Soh[153], G. Sokhrannyi[78], C.A. Solans Sanchez[32], M. Solar[130],
E.Yu. Soldatov[100], U. Soldevila[170], A.A. Solodkov[132], A. Soloshenko[68], O.V. Solovyanov[132],
V. Solovyev[125], P. Sommer[51], H. Son[165], H.Y. Song[36a,ar], A. Sopczak[130], D. Sosa[60b],
C.L. Sotiropoulou[126a,126b], R. Soualah[167a,167c], A.M. Soukharev[111,c], D. South[45], B.C. Sowden[80],
S. Spagnolo[76a,76b], M. Spalla[126a,126b], M. Spangenberg[173], F. Spanò[80], D. Sperlich[17], F. Spettel[103],
T.M. Spieker[60a], R. Spighi[22a], G. Spigo[32], L.A. Spiller[91], M. Spousta[131], R.D. St. Denis[56,*],
A. Stabile[94a], R. Stamen[60a], S. Stamm[17], E. Stanecka[42], R.W. Stanek[6], C. Stanescu[136a],
M.M. Stanitzki[45], S. Stapnes[121], E.A. Starchenko[132], G.H. Stark[33], J. Stark[58], S.H Stark[39],
P. Staroba[129], P. Starovoitov[60a], S. Stärz[32], R. Staszewski[42], P. Steinberg[27], B. Stelzer[144],
H.J. Stelzer[32], O. Stelzer-Chilton[163a], H. Stenzel[55], G.A. Stewart[56], M.C. Stockton[118],
M. Stoebe[90], G. Stoicea[28b], P. Stolte[57], S. Stonjek[103], A.R. Stradling[8], A. Straessner[47],
M.E. Stramaglia[18], J. Strandberg[149], S. Strandberg[148a,148b], A. Strandlie[121], M. Strauss[115],
P. Strizenec[146b], R. Ströhmer[177], D.M. Strom[118], R. Stroynowski[43], A. Strubig[108], S.A. Stucci[27],
B. Stugu[15], N.A. Styles[45], D. Su[145], J. Su[127], S. Suchek[60a], Y. Sugaya[120], M. Suk[130], V.V. Sulin[98],
S. Sultansoy[4c], T. Sumida[71], S. Sun[59], X. Sun[3], K. Suruliz[151], C.J.E. Suster[152], M.R. Sutton[151],
S. Suzuki[69], M. Svatos[129], M. Swiatlowski[33], S.P. Swift[2], I. Sykora[146a], T. Sykora[131], D. Ta[51],

K. Tackmann[45], J. Taenzer[155], A. Taffard[166], R. Tafirout[163a], N. Taiblum[155], H. Takai[27],
R. Takashima[72], T. Takeshita[142], Y. Takubo[69], M. Talby[88], A.A. Talyshev[111,c], J. Tanaka[157],
M. Tanaka[159], R. Tanaka[119], S. Tanaka[69], R. Tanioka[70], B.B. Tannenwald[113], S. Tapia Araya[34b],
S. Tapprogge[86], S. Tarem[154], G.F. Tartarelli[94a], P. Tas[131], M. Tasevsky[129], T. Tashiro[71],
E. Tassi[40a,40b], A. Tavares Delgado[128a,128b], Y. Tayalati[137e], A.C. Taylor[107], G.N. Taylor[91],
P.T.E. Taylor[91], W. Taylor[163b], P. Teixeira-Dias[80], D. Temple[144], H. Ten Kate[32], P.K. Teng[153],
J.J. Teoh[120], F. Tepel[178], S. Terada[69], K. Terashi[157], J. Terron[85], S. Terzo[13], M. Testa[50],
R.J. Teuscher[161,o], T. Theveneaux-Pelzer[88], J.P. Thomas[19], J. Thomas-Wilsker[80],
P.D. Thompson[19], A.S. Thompson[56], L.A. Thomsen[179], E. Thomson[124], M.J. Tibbetts[16],
R.E. Ticse Torres[88], V.O. Tikhomirov[98,as], Yu.A. Tikhonov[111,c], S. Timoshenko[100], P. Tipton[179],
S. Tisserant[88], K. Todome[159], S. Todorova-Nova[5], J. Tojo[73], S. Tokár[146a], K. Tokushuku[69],
E. Tolley[59], L. Tomlinson[87], M. Tomoto[105], L. Tompkins[145,at], K. Toms[107], B. Tong[59],
P. Tornambe[51], E. Torrence[118], H. Torres[144], E. Torró Pastor[140], J. Toth[88,au], F. Touchard[88],
D.R. Tovey[141], C.J. Treado[112], T. Trefzger[177], F. Tresoldi[151], A. Tricoli[27], I.M. Trigger[163a],
S. Trincaz-Duvoid[83], M.F. Tripiana[13], W. Trischuk[161], B. Trocmé[58], A. Trofymov[45],
C. Troncon[94a], M. Trottier-McDonald[16], M. Trovatelli[172], L. Truong[167a,167c], M. Trzebinski[42],
A. Trzupek[42], K.W. Tsang[62a], J.C-L. Tseng[122], P.V. Tsiareshka[95], G. Tsipolitis[10],
N. Tsirintanis[9], S. Tsiskaridze[13], V. Tsiskaridze[51], E.G. Tskhadadze[54a], K.M. Tsui[62a],
I.I. Tsukerman[99], V. Tsulaia[16], S. Tsuno[69], D. Tsybychev[150], Y. Tu[62b], A. Tudorache[28b],
V. Tudorache[28b], T.T. Tulbure[28a], A.N. Tuna[59], S.A. Tupputi[22a,22b], S. Turchikhin[68],
D. Turgeman[175], I. Turk Cakir[4b,av], R. Turra[94a], P.M. Tuts[38], G. Ucchielli[22a,22b], I. Ueda[69],
M. Ughetto[148a,148b], F. Ukegawa[164], G. Unal[32], A. Undrus[27], G. Unel[166], F.C. Ungaro[91],
Y. Unno[69], C. Unverdorben[102], J. Urban[146b], P. Urquijo[91], P. Urrejola[86], G. Usai[8], J. Usui[69],
L. Vacavant[88], V. Vacek[130], B. Vachon[90], C. Valderanis[102], E. Valdes Santurio[148a,148b],
S. Valentinetti[22a,22b], A. Valero[170], L. Valéry[13], S. Valkar[131], A. Vallier[5], J.A. Valls Ferrer[170],
W. Van Den Wollenberg[109], H. van der Graaf[109], N. van Eldik[154], P. van Gemmeren[6],
J. Van Nieuwkoop[144], I. van Vulpen[109], M.C. van Woerden[109], M. Vanadia[134a,134b], W. Vandelli[32],
R. Vanguri[124], A. Vaniachine[160], P. Vankov[109], G. Vardanyan[180], R. Vari[134a], E.W. Varnes[7],
C. Varni[53a,53b], T. Varol[43], D. Varouchas[119], A. Vartapetian[8], K.E. Varvell[152], J.G. Vasquez[179],
G.A. Vasquez[34b], F. Vazeille[37], T. Vazquez Schroeder[90], J. Veatch[57], V. Veeraraghavan[7],
L.M. Veloce[161], F. Veloso[128a,128c], S. Veneziano[134a], A. Ventura[76a,76b], M. Venturi[172],
N. Venturi[161], A. Venturini[25], V. Vercesi[123a], M. Verducci[136a,136b], W. Verkerke[109],
J.C. Vermeulen[109], M.C. Vetterli[144,d], N. Viaux Maira[34b], O. Viazlo[84], I. Vichou[169,*],
T. Vickey[141], O.E. Vickey Boeriu[141], G.H.A. Viehhauser[122], S. Viel[16], L. Vigani[122],
M. Villa[22a,22b], M. Villaplana Perez[94a,94b], E. Vilucchi[50], M.G. Vincter[31], V.B. Vinogradov[68],
A. Vishwakarma[45], C. Vittori[22a,22b], I. Vivarelli[151], S. Vlachos[10], M. Vlasak[130], M. Vogel[178],
P. Vokac[130], G. Volpi[126a,126b], H. von der Schmitt[103], E. von Toerne[23], V. Vorobel[131],
K. Vorobev[100], M. Vos[170], R. Voss[32], J.H. Vossebeld[77], N. Vranjes[14], M. Vranjes Milosavljevic[14],
V. Vrba[130], M. Vreeswijk[109], R. Vuillermet[32], I. Vukotic[33], P. Wagner[23], W. Wagner[178],
J. Wagner-Kuhr[102], H. Wahlberg[74], S. Wahrmund[47], J. Wakabayashi[105], J. Walder[75],
R. Walker[102], W. Walkowiak[143], V. Wallangen[148a,148b], C. Wang[35b], C. Wang[36b,aw], F. Wang[176],
H. Wang[16], H. Wang[3], J. Wang[45], J. Wang[152], Q. Wang[115], R. Wang[6], S.M. Wang[153], T. Wang[38],
W. Wang[153,ax], W. Wang[36a], Z. Wang[36c], C. Wanotayaroj[118], A. Warburton[90], C.P. Ward[30],
D.R. Wardrope[81], A. Washbrook[49], P.M. Watkins[19], A.T. Watson[19], M.F. Watson[19], G. Watts[140],
S. Watts[87], B.M. Waugh[81], A.F. Webb[11], S. Webb[86], M.S. Weber[18], S.W. Weber[177],
S.A. Weber[31], J.S. Webster[6], A.R. Weidberg[122], B. Weinert[64], J. Weingarten[57], C. Weiser[51],
H. Weits[109], P.S. Wells[32], T. Wenaus[27], T. Wengler[32], S. Wenig[32], N. Wermes[23], M.D. Werner[67],
P. Werner[32], M. Wessels[60a], K. Whalen[118], N.L. Whallon[140], A.M. Wharton[75], A. White[8],

M.J. White[1], R. White[34b], D. Whiteson[166], F.J. Wickens[133], W. Wiedenmann[176], M. Wielers[133], C. Wiglesworth[39], L.A.M. Wiik-Fuchs[23], A. Wildauer[103], F. Wilk[87], H.G. Wilkens[32], H.H. Williams[124], S. Williams[109], C. Willis[93], S. Willocq[89], J.A. Wilson[19], I. Wingerter-Seez[5], E. Winkels[151], F. Winklmeier[118], O.J. Winston[151], B.T. Winter[23], M. Wittgen[145], M. Wobisch[82,u], T.M.H. Wolf[109], R. Wolff[88], M.W. Wolter[42], H. Wolters[128a,128c], S.D. Worm[19], B.K. Wosiek[42], J. Wotschack[32], M.J. Woudstra[87], K.W. Wozniak[42], M. Wu[33], S.L. Wu[176], X. Wu[52], Y. Wu[92], T.R. Wyatt[87], B.M. Wynne[49], S. Xella[39], Z. Xi[92], L. Xia[35c], D. Xu[35a], L. Xu[27], B. Yabsley[152], S. Yacoob[147a], D. Yamaguchi[159], Y. Yamaguchi[120], A. Yamamoto[69], S. Yamamoto[157], T. Yamanaka[157], K. Yamauchi[105], Y. Yamazaki[70], Z. Yan[24], H. Yang[36c], H. Yang[16], Y. Yang[153], Z. Yang[15], W-M. Yao[16], Y.C. Yap[83], Y. Yasu[69], E. Yatsenko[5], K.H. Yau Wong[23], J. Ye[43], S. Ye[27], I. Yeletskikh[68], E. Yigitbasi[24], E. Yildirim[86], K. Yorita[174], K. Yoshihara[124], C. Young[145], C.J.S. Young[32], D.R. Yu[16], J. Yu[8], J. Yu[67], S.P.Y. Yuen[23], I. Yusuff[30,ay], B. Zabinski[42], G. Zacharis[10], R. Zaidan[13], A.M. Zaitsev[132,ak], N. Zakharchuk[45], J. Zalieckas[15], A. Zaman[150], S. Zambito[59], D. Zanzi[91], C. Zeitnitz[178], M. Zeman[130], A. Zemla[41a], J.C. Zeng[169], Q. Zeng[145], O. Zenin[132], T. Ženiš[146a], D. Zerwas[119], D. Zhang[92], F. Zhang[176], G. Zhang[36a,ar], H. Zhang[35b], J. Zhang[6], L. Zhang[51], L. Zhang[36a], M. Zhang[169], R. Zhang[23], R. Zhang[36a,aw], X. Zhang[36b], Y. Zhang[35a], Z. Zhang[119], X. Zhao[43], Y. Zhao[36b,az], Z. Zhao[36a], A. Zhemchugov[68], J. Zhong[122], B. Zhou[92], C. Zhou[176], L. Zhou[43], M. Zhou[35a], M. Zhou[150], N. Zhou[35c], C.G. Zhu[36b], H. Zhu[35a], J. Zhu[92], Y. Zhu[36a], X. Zhuang[35a], K. Zhukov[98], A. Zibell[177], D. Zieminska[64], N.I. Zimine[68], C. Zimmermann[86], S. Zimmermann[51], Z. Zinonos[103], M. Zinser[86], M. Ziolkowski[143], L. Živković[14], G. Zobernig[176], A. Zoccoli[22a,22b], R. Zou[33], M. zur Nedden[17], L. Zwalinski[32]

1   *Department of Physics, University of Adelaide, Adelaide, Australia*
2   *Physics Department, SUNY Albany, Albany NY, U.S.A.*
3   *Department of Physics, University of Alberta, Edmonton AB, Canada*
4   [a] *Department of Physics, Ankara University, Ankara;* [b] *Istanbul Aydin University, Istanbul;* [c] *Division of Physics, TOBB University of Economics and Technology, Ankara, Turkey*
5   *LAPP, CNRS/IN2P3 and Université Savoie Mont Blanc, Annecy-le-Vieux, France*
6   *High Energy Physics Division, Argonne National Laboratory, Argonne IL, U.S.A.*
7   *Department of Physics, University of Arizona, Tucson AZ, U.S.A.*
8   *Department of Physics, The University of Texas at Arlington, Arlington TX, U.S.A.*
9   *Physics Department, National and Kapodistrian University of Athens, Athens, Greece*
10 *Physics Department, National Technical University of Athens, Zografou, Greece*
11 *Department of Physics, The University of Texas at Austin, Austin TX, U.S.A.*
12 *Institute of Physics, Azerbaijan Academy of Sciences, Baku, Azerbaijan*
13 *Institut de Física d'Altes Energies (IFAE), The Barcelona Institute of Science and Technology, Barcelona, Spain*
14 *Institute of Physics, University of Belgrade, Belgrade, Serbia*
15 *Department for Physics and Technology, University of Bergen, Bergen, Norway*
16 *Physics Division, Lawrence Berkeley National Laboratory and University of California, Berkeley CA, U.S.A.*
17 *Department of Physics, Humboldt University, Berlin, Germany*
18 *Albert Einstein Center for Fundamental Physics and Laboratory for High Energy Physics, University of Bern, Bern, Switzerland*
19 *School of Physics and Astronomy, University of Birmingham, Birmingham, U.K.*
20 [a] *Department of Physics, Bogazici University, Istanbul;* [b] *Department of Physics Engineering, Gaziantep University, Gaziantep;* [d] *Istanbul Bilgi University, Faculty of Engineering and Natural Sciences, Istanbul;* [e] *Bahcesehir University, Faculty of Engineering and Natural Sciences, Istanbul, Turkey*
21 *Centro de Investigaciones, Universidad Antonio Narino, Bogota, Colombia*

22 [a] *INFN Sezione di Bologna;* [b] *Dipartimento di Fisica e Astronomia, Università di Bologna, Bologna, Italy*

23 *Physikalisches Institut, University of Bonn, Bonn, Germany*

24 *Department of Physics, Boston University, Boston MA, U.S.A.*

25 *Department of Physics, Brandeis University, Waltham MA, U.S.A.*

26 [a] *Universidade Federal do Rio De Janeiro COPPE/EE/IF, Rio de Janeiro;* [b] *Electrical Circuits Department, Federal University of Juiz de Fora (UFJF), Juiz de Fora;* [c] *Federal University of Sao Joao del Rei (UFSJ), Sao Joao del Rei;* [d] *Instituto de Fisica, Universidade de Sao Paulo, Sao Paulo, Brazil*

27 *Physics Department, Brookhaven National Laboratory, Upton NY, U.S.A.*

28 [a] *Transilvania University of Brasov, Brasov;* [b] *Horia Hulubei National Institute of Physics and Nuclear Engineering, Bucharest;* [c] *Department of Physics, Alexandru Ioan Cuza University of Iasi, Iasi;* [d] *National Institute for Research and Development of Isotopic and Molecular Technologies, Physics Department, Cluj Napoca;* [e] *University Politehnica Bucharest, Bucharest;* [f] *West University in Timisoara, Timisoara, Romania*

29 *Departamento de Física, Universidad de Buenos Aires, Buenos Aires, Argentina*

30 *Cavendish Laboratory, University of Cambridge, Cambridge, U.K.*

31 *Department of Physics, Carleton University, Ottawa ON, Canada*

32 *CERN, Geneva, Switzerland*

33 *Enrico Fermi Institute, University of Chicago, Chicago IL, U.S.A.*

34 [a] *Departamento de Física, Pontificia Universidad Católica de Chile, Santiago;* [b] *Departamento de Física, Universidad Técnica Federico Santa María, Valparaíso, Chile*

35 [a] *Institute of High Energy Physics, Chinese Academy of Sciences, Beijing;* [b] *Department of Physics, Nanjing University, Jiangsu;* [c] *Physics Department, Tsinghua University, Beijing 100084, China*

36 [a] *Department of Modern Physics and State Key Laboratory of Particle Detection and Electronics, University of Science and Technology of China, Anhui;* [b] *School of Physics, Shandong University, Shandong;* [c] *Department of Physics and Astronomy, Key Laboratory for Particle Physics, Astrophysics and Cosmology, Ministry of Education; Shanghai Key Laboratory for Particle Physics and Cosmology, Shanghai Jiao Tong University, Shanghai (also at PKU-CHEP), China*

37 *Université Clermont Auvergne, CNRS/IN2P3, LPC, Clermont-Ferrand, France*

38 *Nevis Laboratory, Columbia University, Irvington NY, U.S.A.*

39 *Niels Bohr Institute, University of Copenhagen, Kobenhavn, Denmark*

40 [a] *INFN Gruppo Collegato di Cosenza, Laboratori Nazionali di Frascati;* [b] *Dipartimento di Fisica, Università della Calabria, Rende, Italy*

41 [a] *AGH University of Science and Technology, Faculty of Physics and Applied Computer Science, Krakow;* [b] *Marian Smoluchowski Institute of Physics, Jagiellonian University, Krakow, Poland*

42 *Institute of Nuclear Physics Polish Academy of Sciences, Krakow, Poland*

43 *Physics Department, Southern Methodist University, Dallas TX, U.S.A.*

44 *Physics Department, University of Texas at Dallas, Richardson TX, U.S.A.*

45 *DESY, Hamburg and Zeuthen, Germany*

46 *Lehrstuhl für Experimentelle Physik IV, Technische Universität Dortmund, Dortmund, Germany*

47 *Institut für Kern- und Teilchenphysik, Technische Universität Dresden, Dresden, Germany*

48 *Department of Physics, Duke University, Durham NC, U.S.A.*

49 *SUPA - School of Physics and Astronomy, University of Edinburgh, Edinburgh, U.K.*

50 *INFN Laboratori Nazionali di Frascati, Frascati, Italy*

51 *Fakultät für Mathematik und Physik, Albert-Ludwigs-Universität, Freiburg, Germany*

52 *Departement de Physique Nucleaire et Corpusculaire, Université de Genève, Geneva, Switzerland*

53 [a] *INFN Sezione di Genova;* [b] *Dipartimento di Fisica, Università di Genova, Genova, Italy*

54 [a] *E. Andronikashvili Institute of Physics, Iv. Javakhishvili Tbilisi State University, Tbilisi;* [b] *High Energy Physics Institute, Tbilisi State University, Tbilisi, Georgia*

55 *II Physikalisches Institut, Justus-Liebig-Universität Giessen, Giessen, Germany*

[56] SUPA - School of Physics and Astronomy, University of Glasgow, Glasgow, U.K.

[57] II Physikalisches Institut, Georg-August-Universität, Göttingen, Germany

[58] Laboratoire de Physique Subatomique et de Cosmologie, Université Grenoble-Alpes, CNRS/IN2P3, Grenoble, France

[59] Laboratory for Particle Physics and Cosmology, Harvard University, Cambridge MA, U.S.A.

[60] [a] Kirchhoff-Institut für Physik, Ruprecht-Karls-Universität Heidelberg, Heidelberg; [b] Physikalisches Institut, Ruprecht-Karls-Universität Heidelberg, Heidelberg; [c] ZITI Institut für technische Informatik, Ruprecht-Karls-Universität Heidelberg, Mannheim, Germany

[61] Faculty of Applied Information Science, Hiroshima Institute of Technology, Hiroshima, Japan

[62] [a] Department of Physics, The Chinese University of Hong Kong, Shatin, N.T., Hong Kong; [b] Department of Physics, The University of Hong Kong, Hong Kong; [c] Department of Physics and Institute for Advanced Study, The Hong Kong University of Science and Technology, Clear Water Bay, Kowloon, Hong Kong, China

[63] Department of Physics, National Tsing Hua University, Taiwan, Taiwan

[64] Department of Physics, Indiana University, Bloomington IN, U.S.A.

[65] Institut für Astro- und Teilchenphysik, Leopold-Franzens-Universität, Innsbruck, Austria

[66] University of Iowa, Iowa City IA, U.S.A.

[67] Department of Physics and Astronomy, Iowa State University, Ames IA, U.S.A.

[68] Joint Institute for Nuclear Research, JINR Dubna, Dubna, Russia

[69] KEK, High Energy Accelerator Research Organization, Tsukuba, Japan

[70] Graduate School of Science, Kobe University, Kobe, Japan

[71] Faculty of Science, Kyoto University, Kyoto, Japan

[72] Kyoto University of Education, Kyoto, Japan

[73] Research Center for Advanced Particle Physics and Department of Physics, Kyushu University, Fukuoka, Japan

[74] Instituto de Física La Plata, Universidad Nacional de La Plata and CONICET, La Plata, Argentina

[75] Physics Department, Lancaster University, Lancaster, U.K.

[76] [a] INFN Sezione di Lecce; [b] Dipartimento di Matematica e Fisica, Università del Salento, Lecce, Italy

[77] Oliver Lodge Laboratory, University of Liverpool, Liverpool, U.K.

[78] Department of Experimental Particle Physics, Jožef Stefan Institute and Department of Physics, University of Ljubljana, Ljubljana, Slovenia

[79] School of Physics and Astronomy, Queen Mary University of London, London, U.K.

[80] Department of Physics, Royal Holloway University of London, Surrey, U.K.

[81] Department of Physics and Astronomy, University College London, London, U.K.

[82] Louisiana Tech University, Ruston LA, U.S.A.

[83] Laboratoire de Physique Nucléaire et de Hautes Energies, UPMC and Université Paris-Diderot and CNRS/IN2P3, Paris, France

[84] Fysiska institutionen, Lunds universitet, Lund, Sweden

[85] Departamento de Fisica Teorica C-15, Universidad Autonoma de Madrid, Madrid, Spain

[86] Institut für Physik, Universität Mainz, Mainz, Germany

[87] School of Physics and Astronomy, University of Manchester, Manchester, U.K.

[88] CPPM, Aix-Marseille Université and CNRS/IN2P3, Marseille, France

[89] Department of Physics, University of Massachusetts, Amherst MA, U.S.A.

[90] Department of Physics, McGill University, Montreal QC, Canada

[91] School of Physics, University of Melbourne, Victoria, Australia

[92] Department of Physics, The University of Michigan, Ann Arbor MI, U.S.A.

[93] Department of Physics and Astronomy, Michigan State University, East Lansing MI, U.S.A.

[94] [a] INFN Sezione di Milano; [b] Dipartimento di Fisica, Università di Milano, Milano, Italy

[95] B.I. Stepanov Institute of Physics, National Academy of Sciences of Belarus, Minsk, Republic of Belarus

[96] Research Institute for Nuclear Problems of Byelorussian State University, Minsk, Republic of Belarus

[97] Group of Particle Physics, University of Montreal, Montreal QC, Canada

[98] P.N. Lebedev Physical Institute of the Russian Academy of Sciences, Moscow, Russia

[99] Institute for Theoretical and Experimental Physics (ITEP), Moscow, Russia

[100] National Research Nuclear University MEPhI, Moscow, Russia

[101] D.V. Skobeltsyn Institute of Nuclear Physics, M.V. Lomonosov Moscow State University, Moscow, Russia

[102] Fakultät für Physik, Ludwig-Maximilians-Universität München, München, Germany

[103] Max-Planck-Institut für Physik (Werner-Heisenberg-Institut), München, Germany

[104] Nagasaki Institute of Applied Science, Nagasaki, Japan

[105] Graduate School of Science and Kobayashi-Maskawa Institute, Nagoya University, Nagoya, Japan

[106] [a] INFN Sezione di Napoli; [b] Dipartimento di Fisica, Università di Napoli, Napoli, Italy

[107] Department of Physics and Astronomy, University of New Mexico, Albuquerque NM, U.S.A.

[108] Institute for Mathematics, Astrophysics and Particle Physics, Radboud University Nijmegen/Nikhef, Nijmegen, Netherlands

[109] Nikhef National Institute for Subatomic Physics and University of Amsterdam, Amsterdam, Netherlands

[110] Department of Physics, Northern Illinois University, DeKalb IL, U.S.A.

[111] Budker Institute of Nuclear Physics, SB RAS, Novosibirsk, Russia

[112] Department of Physics, New York University, New York NY, U.S.A.

[113] Ohio State University, Columbus OH, U.S.A.

[114] Faculty of Science, Okayama University, Okayama, Japan

[115] Homer L. Dodge Department of Physics and Astronomy, University of Oklahoma, Norman OK, U.S.A.

[116] Department of Physics, Oklahoma State University, Stillwater OK, U.S.A.

[117] Palacký University, RCPTM, Olomouc, Czech Republic

[118] Center for High Energy Physics, University of Oregon, Eugene OR, U.S.A.

[119] LAL, Univ. Paris-Sud, CNRS/IN2P3, Université Paris-Saclay, Orsay, France

[120] Graduate School of Science, Osaka University, Osaka, Japan

[121] Department of Physics, University of Oslo, Oslo, Norway

[122] Department of Physics, Oxford University, Oxford, U.K.

[123] [a] INFN Sezione di Pavia; [b] Dipartimento di Fisica, Università di Pavia, Pavia, Italy

[124] Department of Physics, University of Pennsylvania, Philadelphia PA, U.S.A.

[125] National Research Centre "Kurchatov Institute" B.P.Konstantinov Petersburg Nuclear Physics Institute, St. Petersburg, Russia

[126] [a] INFN Sezione di Pisa; [b] Dipartimento di Fisica E. Fermi, Università di Pisa, Pisa, Italy

[127] Department of Physics and Astronomy, University of Pittsburgh, Pittsburgh PA, U.S.A.

[128] [a] Laboratório de Instrumentação e Física Experimental de Partículas - LIP, Lisboa; [b] Faculdade de Ciências, Universidade de Lisboa, Lisboa; [c] Department of Physics, University of Coimbra, Coimbra; [d] Centro de Física Nuclear da Universidade de Lisboa, Lisboa; [e] Departamento de Fisica, Universidade do Minho, Braga; [f] Departamento de Fisica Teorica y del Cosmos and CAFPE, Universidad de Granada, Granada; [g] Dep Fisica and CEFITEC of Faculdade de Ciencias e Tecnologia, Universidade Nova de Lisboa, Caparica, Portugal

[129] Institute of Physics, Academy of Sciences of the Czech Republic, Praha, Czech Republic

[130] Czech Technical University in Prague, Praha, Czech Republic

[131] Charles University, Faculty of Mathematics and Physics, Prague, Czech Republic

[132] State Research Center Institute for High Energy Physics (Protvino), NRC KI, Russia

[133] Particle Physics Department, Rutherford Appleton Laboratory, Didcot, U.K.

[134] [a] INFN Sezione di Roma; [b] Dipartimento di Fisica, Sapienza Università di Roma, Roma, Italy

[135] [a] INFN Sezione di Roma Tor Vergata; [b] Dipartimento di Fisica, Università di Roma Tor Vergata, Roma, Italy

[136] [a] *INFN Sezione di Roma Tre;* [b] *Dipartimento di Matematica e Fisica, Università Roma Tre, Roma, Italy*

[137] [a] *Faculté des Sciences Ain Chock, Réseau Universitaire de Physique des Hautes Energies - Université Hassan II, Casablanca;* [b] *Centre National de l'Energie des Sciences Techniques Nucleaires, Rabat;* [c] *Faculté des Sciences Semlalia, Université Cadi Ayyad, LPHEA-Marrakech;* [d] *Faculté des Sciences, Université Mohamed Premier and LPTPM, Oujda;* [e] *Faculté des sciences, Université Mohammed V, Rabat, Morocco*

[138] *DSM/IRFU (Institut de Recherches sur les Lois Fondamentales de l'Univers), CEA Saclay (Commissariat à l'Energie Atomique et aux Energies Alternatives), Gif-sur-Yvette, France*

[139] *Santa Cruz Institute for Particle Physics, University of California Santa Cruz, Santa Cruz CA, U.S.A.*

[140] *Department of Physics, University of Washington, Seattle WA, U.S.A.*

[141] *Department of Physics and Astronomy, University of Sheffield, Sheffield, U.K.*

[142] *Department of Physics, Shinshu University, Nagano, Japan*

[143] *Department Physik, Universität Siegen, Siegen, Germany*

[144] *Department of Physics, Simon Fraser University, Burnaby BC, Canada*

[145] *SLAC National Accelerator Laboratory, Stanford CA, U.S.A.*

[146] [a] *Faculty of Mathematics, Physics & Informatics, Comenius University, Bratislava;* [b] *Department of Subnuclear Physics, Institute of Experimental Physics of the Slovak Academy of Sciences, Kosice, Slovak Republic*

[147] [a] *Department of Physics, University of Cape Town, Cape Town;* [b] *Department of Physics, University of Johannesburg, Johannesburg;* [c] *School of Physics, University of the Witwatersrand, Johannesburg, South Africa*

[148] [a] *Department of Physics, Stockholm University;* [b] *The Oskar Klein Centre, Stockholm, Sweden*

[149] *Physics Department, Royal Institute of Technology, Stockholm, Sweden*

[150] *Departments of Physics & Astronomy and Chemistry, Stony Brook University, Stony Brook NY, U.S.A.*

[151] *Department of Physics and Astronomy, University of Sussex, Brighton, U.K.*

[152] *School of Physics, University of Sydney, Sydney, Australia*

[153] *Institute of Physics, Academia Sinica, Taipei, Taiwan*

[154] *Department of Physics, Technion: Israel Institute of Technology, Haifa, Israel*

[155] *Raymond and Beverly Sackler School of Physics and Astronomy, Tel Aviv University, Tel Aviv, Israel*

[156] *Department of Physics, Aristotle University of Thessaloniki, Thessaloniki, Greece*

[157] *International Center for Elementary Particle Physics and Department of Physics, The University of Tokyo, Tokyo, Japan*

[158] *Graduate School of Science and Technology, Tokyo Metropolitan University, Tokyo, Japan*

[159] *Department of Physics, Tokyo Institute of Technology, Tokyo, Japan*

[160] *Tomsk State University, Tomsk, Russia*

[161] *Department of Physics, University of Toronto, Toronto ON, Canada*

[162] [a] *INFN-TIFPA;* [b] *University of Trento, Trento, Italy*

[163] [a] *TRIUMF, Vancouver BC;* [b] *Department of Physics and Astronomy, York University, Toronto ON, Canada*

[164] *Faculty of Pure and Applied Sciences, and Center for Integrated Research in Fundamental Science and Engineering, University of Tsukuba, Tsukuba, Japan*

[165] *Department of Physics and Astronomy, Tufts University, Medford MA, U.S.A.*

[166] *Department of Physics and Astronomy, University of California Irvine, Irvine CA, U.S.A.*

[167] [a] *INFN Gruppo Collegato di Udine, Sezione di Trieste, Udine;* [b] *ICTP, Trieste;* [c] *Dipartimento di Chimica, Fisica e Ambiente, Università di Udine, Udine, Italy*

[168] *Department of Physics and Astronomy, University of Uppsala, Uppsala, Sweden*

[169] *Department of Physics, University of Illinois, Urbana IL, U.S.A.*

[170] *Instituto de Física Corpuscular (IFIC), Centro Mixto Universidad de Valencia - CSIC, Spain*

[171] Department of Physics, University of British Columbia, Vancouver BC, Canada

[172] Department of Physics and Astronomy, University of Victoria, Victoria BC, Canada

[173] Department of Physics, University of Warwick, Coventry, U.K.

[174] Waseda University, Tokyo, Japan

[175] Department of Particle Physics, The Weizmann Institute of Science, Rehovot, Israel

[176] Department of Physics, University of Wisconsin, Madison WI, U.S.A.

[177] Fakultät für Physik und Astronomie, Julius-Maximilians-Universität, Würzburg, Germany

[178] Fakultät für Mathematik und Naturwissenschaften, Fachgruppe Physik, Bergische Universität Wuppertal, Wuppertal, Germany

[179] Department of Physics, Yale University, New Haven CT, U.S.A.

[180] Yerevan Physics Institute, Yerevan, Armenia

[181] CH-1211 Geneva 23, Switzerland

[182] Centre de Calcul de l'Institut National de Physique Nucléaire et de Physique des Particules (IN2P3), Villeurbanne, France

[a] Also at Department of Physics, King's College London, London, U.K.

[b] Also at Institute of Physics, Azerbaijan Academy of Sciences, Baku, Azerbaijan

[c] Also at Novosibirsk State University, Novosibirsk, Russia

[d] Also at TRIUMF, Vancouver BC, Canada

[e] Also at Department of Physics & Astronomy, University of Louisville, Louisville, KY, U.S.A.

[f] Also at Physics Department, An-Najah National University, Nablus, Palestine

[g] Also at Department of Physics, California State University, Fresno CA, U.S.A.

[h] Also at Department of Physics, University of Fribourg, Fribourg, Switzerland

[i] Also at II Physikalisches Institut, Georg-August-Universität, Göttingen, Germany

[j] Also at Departament de Fisica de la Universitat Autonoma de Barcelona, Barcelona, Spain

[k] Also at Departamento de Fisica e Astronomia, Faculdade de Ciencias, Universidade do Porto, Portugal

[l] Also at Tomsk State University, Tomsk, Russia

[m] Also at The Collaborative Innovation Center of Quantum Matter (CICQM), Beijing, China

[n] Also at Universita di Napoli Parthenope, Napoli, Italy

[o] Also at Institute of Particle Physics (IPP), Canada

[p] Also at Horia Hulubei National Institute of Physics and Nuclear Engineering, Bucharest, Romania

[q] Also at Department of Physics, St. Petersburg State Polytechnical University, St. Petersburg, Russia

[r] Also at Borough of Manhattan Community College, City University of New York, New York City, U.S.A.

[s] Also at Department of Physics, The University of Michigan, Ann Arbor MI, U.S.A.

[t] Also at Centre for High Performance Computing, CSIR Campus, Rosebank, Cape Town, South Africa

[u] Also at Louisiana Tech University, Ruston LA, U.S.A.

[v] Also at Institucio Catalana de Recerca i Estudis Avancats, ICREA, Barcelona, Spain

[w] Also at Graduate School of Science, Osaka University, Osaka, Japan

[x] Also at Fakultät für Mathematik und Physik, Albert-Ludwigs-Universität, Freiburg, Germany

[y] Also at Institute for Mathematics, Astrophysics and Particle Physics, Radboud University Nijmegen/Nikhef, Nijmegen, Netherlands

[z] Also at Department of Physics, The University of Texas at Austin, Austin TX, U.S.A.

[aa] Also at Institute of Theoretical Physics, Ilia State University, Tbilisi, Georgia

[ab] Also at CERN, Geneva, Switzerland

[ac] Also at Georgian Technical University (GTU),Tbilisi, Georgia

[ad] Also at Ochadai Academic Production, Ochanomizu University, Tokyo, Japan

[ae] Also at Manhattan College, New York NY, U.S.A.

[af] Also at Departamento de Física, Pontificia Universidad Católica de Chile, Santiago, Chile

[ag] Also at Academia Sinica Grid Computing, Institute of Physics, Academia Sinica, Taipei, Taiwan

[ah] Also at School of Physics, Shandong University, Shandong, China

[ai] Also at Departamento de Fisica Teorica y del Cosmos and CAFPE, Universidad de Granada, Granada, Portugal

[aj] Also at Department of Physics, California State University, Sacramento CA, U.S.A.

[ak] Also at Moscow Institute of Physics and Technology State University, Dolgoprudny, Russia

[al] Also at Departement de Physique Nucleaire et Corpusculaire, Université de Genève, Geneva, Switzerland

[am] Also at International School for Advanced Studies (SISSA), Trieste, Italy

[an] Also at Institut de Física d'Altes Energies (IFAE), The Barcelona Institute of Science and Technology, Barcelona, Spain

[ao] Also at School of Physics, Sun Yat-sen University, Guangzhou, China

[ap] Also at Institute for Nuclear Research and Nuclear Energy (INRNE) of the Bulgarian Academy of Sciences, Sofia, Bulgaria

[aq] Also at Faculty of Physics, M.V.Lomonosov Moscow State University, Moscow, Russia

[ar] Also at Institute of Physics, Academia Sinica, Taipei, Taiwan

[as] Also at National Research Nuclear University MEPhI, Moscow, Russia

[at] Also at Department of Physics, Stanford University, Stanford CA, U.S.A.

[au] Also at Institute for Particle and Nuclear Physics, Wigner Research Centre for Physics, Budapest, Hungary

[av] Also at Giresun University, Faculty of Engineering, Turkey

[aw] Also at CPPM, Aix-Marseille Université and CNRS/IN2P3, Marseille, France

[ax] Also at Department of Physics, Nanjing University, Jiangsu, China

[ay] Also at University of Malaya, Department of Physics, Kuala Lumpur, Malaysia

[az] Also at LAL, Univ. Paris-Sud, CNRS/IN2P3, Université Paris-Saclay, Orsay, France

[*] Deceased